

UNIVERSITE DE NICE-SOPHIA ANTIPOLIS

ECOLE DOCTORALE STIC
SCIENCES ET TECHNOLOGIES DE L'INFORMATION ET DE LA
COMMUNICATION

THESE

pour obtenir le titre de

DOCTEUR EN SCIENCES

de l'Université de Nice-Sophia Antipolis

Discipline: Automatique, Traitement du Signal et des Images

présentée et soutenue par

Fadi ABI ABDALLAH

**SOURCE-CHANNEL CODING TECHNIQUES
APPLIED TO WIRELESS SENSOR NETWORKS**

Thèse dirigée par **Raymond KNOPP**
soutenue le 19 Décembre 2008 à Eurécom

Jury:

M. Pierre COMON	Directeur de Recherches au CNRS, UNSA	Président
M. João BARROS	Professeur Associé à l'Université de Porto	Rapporteur
M. Walid HACHEM	Professeur Associé au CNRS, ENST	Rapporteur
Mme Aline ROUMY	Chargé de Recherches à l'INRIA	Examinateur
M. Dirk SLOCK	Professeur à Eurécom	Examinateur
M. Raymond KNOPP	Professeur à Eurécom	Directeur de thèse

Acknowledgements

I would like to thank my God for all what he did and gave me during the whole period of this thesis. I would like to express my gratitude to all those who gave me the possibility to complete this work.

I am deeply indebted to my supervisor Prof. Raymond Knopp for his encouragement, enthusiasm and for the practical advices he gave me throughout the course of this thesis. In the same way, I thank all the jury members for their valuable comments and suggestions for improvements of this work.

In the end, I would like to give my special thanks to my parents whose patient love enabled me to complete this work.

December 2008
Fadi Abi Abdallah
Sophia Antipolis, France

Abstract

Wireless sensor networks are networks consisting of spatially distributed autonomous devices called sensors, deployed to cooperatively collect information and send it back to a location in which it can be extracted and analyzed. One of the most challenging topic in these networks is how to efficiently use the limited energy resource in each sensor node in order to increase the lifetime of the whole network.

In this thesis, we address the source-channel coding problem applied to wireless sensor network models where sensor nodes are observing sources of information and sending back their gathered data through a Gaussian multiple-access channel to a given receiver or collector node.

In a first part, independent random sources varying slowly in time are considered. A source-channel code adapted with the application characteristics is proposed and bounds on the optimal achievable performance are derived. Several model variants involving noncoherent detection and the presence of observation noise are also studied.

In a second part, arbitrarily correlated discrete sources of finite alphabets are considered. After being encoded, they are sent through a Gaussian multiple-access channel with phase shifts unknown at the transmitters and completely known at the receiver. For both random ergodic and arbitrary non-random models for the phase shifts, it is proved that the separation theorem holds, and consequently, the strategy of combining Slepian-Wolf coding to capacity achieving channel encoders is optimal. For continuous sources, it is shown that the source-channel separation is asymptotically optimal.

Finally, a wireless sensor network monitoring a random physical field is considered. The performance of a linear encoder scheme is investigated and bounds on the optimal achievable performance are derived.

Résumé

Les réseaux de capteurs sans fil sont des réseaux qui se composent de plusieurs noeuds autonomes appelés capteurs, déployés sur une surface pour collecter des informations et les transmettre à un endroit où elles peuvent être extraites et analysées. Un des plus grands défis de ces réseaux est de savoir utiliser efficacement la ressource d'énergie limitée de chaque capteur afin d'augmenter la durée de vie du réseau tout entier.

Dans cette thèse, nous abordons le problème de codage source-canal appliqué à certains modèles de réseaux où des capteurs observent des sources d'information, et renvoient les données recueillies à travers un canal gaussien à accès multiple vers un récepteur ou un noeud collecteur.

Dans une première partie, des sources aléatoires indépendantes qui varient lentement dans le temps sont considérées. Un code source-canal adapté aux caractéristiques de l'application est proposé et des bornes sur la performance optimale sont dérivées. Plusieurs variantes de ce modèle, comportant la détection non cohérente et la présence de bruit d'observation, sont également étudiées.

Dans une deuxième partie, des sources discrètes à alphabets finis et arbitrairement corrélées sont considérées. Après avoir été codées, elles sont transmises à travers un canal gaussien à accès multiple soumis à des décalages de phase inconnus aux émetteurs et complètement connus au récepteur. Pour les modèles aléatoires et arbitraires des phases, on montre que le théorème de séparation s'applique, et par conséquent, la stratégie de combiner le codage de Slepian-Wolf avec des encodeurs atteignant la capacité du canal est optimale. Pour des sources continues, on montre que la séparation source-canal est asymptotiquement optimale.

Finalement, un réseau de capteurs sans fil surveillant un champ physique aléatoire est considéré. La performance du codage linéaire est étudiée et des bornes sur la performance optimale sont dérivées.

Contents

Acknowledgements	i
Abstract	iii
Abstract	iii
List of Figures	xi
1 Introduction	1
1.1 General Introduction	1
1.2 Applications	2
1.2.1 Military Applications	2
1.2.2 Civil Applications	2
1.2.3 Environmental Applications	3
1.2.4 Medical Applications	3
1.3 Motivation and Challenges	3
1.4 Thesis Outline and Contributions	6
2 Source-Channel Coding for Very-Low Bandwidth Sources	11
2.1 Introduction	13
2.2 System performance with coherent reception	16
2.2.1 Lower Bound	16
2.2.2 Performance of a Linear Encoder	18
2.2.3 Analytical Upper Bound	18
2.2.4 Other Types of Quantizers	22
2.2.5 An MMSE-Based Scheme	22
2.2.6 Comparison with Other Joint Source-Channel Coding Schemes	24
2.2.7 Extension to Sequence Coding	26
2.3 System Performance with Noncoherent Reception	27
2.3.1 Lower Bound	28
2.3.2 Upper Bound	28
2.3.3 Noisy Observations	30

2.3.4	Numerical Results	32
2.4	Multiple sensors	38
2.4.1	Lower Bound for the Multiple Sensor Case	38
2.4.2	Upper Bound for the Multiple Sensor Case	39
2.5	Conclusion	40
2.A	Probability of Error	42
2.B	Lower Bound on D_e	42
2.C	Symmetric Encoder Characteristic	44
3	Correlated Discrete Sources Over GMACs with Phase Shifts	45
3.1	Introduction	46
3.2	Model	48
3.3	Coding Theorems for Correlated Sources Over GMAC with Phase Shifts	50
3.3.1	Ergodic Phase Sequences	50
3.3.2	Arbitrary Phase Sequences	51
3.4	Discussion	52
3.5	Conclusion	54
3.A	Proof of the Converse of Theorem 1	56
3.B	Proof of the Converse of Theorem 2	58
4	Correlated Continuous Sources Over GMACs with Phase Shifts	63
4.1	Introduction	64
4.2	Model	65
4.3	Two Correlated Gaussian Sources	66
4.3.1	Inner Region	67
4.3.2	Lower Bounds on the Distortion	68
4.4	Outer Region and High Fidelity Regime	71
4.5	Generalisation	72
4.6	Conclusion	73
5	Distributed Sensing of Random Fields	75
5.1	Introduction	76
5.2	Model	77
5.3	Performance Limits Of Linear Coding	79
5.3.1	Achievable Distortion	79
5.3.2	Lower-Bound	81
5.4	General Lower-Bound	82
5.5	Ideal Model	83

5.5.1	Scaling Law	83
5.5.2	Comparison With a TDMA Scheme	84
5.6	Numerical Results	85
5.7	Conclusion	85
5.A	Proof of D_{lower}	87
6	Conclusions and Future Work Directions	89

List of Figures

1.1	Wireless sensor network deployed over an area.	4
1.2	Wireless sensor network model.	4
1.3	Hierarchical wireless sensor network model.	5
2.1	System model	13
2.2	The proposed coding scheme based on a linear quantizer followed by an orthogonal modulation and a MAP receiver . . .	19
2.3	The linear quantizer	20
2.4	Comparison between the spherical code and the upper bound corresponding to our digital code, applied to a source uniformly distributed in an interval of length 0.5.	26
2.5	System model with phase shift.	27
2.6	The model scheme with noisy observations.	30
2.7	Performances of the MAP-based scheme compared to the linear encoder and the theoretical lower bound.	33
2.8	Comparison between the MAP and the MMSE based scheme.	34
2.9	Comparison between the orthogonal and the biorthogonal modulation performances combined with the MMSE estimator.	34
2.10	The lower bound compared to the upper bound corresponding to sequence coding of length K	35
2.11	Performances of the MAP-based scheme compared to the theoretical lower and upper bound for noncoherent reception. . .	35
2.12	Comparison between the MAP and the MMSE-based schemes for the noncoherent reception case.	36
2.13	Comparison of the performances of the MAP-based scheme in both coherent and noncoherent cases.	36
2.14	Comparison of the performances of the MMSE-based scheme in both coherent and noncoherent cases.	37
2.15	The model scheme of multiple sensors observing independent sources.	40

3.1	Correlated sources over GMAC with phase shifts perfectly known at the receiver	49
4.1	Bivariate Gaussian sources over GMAC with phase shifts perfectly known at the receiver	66
4.2	Two correlated Gaussian sources separately encoded at rates R_1 and R_2	68
4.3	Model scheme of M arbitrarily correlated sources sent through a GMAC with phase shifts perfectly known at the receiver . .	74
5.1	The scheme of the considered wireless sensor network model .	78
5.2	Comparison between D_{lower} , D_{ach} , $D_{remote}(C)$ and Gastpar-Vetterli distortion: $\mathcal{A} = [9, 15, 18, 12, 6, 7, 3, 13, 7, 10]$, $N = N' = 10$, $\lambda_1 = \dots = \lambda_{10} = 10$, $\alpha_i = 1$ for $i = 1, \dots, M$, $\sigma_Z = 1.5$, $\sigma_W = 0.01$	88

Chapter 1

Introduction

1.1 General Introduction

A wireless sensor network (WSN) is a wireless network consisting of spatially distributed autonomous devices called sensors that cooperatively monitor physical fields or environmental conditions, such as temperature, sound, vibration, pressure or motion, at different locations [1, 2, 3, 4, 5, 6]. Originally, the development of such networks was motivated by military applications such as battlefield surveillance or border security. However, they are now used in many civilian applications, including environment and habitat monitoring [7, 8], home automation and traffic control. The application requirements and the unique features of WSNs make them different from the traditional ad hoc networks. The characteristics of WSNs and their differences with ad hoc networks can be summarized as follows [9, 10]:

- Sensor nodes in a WSN are in general tiny devices limited in power, computational capacities and memory. They use short-range transceiver for the transmission or the reception of messages and are equipped with small nonrenewable batteries.
- The number of sensor nodes in a WSN depends on the application and can be several orders of magnitude higher than in an ad hoc network.
- Sensor nodes are generally densely deployed and have the possibility of

cooperating between themselves before relaying back the information to the base station.

- Sensor nodes are prone to failure which can have several reasons, such as environmental factors, hardware failure, depleted battery, etc...
- Sensor network topologies change and evolve very frequently in time which is mainly due to sensor node failures. Also, new sensor nodes may be deployed to replace dead nodes or to extend the coverage of the network.
- Sensor nodes use a broadcast communication paradigm while ad hoc networks are based on point-to-point communications.

1.2 Applications

The range of applications of wireless sensor networks is increasing very fast and covering several domains: military, civil, environmental, health, etc...In this section, we will talk more about WSN applications in each of these domains [11]:

1.2.1 Military Applications

Asset monitoring: commanders can monitor locations of the troops, weapons and supplies to enhance the control and the communication.

battlefield monitoring: vibration and magnetic sensors can locate and track enemy forces in the battlefield.

Urban warfare: Deploying sensors in cleared buildings can prevent their re-occupation and track the enemy activity inside them.

Protection: prevention and protection from radiations, biological and chemical weapons can be achieved by the deployment of a network of sensor nodes in the area of interest detecting the level of radiation or the presence of toxic products.

1.2.2 Civil Applications

surveillance: a sensor network can detect fire in buildings and give information about its location. It can also detect intrusions and track human activity.

Disaster prevention: sensor nodes deployed under water can prevent from

disaster like oceanic earthquake or impending tsunami.

Disaster recovery: after an earthquake or a terrorist attack, sensor nodes can detect signs of life inside a damaged building.

1.2.3 Environmental Applications

Environment and habitat monitoring: a WSN deployed in a subglacial environment [12, 13] can collect information about ice caps and glaciers. Sensor networks can also be deployed to measure population of birds and other species [14]. Also, WSN can provide a flood warning [15] and monitor coastal erosion [16].

Disaster detection: forest fire can be detected and localized by a densely deployed WSN.

1.2.4 Medical Applications

Home monitoring: home monitoring for chronic and elderly patients allows long-term care and can reduce the length of hospital stay.

Patient monitoring: sensor nodes deployed on the body of patients in hospitals ([17]) allow the collection of periodic or continuous data like temperature, blood pressure, etc...

1.3 Motivation and Challenges

Recent advances in wireless communications, low-power circuit design and electronics have enabled the development of low-cost, low-power, multifunctional sensors to be used in a WSN context. As sensor nodes are equipped with small batteries, one of the most challenging research subjects is how to increase the lifetime of a WSN by preserving as much as possible the small amount of energy in each node. Power consumption in a sensor node can be divided into three domains: sensing, communicating, and data processing. Sensing power varies with the nature of applications while energy consumption at the data processing stage is much less than the one consumed for the communication process. Hence, the major problem of energy consumption is restrained to designing energy-efficient communication protocols. In large scale sensor networks, routing protocols have their great impact on the energy consumption of each sensor node. For this sake, different strategy of routing has been proposed in the literature: directed diffusion [18], LEACH protocol [19], PEGASIS [20], TEEN [21, 22], and many others as in [23, 24, 25, 26].

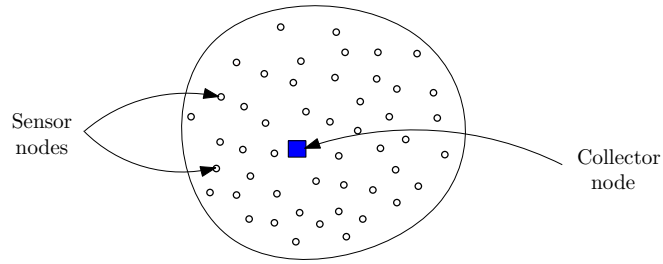


Figure 1.1: Wireless sensor network deployed over an area.

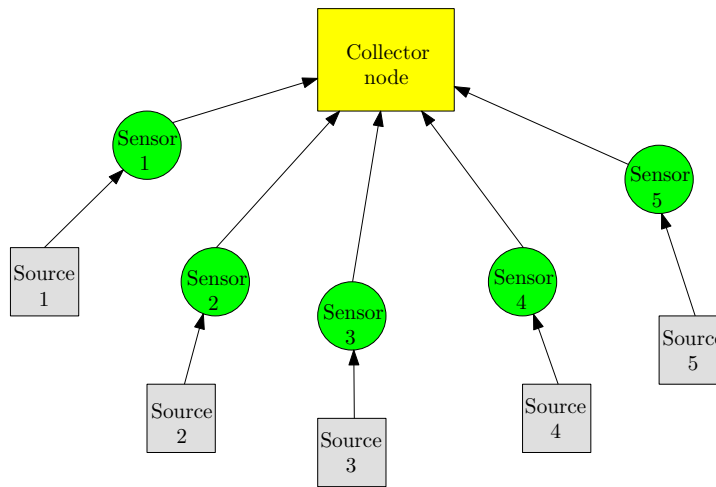


Figure 1.2: Wireless sensor network model.

In this thesis, we are more concerned with working in the physical layer, and more precisely with designing energy-efficient coding strategies that ensure an efficient use of the limited power resources in each sensor node. We consider applications where deployed sensor nodes are observing random sources and sending their observations through a multiple-access channel (MAC) to a common receiver or collector node (see Fig. 1.1 and Fig. 1.2). Typical applications for such models can be found in healthcare area where sensors deployed on a patient send information periodically to a given receiver. In general, small scale sensor networks like the ones used for indoor applications are also concerned by this type of model. In hierarchical sensor networks [27, 28, 29, 30](Fig. 1.3), our model can represent the communi-

cation inside each cluster between the sensors and the cluster head. It can also represent the communication between the cluster heads and the fusion node. Note that a cluster head may have more resources than a sensor node especially in terms of energy which allows it to have more processing capacities and longer range communications. For example, in a hospital we need to collect information from several patients. In this case, a cluster (i.e. one cluster head and a given number of sensors) can be dedicated to each patient. The sensors send their data to the cluster head that could be put on the patient, on his bed or in his room. Then, the cluster heads collect all the received information and relay it back to a given fusion node.

The coding problem for such kind of applications is also known in the literature as the *sensor reachback problem* [31]. Depending on the application, the observations at the sensor nodes might be independent or correlated; in the latter case, coding schemes that exploit this correlation in order to enhance the system performance should be considered. Besides, the receiver might be interested in decoding all the observed sources or to reconstruct a random field based on the sensors observations.

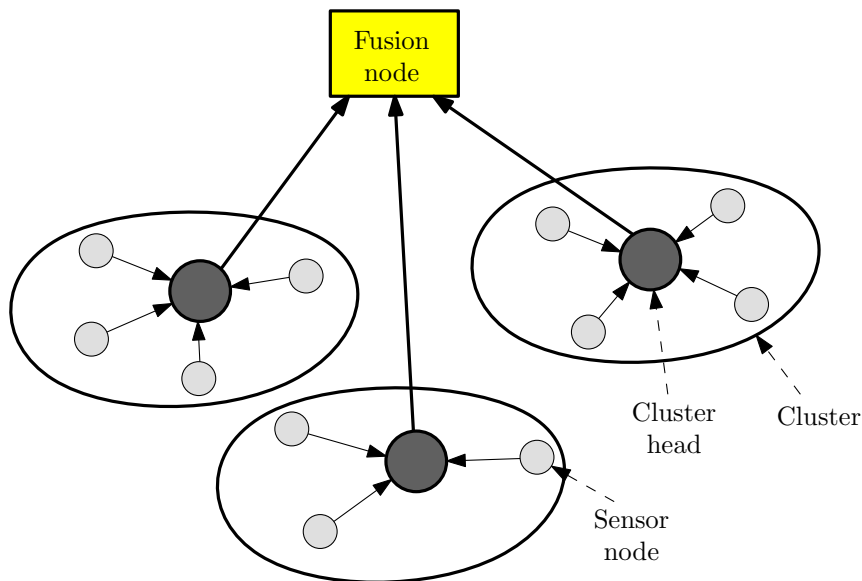


Figure 1.3: Hierarchical wireless sensor network model.

1.4 Thesis Outline and Contributions

As mentioned above, we focus our study on the communication problem that may arise in such models, and more precisely on coding strategies leading to optimal system performance. The thesis report can be divided into three main parts:

- The first part deals with independent sources observed by a deployed WSN where the receiver is interested in decoding all the sources with the best possible fidelity. The work in this part is done in chapter 2. Here, we consider the case where sensor nodes are tracking information sources that are varying very slowly in time; this case represents a typical application for WSNs where sources like temperature, light, radiations, etc...are not fast-varying in time. We start the chapter by addressing the coding problem of one sensor node observing a slowly time-varying source and sending its information to a given receiver. The slowly-time varying characteristic of the source implies that the time interval between two i.i.d. source samples is large enough (it can be minutes, hours or even days depending on the application), and therefore, the communication channel can be used a large number of times to transmit the information from the sender to the receiver. Therefore, for practical reasons, the energy constraint has to be considered per source sample and not per channel use. Due to the large interval of time between two i.i.d. source samples, the sensor node will not have the possibility to encode long sequences of i.i.d. source realisations and therefore it is constrained to encode one single realisation, to send it through the channel and then to decode it at the receiver. From channel coding point of view, it is well-known that Shannon capacity can be achieved when encoding sequences of increasing blocklength which is not the case of the considered WSN application; apart from some special cases of source-channel matching where uncoded delay-free transmission achieve optimal system performance, new codes making use of a single source realisation and exploiting large channel dimensionality should be constructed. In this chapter, we propose a simple code based on a quantizer followed by a modulator and combined with a MAP decoder at the receiver. We derive achievable bounds on the performance and lower bounds using the classical information theory; we compare the proposed coding scheme performance with other existing joint source-channel codes in the literature. We make several practical generalisations of the consid-

ered point-to-point communication model, like the one involving short sequence coding, noncoherent detection at the receiver and noisy observations at the sensor node. We prove that significant gain can be obtained with our proposed code when short sequences of i.i.d source samples are encoded, and show that noncoherent detection results in very small loss in the system performance. At the end of this chapter, we generalise the point-to-point model to the one described in Fig. 1.2 where multiple sensors observing independent, slowly time varying sources, send their information through a noisy MAC to the collector node. Also for this case, we use the code proposed for the single sensor case while the multiple access problem is solved by using a suitable protocol that change the MAC into a set of parallel channels.

- Chapters 3 and 4 constitute the second and the most important part of this thesis. In these chapters, we consider the same WSN model as the one depicted in Fig. 1.1; however, we assume that the sources observed by the sensor nodes are arbitrarily correlated. In chapter 3, the sources are represented by discrete sources of finite alphabets and the receiver wishes to reconstruct these sources with an arbitrarily small probability of error. Here, we address the coding problem from a theoretical point of view, which means that we are interested in deriving necessary and sufficient conditions for lossless transmission of the sources regardless of the code complexity and of its incurred delay. This means that each sensor is supposed to have very powerful computational capacities and also the possibility of encoding long sequences of i.i.d source samples. In our model, we consider that the channel noise has a Gaussian distribution and suppose the existence of phase shifts in the MAC that are unknown at the transmitters while being completely known at the receiver. Note that the optimal coding strategy of correlated sources separately encoded and sent through a real MAC (i.e. when no phase shifts are considered) is not known until now, and the best achievable performance still remains an open problem in information theory [32]; in this case, it is well-known that the coding strategy that consists of compressing the sources in the Slepian-Wolf sense and then adding capacity achieving channel encoders is sub-optimal. This strategy known also as the *separation theorem* or the *source-channel separation* was first introduced by Shannon in [33], and was proved to be optimal in point-to-point communication scenarios. Unfortunately, this separation does not hold for general models in network information theory. However, in our model where phase shifts are considered

to be unknown at the transmitters and completely known at the receiver, we prove that the source-channel separation is the best coding strategy, hence, combining Slepian-Wolf coding to capacity attaining channel encoders leads to optimal system performance. First, this result is important from a theoretical point of view since our model constitutes one of the rare scenarios in network information theory where the separation theorem holds; it tells us also that if the phases are not known at the transmitters, we cannot get better performance than the one achieved by a separation-based coding scheme. Second, it is important to point out that it is not convenient to acquire the phase knowledge at the transmitters, since this operation reveals to be very costly and energy consuming for the sensor nodes; this shows the practical side of our model and reveals the utility of our separation result in real-life applications.

The same model scheme is considered in chapter 4; the main difference remains in considering the sources as continuous random variables of finite energies. Given power constraints on the channel inputs, the receiver wishes to reconstruct estimates of the sources with the best achievable fidelity. We prove that in the high fidelity regime, the separation based on lossy source coding combined to channel encoders achieving the MAC capacity is asymptotically optimal. This implies that in practical applications where small distortions are required when estimating the sources, a separation-based coding scheme is quasi-optimal. This separation can be viewed as an extension of the one obtained in chapter 3 to the lossy coding case where some information loss on the sources is allowed. We note here that we have used the asymptotic characterization of the rate distortion region of the lossy multiterminal source coding problem (see [34]) to prove the quasi-optimality of the separation in the high fidelity regime, its full characterization remaining one of the most longstanding open problem in information theory.

- Chapter 5 constitutes the third and last part of this thesis. In this chapter, we consider a WSN deployed in an area to monitor a random physical field. We assume here a real Gaussian multiple-access channel and consider that the random field is generated by a fixed number of Gaussian random variables. Each observation at the sensor node is encoded linearly before being transmitted to the receiver which has to reconstruct an estimate of the random field with the best possible fidelity. Linear coding is also known under *uncoded transmission* where

the observation is just multiplied by a constant in order to satisfy the considered energy constraint in each sensor; this coding strategy is known to be optimal in several cases like the ones presented in [35] and [36]. We derive lower and upper bounds on the performance and find the asymptotic decreasing behavior of the distortion as a function of the number of sensors.

Chapter 2

Source-Channel Coding for Very-Low Bandwidth Sources

In this chapter, we address the source-channel coding problem of a sensor observing a slowly time-varying Gaussian source and communicating its information to a receiver through a Gaussian channel. Due to the slowly time-varying characteristic of the source, we consider that the sensor is capable of using many channel dimensions per source symbol. Under an energy constraint per source realisation, we derive a theoretical lower bound on the MSE distortion as well as an analytical upper bound based on a practical coding scheme involving a linear uniform quantizer followed by an orthogonal modulation and a MAP receiver. For this coding scheme, we prove the optimality of the linear uniform quantizer in the high energy regime in the sense that it achieves the best rate of decay of the upper bound among all other types of quantizer. Other coding schemes coupled with an MMSE estimator are also proposed and their performances are compared. An extension to the case where the sensor has the capability of encoding a sequence of K source components is studied and a general upper bound in that case is obtained. Assuming the presence of a channel phase in the transmission unknown at the receiver, we derive upper and lower bounds on the system performance and plot numerical results comparing the coherent reception case to the non-

12Chapter 2 Source-Channel Coding for Very-Low Bandwidth Sources

coherent one. A variant of the system model involving the presence of an observation noise at the sensing stage is studied. Finally, we extend the work to the case of multiple sensor nodes observing independent sources and sending their observations to a single receiver through a Gaussian multiple access channel.

2.1 Introduction

We consider one sensor node tracking a slowly time-varying random sequence and sending its observations over a wireless channel to a receiver. The source is represented by a Gaussian random variable U of zero mean and variance $\sigma_u^2 = 1$. The sensor is in general a tiny device with strict energy constraints. The communication channel between the sender and the receiver is an additive white Gaussian noise channel. An important question is how to efficiently encode the random source, and what performance can be achieved. The slowly time-varying characteristic of the source has two main impacts on the way the coding problem should be addressed: firstly, the time between two observations is long, and the sensor will not wait for a sequence of observations to encode it. Therefore, the sensor will encode only one observation before sending it through the channel. Secondly, for each source realisation the channel can be used a large number of times, hence, there is no constraint on the dimensionality of the channel codebook. The latter condition amounts to saying that very low-rate codes should be used.

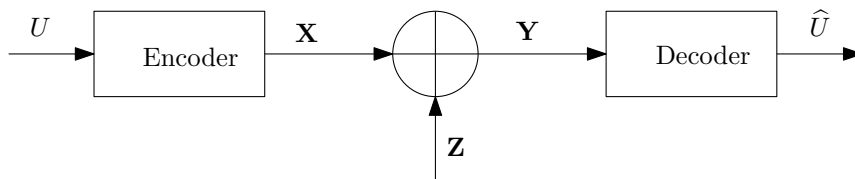


Figure 2.1: System model

The model is depicted in Fig. 2.1. The encoder maps one realisation of the source $U \sim \mathcal{N}(0,1)$ into $\mathbf{X} \triangleq (X_1, \dots, X_N)$ where N denotes the dimension of the channel input. \mathbf{X} is then sent across the channel corrupted by a white Gaussian noise sequence \mathbf{Z} , and is received as \mathbf{Y} . The receiver is a mapping function which tries to construct an estimate \hat{U} of U given \mathbf{Y} . The fidelity criterion that we wish to minimize is the MSE distortion defined as

$$D \triangleq \mathbb{E}[(U - \hat{U})^2], \quad (2.1)$$

under the mean energy constraint

$$\mathbb{E}[|\mathbf{X}|^2] \leq E. \quad (2.2)$$

It is well-known that the linear encoder (i.e. $X = \sqrt{E}U$) achieves the best performance under the mean energy constraint for the special case $N = 1$

[35], [37], [38]. We extended the optimality of the linear encoder as $E \rightarrow 0$ to the case where the source-channel rate is less than one. In the high energy regime, this optimality no longer holds and the best we can do is to bound the MSE distortion by deriving a lower and an upper bound and trying to minimize the gap between these two bounds.

In fact, a lower bound on the distortion over all possible encoders and decoders is easily derived using classical information theory. For an upper bound on the optimal performance, we propose several achievable schemes based on separated source-channel encoders combined with a MAP receiver or an MMSE estimator. Note that an MMSE estimator is the one which minimizes the MSE distortion, but, from a practical point of view, it is too complex to implement. The separate source-channel encoder is based on a quantizer followed by a modulator. Here, the Gaussian source is quantized in b bits which are mapped onto an appropriate modulation before being transmitted over the channel. The distortion is caused by the quantization process and the noisy channel. Increasing the number of quantization bits per source component has the effect of reducing the quantization error and simultaneously increasing the error induced by the channel; decreasing it will have the opposite effect. Thus, the number of quantization bits has to be optimized as a function of the energy. Such optimization can be found in the literature for example in [39] and [40], where the authors try to bound the optimal number of quantization bits that minimizes distortion; the main difference with our model remains in the power constraint they are considering. The choice of the quantizer and the modulator has a great impact on the upper bound and is discussed in section 2.2. We show that for high SNR the chosen quantizer is quasi-optimal among all other symmetric ones, in the sense that it achieves the best rate of decay of the upper bound.

In this chapter, we make comparisons with two quite related works in the literature based on joint source-channel coding schemes and presented in [41, 42]: In [41], the authors developed the theory of non-linear mapping (known also under the name of twisted modulation schemes) where a source sample is directly mapped to an N -dimensional curve. A comparison between a PPM (Pulse Position Modulation) scheme and our digital encoder shows that this latter can achieve the same performance attained by the PPM modulator for a source belonging to $[-1; 1]$. In [42], the authors present a joint source-channel type of codes based on dynamical systems; although these codes exhibit an interesting scaling property of MSE with the SNR for fixed bandwidth expansion, the comparison shows that our digital scheme still achieves better performance than these codes. Other kind of analog codes are developed by Chen and Wornell in [43]; it is shown that

the MSE distortion decreases as $E^{-(3/2)}$. In [44], assuming weak noise, the distortion corresponding to $1 : N$ dimension expansion systems is generalised to $K : N$ dimension expanding mappings. In [45], the authors use a digital coding scheme that can exploit the channel bandwidth expansion and try to optimize numerically both the quantizer and the modulator for a fixed $K:N$ mapping. Note that this optimization is computationally hard, subject to local minima, does not lead to theoretical bound on the distortion as a function of energy and does not give the optimal source-channel rate $r \triangleq K/N$ for minimal distortion.

After making comparisons with previous related works, we extend our coding and decoding schemes to more practical models:

1. Firstly, it is extended to the case where the encoder maps K source realisations; here we assume that the sensor node can wait until having K i.i.d realisations of the source. It is shown that significant improvements can be achieved while performing short sequence coding.
2. Secondly, we generalise the performance bounds to the case of non-coherent reception where the channel induces a phase unknown at the receiver that is constrained to noncoherently decode the message. Here, we consider that obtaining this channel knowledge at the receiver is energy consuming for the sensor node especially when the phase state is changing in time. Theoretical lower and upper bounds are derived for the noncoherent case that are practically the same as for the coherent one. Comparisons based on simulations show a small performance gap that is decreasing with energy. As we are seeking more realistic models, we consider the case where the observations are noisy since no sensor node has perfect sensing capabilities. Also for this case, lower and upper bounds on the performance are derived.
3. Finally, we study the case of multiple sensors monitoring independent sources and sending their informations to a single collector node through a multiple-access channel (MAC). Here also, we derive a lower bound on the optimal performance using the classical information theory. To upper bound the optimal performance, we use the same coding scheme as for the single sensor case, and we assume that the bandwidth of the MAC is large enough so that the sensor nodes can send their informations through parallel channels with unconstrained bandwidth. While in this chapter, the multiple sensor case will be limited to independent sources, in the next chapter, we will address the coding problem when correlation between the sources is involved.

2.2 System performance with coherent reception

2.2.1 Lower Bound

Let us take first the more general case where the encoder maps K source components $\mathbf{U} \triangleq (U_1, \dots, U_K)$ into $\mathbf{X} = (X_1, \dots, X_N)$, and the decoder maps $\mathbf{Y} = (Y_1, \dots, Y_N)$ into $\hat{\mathbf{U}} \triangleq (\hat{U}_1, \dots, \hat{U}_K)$; the source-channel code rate is equal to $r \triangleq \frac{K}{N}$. Define the distortion as $D_K \triangleq \frac{1}{K} \mathbb{E}[\|\mathbf{U} - \hat{\mathbf{U}}\|^2]$ and the mean energy constraint as

$$\sum_{i=1}^N \mathbb{E}[X_i^2] \leq KE. \quad (2.3)$$

Clearly, it suffices to put $K = 1$ to return to our special model stated above in the introduction section and depicted in Fig. 2.1. Now, let us find a lower bound on the distortion D_K over all possible encoders and decoders satisfying (2.3). We have these standard inequalities [46]

$$I(\mathbf{U}; \hat{\mathbf{U}}) = h(\mathbf{U}) - h(\mathbf{U}|\hat{\mathbf{U}}) \quad (2.4)$$

$$= h(\mathbf{U}) - h(\mathbf{U} - \hat{\mathbf{U}}|\hat{\mathbf{U}}) \quad (2.5)$$

$$\geq h(\mathbf{U}) - h(\mathbf{U} - \hat{\mathbf{U}}) \quad (2.6)$$

$$\geq \frac{K}{2} \log(2\pi e) - \sum_{i=1}^K h(U_i - \hat{U}_i) \quad (2.7)$$

$$\geq - \sum_{i=1}^K \frac{1}{2} \log(\mathbb{E}[(U_i - \hat{U}_i)^2]) \quad (2.8)$$

$$\geq \frac{K}{2} \log\left(\frac{1}{D_K}\right), \quad (2.9)$$

and

$$I(\mathbf{U}; \hat{\mathbf{U}}) \leq I(\mathbf{X}, \mathbf{Y}) \quad (2.10)$$

$$= h(\mathbf{Y}) - h(\mathbf{Y}|\mathbf{X}) \quad (2.11)$$

$$\leq \sum_{i=1}^N h(Y_i) - h(\mathbf{Z}) \quad (2.12)$$

$$\leq \sum_{i=1}^N \frac{1}{2} \log(\mathbb{E}[Y_i^2]) - \frac{N}{2} \log(\sigma_z^2) \quad (2.13)$$

$$\leq \frac{N}{2} \log\left(\frac{\sum_{i=1}^N \mathbb{E}[Y_i^2]}{N\sigma_z^2}\right) \quad (2.14)$$

$$= \frac{N}{2} \log\left(\frac{KE + N\sigma_z^2}{N\sigma_z^2}\right). \quad (2.15)$$

From these inequalities, we obtain

$$D_K \geq \frac{1}{\left(1 + \frac{KE}{N\sigma_z^2}\right)^{N/K}} \quad (2.16)$$

Therefore,

$$D = D_1 \geq \frac{1}{\left(1 + \frac{E}{N\sigma_z^2}\right)^N}. \quad (2.17)$$

The RHS of that inequality is a decreasing function of N . Since it is unconstrained in our model specifications, we obtain that

$$D \geq \lim_{N \rightarrow \infty} \frac{1}{\left(1 + \frac{E}{N\sigma_z^2}\right)^N} = e^{-E/\sigma_z^2} \triangleq D_{lower}. \quad (2.18)$$

The RHS term in (2.18) constitutes a lower bound over D and coincides with $D(C)$ where $D(R)$ is the rate distortion function of the source U , $C = \lim_{N \rightarrow \infty} C_N$, and C_N is the capacity of the N -dimensional channel defined by

$$C_N \triangleq \max_{p(\mathbf{x}): \mathbb{E}[|\mathbf{X}|^2] \leq E} I(\mathbf{X}, \mathbf{Y}). \quad (2.19)$$

Note that the lower bound could be achieved by encoding infinite-length source sequences but, when we are constrained to encode one source component, it is not the case anymore; in fact, the equality in $h(\mathbf{Y}) \leq \sum_{j=1}^N h(Y_j)$ is achieved when Y_j and thus X_j are independent; but X_j are all functions of one realisation of U , therefore they must be correlated. Thus, for the case of one source component coding, the inequality in (2.12) is strict and the lower bound is not achievable.

2.2.2 Performance of a Linear Encoder

The linear encoder is the one that simply multiplies the source output by a scaling factor in order to match the energy requirement of the system before sending it through the noisy channel. Followed by an MMSE estimator at the receiver, the achieved distortion is given by [38]

$$D = \frac{\sigma_z^2}{\sigma_z^2 + E}. \quad (2.20)$$

As said previously in the introduction, it is well-known that the linear encoder is optimal when the source-channel rate is equal to one. But when this rate goes to zero, it is no longer the case as it can be seen by comparing (2.20) to (2.18). Although this bad performance of the linear encoder when one source component can be mapped onto an infinite dimensional channel, it still has a very nice behaviour when the amount of the transmitted energy is small. In fact, by expanding D_{lower} and the distortion in (2.20) as $E \rightarrow 0$, we can write

$$D_{lower} = e^{-E/\sigma_z^2} \approx 1 - \frac{E}{\sigma_z^2} \quad \text{and} \quad D = \frac{1}{1 + E/\sigma_z^2} \approx 1 - \frac{E}{\sigma_z^2}. \quad (2.21)$$

Therefore, the linear encoder is still optimal when $E \rightarrow 0$ even if the source-channel rate is less than one. In the sequel, we will be more interested in constructing codes that have nice performance in the high energy regime.

2.2.3 Analytical Upper Bound

As shown in the previous section, the resultant distortion corresponding to the linear coding scheme decreases linearly with the energy E while in the case of very-low bandwidth sources, the lower bound is exponentially decreasing in E . In order to minimize this gap, we propose a separate source-channel coding scheme and derive an analytical upper bound on the minimal achievable distortion. As presented in Fig. 2.2, the encoder is formed by a uniform linear quantizer followed by an orthogonal modulator. The choice of an orthogonal modulation is motivated by the fact that the probability of correct detection approaches that of the regular simplex constellation when the size of the modulation becomes large [47, p. 381]. The optimality of the regular simplex is proved in [48] and [49] for different energy constraints and assumptions on *a priori* probabilities, although not those arising in our model (i.e. average energy constraint and non-uniform priors). However, it is also shown in [50] that, under an average energy constraint, the regular

simplex still optimizes the union bound even if its 'strong' optimality does not hold.

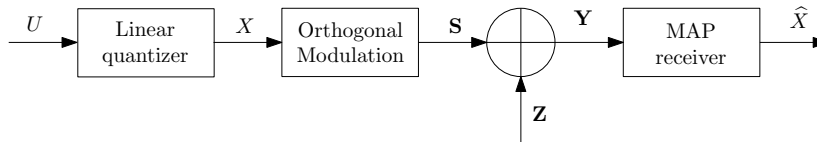


Figure 2.2: The proposed coding scheme based on a linear quantizer followed by an orthogonal modulation and a MAP receiver

The choice of a uniform quantizer is motivated first by its simplicity, secondly by its easy-calculated analytical upper bound on its quantization distortion, and finally for its quasi-optimality in the high resolution regime from source coding point of view. It is perhaps interesting to point out that the use of a Max-Lloyd quantizer will reduce the quantization distortion and not the MSE distortion that we wish to minimize. The optimal quantizer design of a source sent over a noisy channel was found by Kurtenbach and Wintz in [51] and [52]. The corresponding quantization values and levels are written in terms of the source input distribution and the channel transition matrix. Besides, it is shown that when the noise power vanishes, the quantizer coincides with the Max-Lloyd one. After introducing our coding scheme, we will return to these results and discuss about the complexity of applying them to our case.

The uniform quantizer that we used is a function $f : \mathcal{U} \rightarrow \mathcal{X} \triangleq \{x_1, \dots, x_M\}$ that assigns a value x_i to each $u \in I_i$ for $i = 1, \dots, M$, where x_i and I_i are respectively the quantization values and intervals. The partition of \mathcal{U} is as follows: $I_1 =]-\infty; \Delta[$, $I_M = [\Delta; \infty[$, and for $i = 2, \dots, M - 1$,

$$I_i = \left[-\Delta + \frac{\Delta(i-2)}{2^{b-1}-1}; -\Delta + \frac{\Delta(i-1)}{2^{b-1}-1}\right[, \quad (2.22)$$

where $\Delta = 2\sqrt{b \log 2}$, $M = 2^b$ and $b \geq 2$ is an integer representing the quantization bits per source component. The quantization levels are chosen as follows: $x_1 = -\Delta$, $x_M = \Delta$ and for $i = 2, \dots, M - 1$, x_i is the value in the middle of I_i . This quantizer is easy to build and its corresponding quantization distortion achieves the exponential rate of decay of $2^{-2b(1+o(b))}$, where $o(b)$ is a function that goes to zero when $b \rightarrow \infty$. It is illustrated in Fig. 2.3. The output $X = x_i$ of the quantizer is assigned to a signal $\mathbf{S} = \mathbf{s}_i$ chosen from an orthogonal modulation of size M that is sent through

the Gaussian channel. We assume that the transmitted signals have equal energy. Given the received signal, a MAP receiver makes the decision on

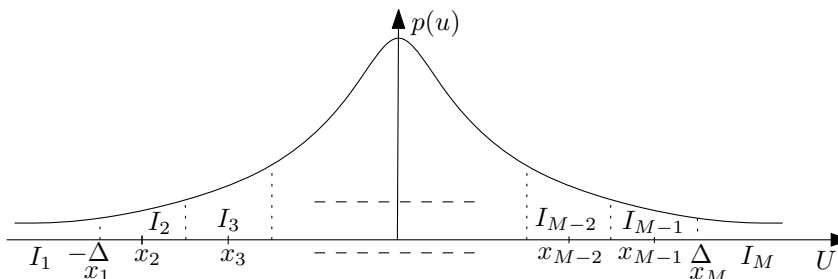


Figure 2.3: The linear quantizer

the signal that has been sent and decodes $\hat{X} = x_j$ where

$$j = \arg \max_{i=1, \dots, M} p(\mathbf{y}|x_i)p_i \quad (2.23)$$

$$= \arg \max_{i=1, \dots, M} \ln p_i - \frac{1}{2\sigma_z^2} \|\mathbf{y} - \mathbf{s}_i\|^2 \quad (2.24)$$

$$= \arg \max_{i=1, \dots, M} \ln p_i + \frac{1}{\sigma_z^2} \mathbf{y}^T \mathbf{s}_i, \quad (2.25)$$

and $p_i = \int_{I_i} p(u) du$ for $i = 1, \dots, M$ denote the *a priori* probabilities. Now let $P_{ij} \triangleq p(x_j|x_i) = p(\mathbf{s}_j|\mathbf{s}_i)$ denotes the probability of decoding x_j given that x_i has been transmitted and $Q(t) \triangleq \int_t^\infty \frac{1}{\sqrt{2\pi}} e^{-u^2/2} du$; the expression of P_{ij} can be easily found: if $i \neq j$

$$P_{ij} = \mathbb{E}_A \left[(1 - Q(T_{ij} - \sqrt{E}/\sigma_z^2)) \prod_{\substack{k=1 \\ k \neq i, j}}^M (1 - Q(T_{kj})) \right] \quad (2.26)$$

$$\text{and } P_{ii} = \mathbb{E}_A \left[\prod_{\substack{k=1 \\ k \neq i}}^M (1 - Q(T_{ki} + \sqrt{E}/\sigma_z^2)) \right] \quad (2.27)$$

where $T_{ij} = A/\sigma_z - \frac{\sigma_z}{E} \log(p_i/p_j)$, and $A \sim \mathcal{N}(0, \sigma_z^2)$. Hence, the exact expression of the distortion is

$$D = \sum_{i,j=1}^M P_{ij} \int_{I_i} (u - x_j)^2 p(u) du. \quad (2.28)$$

The results of Kurtenbach and Wintz in [51] and [52] state that, for a given source distribution and fixed channel transition matrix, the quantization values and transition levels can be optimized; but, on one hand, the calculation of the transition matrix is too hard for computation, and, on the other hand, we desire to bound the distortion in order to be able to optimize the number of quantization bits given a certain amount of energy. It is important to point out that an algorithm based on calculating, after optimizing the quantizer at step 1, the new channel transition matrix that depends on the *apriories* at step 2, then repeating these two steps several times, is not sure to converge because step 2 will minimize the probability of error and not the MSE distortion.

The following bound on the MSE distortion holds:

$$D = D_Q(1 - P_e) + D_e P_e \quad (2.29)$$

$$< D_Q + D_e P_e \quad (2.30)$$

where D_e is the MSE distortion given that an error decision has been made, P_e is the probability of making an error and D_Q represents the quantization distortion. Using the inequality $Q(\Delta) < \frac{e^{-\Delta^2/2}}{\sqrt{2\pi}\Delta}$, we can write

$$\begin{aligned} D_Q &= 2 \int_{\Delta}^{\infty} (u - \Delta)^2 p(u) du + \sum_{i=2}^{M-1} \int_{I_i} (u - x_i)^2 p(u) du \\ &< \frac{2e^{-\Delta^2/2}}{\sqrt{2\pi}\Delta} + \frac{\Delta^2}{(2^b - 2)^2}. \end{aligned} \quad (2.31)$$

Again, using the same upper bound on the function $Q(\Delta)$ and the fact that $D_e < 4\Delta^2$ when $|u| \leq \Delta$, we obtain

$$\begin{aligned} D_e &< 4\Delta^2 + 2 \int_{\Delta}^{\infty} (u + \Delta)^2 p(u) du \\ &< 4\Delta^2 + \frac{2(4\Delta^2 + 1)}{\sqrt{2\pi}\Delta} e^{-\Delta^2/2}. \end{aligned} \quad (2.32)$$

The probability of error can be bounded by

$$P_e \leq M^\rho e^{\left[-\frac{E}{2\sigma_z^2} \left(\frac{\rho}{\rho+1}\right)\right]} \quad (2.33)$$

For the derivation, see Appendix 2.A. Combining all these bounds in (2.30), (2.31), (2.32) and (2.33), we obtain

$$D < 2^{-2b(1+o(b))} + 2^{\rho b(1+o'(b)) - \frac{E \ln(2)}{2\sigma_z^2} \left(\frac{\rho}{\rho+1}\right)} \quad (2.34)$$

where $o'(b)$ is a function that goes to zero when $b \rightarrow \infty$. This bound is a sum of two exponential terms: the first represents the quantization distortion and is independent from the energy while the second represents the distortion due to the channel error. When we increase the amount of energy E , the second term decreases and becomes less than the first one; to minimize the upper bound in that case, the number of quantization bits should be increased so that the two terms will have the same decreasing behaviour. Thus, when E is sufficiently large, optimizing the bound in (2.34) with respect to ρ and b gives $D < e^{-2b_{opt} \log(2)}$, with $b_{opt} = \lfloor \frac{E}{12\sigma_z^2 \log(2)} \rfloor$ and $\rho_{opt} = 1$. Thus, the upper bound approaches the value $e^{-E/(6\sigma_z^2)}$ for large E which represents 7.8dB loss from the lower bound. Notice that the use of a maximum-likelihood decoder instead of a MAP gives exactly the same upper bound even if the performance of the latter is obviously better.

2.2.4 Other Types of Quantizers

The reader may be interested in investigating the use of other types of quantizers and their influence on the upper bound. In fact, changing the quantizer will change the bounds on D_Q and D_e . We will prove in this section that, for high SNR and with any symmetric quantizer, the best rate of decay of the upper bound will be $e^{-E/(6\sigma_z^2)}$.

On one hand, it is clear that D_Q is lowered by 2^{-2b} which represents the distortion-rate function of the source. A necessary condition for a good upper bound is that the quantization distortion should be small compared to $\sigma_u^2 = 1$ when E gets large, i.e. $D_Q \ll 1$; otherwise, we will obtain a bad upper bound. On the other hand, it is shown in Appendix 2.B that in the high energy regime, $D_e \gtrsim 1$ for any symmetric quantizer verifying $D_Q \ll 1$. Therefore, the resultant upper bound will not be smaller than

$$2^{-2b} + 2^{\rho b - \frac{E \ln(2)}{2\sigma_z^2} \left(\frac{\rho}{\rho+1}\right)} \quad (2.35)$$

which, when b and ρ get optimized, will decrease like $e^{-E/(6\sigma_z^2)}$. This proves that the linear uniform quantizer that we have used achieves the best rate of decay of the upper bound among all other symmetric quantizers.

2.2.5 An MMSE-Based Scheme

Since the MAP receiver is the decoder which minimizes the probability of error and not the MSE distortion, it is interesting to see the distortion gain that could be obtained by using an MMSE estimator. To this end, we

propose a scheme where the range of the Gaussian source is partitioned into M intervals I_1, \dots, I_M defined as in section 2.2.3; each of the intervals is mapped onto a signal chosen from a biorthogonal modulation of size M : for $i = 1, \dots, M/2$, the intervals I_i and I_{M+1-i} are assigned respectively to the two signals \mathbf{s}_i and \mathbf{s}_{M+1-i} which belong to the same axis in the bi-orthogonal constellation. For $i, j = 1, \dots, M$, let

$$J_i \triangleq \int_{I_i} up(u) du, \quad K_{ij} \triangleq \int_{-\infty}^{\infty} \frac{p(\mathbf{y}|\mathbf{s}_i)p(\mathbf{y}|\mathbf{s}_j)}{\sum_{k=1}^M p_k p(\mathbf{y}|\mathbf{s}_k)} d\mathbf{y}. \quad (2.36)$$

Due to the symmetry in the construction of the encoder, we have that $J_j = -J_{M+1-j}$ and $K_{i,j} = K_{i,M+1-j}$ for all $i = 1, \dots, M$, $j = 1, \dots, M/2$ and $j \neq i, M+1-i$ (see Appendix 2.C for the proof).

The receiver is an MMSE estimator which minimizes the mean square error distortion. The estimate of u is

$$\hat{u}(\mathbf{y}) = \mathbb{E}[U|\mathbf{y}] = \frac{1}{p(\mathbf{y})} \int_{-\infty}^{\infty} up(\mathbf{y}|u)p(u) du \quad (2.37)$$

$$= \frac{\sum_{i=1}^M \int_{I_i} up(\mathbf{y}|\mathbf{s}_i)p(u) du}{\int_{-\infty}^{\infty} p(\mathbf{y}|u)p(u) du} = \frac{\sum_{i=1}^M p(\mathbf{y}|\mathbf{s}_i) \int_{I_i} up(u) du}{\sum_{i=1}^M \int_{I_i} p(\mathbf{y}|\mathbf{s}_i)p(u) du} \quad (2.38)$$

$$= \frac{\sum_{i=1}^M J_i p(\mathbf{y}|\mathbf{s}_i)}{\sum_{i=1}^M p_i p(\mathbf{y}|\mathbf{s}_i)}. \quad (2.39)$$

The MSE distortion can be written as

$$D = \mathbb{E}[(U - \hat{U}(\mathbf{Y}))^2] = 1 + \mathbb{E}[\hat{U}^2(\mathbf{Y})] - 2\mathbb{E}[U\hat{U}(\mathbf{Y})] \quad (2.40)$$

$$= 1 - \mathbb{E}[\hat{U}^2(\mathbf{Y})] = 1 - \sum_{i=1}^M \sum_{j=1}^M J_i J_j K_{ij} \quad (2.41)$$

$$= 1 + \sum_{i=1}^M J_i^2 K_{i,M+1-i} - \sum_{i=1}^M J_i^2 K_{i,i}. \quad (2.42)$$

We have that

$$\begin{aligned} K_{i,M+1-i} &= \int_{-\infty}^{\infty} \frac{\frac{1}{(2\pi\sigma_z^2)^{M/4}} e^{-\frac{1}{2\sigma_z^2} \sum_{k=1}^{M/2} y_k^2} e^{-E/2\sigma_z^2}}{\sum_{k=1}^{M/2} p_k (e^{-\frac{\sqrt{E}}{\sigma_z^2} y_k} + e^{\frac{\sqrt{E}}{\sigma_z^2} y_k})} d\mathbf{y} \\ &< e^{-E/2\sigma_z^2} \int_{-\infty}^{\infty} \frac{\frac{1}{(2\pi\sigma_z^2)^{M/4}} e^{-\frac{1}{2\sigma_z^2} \sum_{k=1}^{M/2} y_k^2}}{\sum_{k=1}^{M/2} 2p_k} d\mathbf{y} \\ &= e^{-E/2\sigma_z^2}, \end{aligned}$$

$$\text{and } K_{ii} = \mathbb{E}_{\mathbf{Y}|\mathbf{s}_i} \left[\frac{p(\mathbf{y}|\mathbf{s}_i)}{\sum_{k=1}^M p_k p(\mathbf{y}|\mathbf{s}_k)} \right]$$

where $\mathbf{Y}|\mathbf{s}_i$ is a multivariate Gaussian of mean \mathbf{s}_i and covariance matrix $\sigma_z^2 \mathbf{I}_{M/2}$. Thus,

$$D < 1 + 2e^{-E/2\sigma_z^2} \sum_{i=1}^{M/2} J_i^2 - 2 \sum_{i=1}^{M/2} J_i^2 \mathbb{E}_{\mathbf{Y}|\mathbf{s}_i} \left[\frac{e^{\frac{\sqrt{E}}{\sigma_z^2} y_i}}{\sum_{k=1}^{M/2} p_k (e^{-\frac{\sqrt{E}}{\sigma_z^2} y_k} + e^{\frac{\sqrt{E}}{\sigma_z^2} y_k})} \right]. \quad (2.43)$$

Now, suppose that we use an orthogonal modulation instead of the biorthogonal one; for $i = 1, \dots, M$, every interval I_i is mapped into a signal \mathbf{s}_i . Doing similar calculations as for the biorthogonal case, we obtain

$$D = 1 - \sum_{i=1}^M J_i^2 \mathbb{E}_{\mathbf{Y}|\mathbf{s}_i} \left[\frac{e^{\frac{\sqrt{E}}{\sigma_z^2} y_i} - e^{\frac{\sqrt{E}}{\sigma_z^2} y_{M+1-i}}}{\sum_{k=1}^M p_k e^{\frac{\sqrt{E}}{\sigma_z^2} y_k}} \right] \quad (2.44)$$

where $\mathbf{Y} = (Y_1, \dots, Y_M)|\mathbf{s}_i$ is a multivariate Gaussian of mean \mathbf{s}_i and covariance matrix $\sigma_z^2 \mathbf{I}_M$. We currently do not have asymptotic expressions for (2.43) and (2.44) as $E \rightarrow \infty$. We will compare the performance of the MMSE estimator to the MAP one in section (2.3.4).

2.2.6 Comparison with Other Joint Source-Channel Coding Schemes

We now compare our encoder to other joint source-channel encoders that try to exploit the channel bandwidth expansion in order to minimize the resultant distortion.

In [41, pp.623], the authors use a PPM modulator which map a random input m belonging to $[-1; 1]$ into a signal

$$s_m(t) = \sqrt{E} \phi(t - mT_0); \quad -1 \leq m \leq 1 \quad (2.45)$$

where E represents the transmitted energy and

$$\phi(t) \triangleq \sqrt{2W} \frac{\sin 2\pi W t}{2\pi W t} \quad (2.46)$$

is a unit-energy waveform generated by passing an impulse through an ideal lowpass filter of bandwidth W . The modulated signal is then transmitted through a noisy channel where the noise is considered to be white Gaussian. While performing a ML decoding at the receiver, it is shown that the resultant MSE distortion D can be approximated by

$$D \approx \frac{12}{\pi^2} \left(\frac{1}{\beta}\right)^2 \frac{\sigma_z^2}{E} + \frac{2}{3} \frac{\beta - 1}{\sqrt{2\pi E/2\sigma_z^2}} e^{-E/4\sigma_z^2} \quad (2.47)$$

where σ_z^2 denotes the noise variance and $\beta \triangleq 4WT_0$ denotes the effective dimensionality of the transmitted signal. By optimizing β as a function of the transmitted energy, it can be easily shown that in the high energy regime, the distortion $D \approx e^{-E/6\sigma_z^2}$ can be achieved. Note that if we use our encoder to send the random input m in the same channel conditions while using ML decoder at the receiver, the same achievable distortion can be attained. Another point is that the performance achieved while using the joint source-channel encoder is not expected to change for high SNR when the source to transmit is Gaussian; in the latter case, a certain companding function which maps the real line onto $[-1; 1]$ can be used in order to adapt the source to the used coding scheme. Therefore, we deduce that our digital approach gives practically the same performance as for the analog one introduced in [41] at least for sources belonging to $[-1; 1]$.

Another type of joint source-channel encoder with which we can make a comparison is the spherical code based on dynamical systems and introduced in [42]. For fixed bandwidth expansion factor, it is shown in [42] that the spherical code is quasi-optimal for high SNR by the means that the rate of decay of its resultant MSE distortion can be arbitrarily close to the one obtained by the OPTA. In Fig. 2.4, we compare the spherical code performance to the upper bound corresponding to our separate-based coding scheme. The curves correspond to a source uniformly distributed in $[0; 1/2]$ and show the optimality of our scheme compared to the spherical code. It is also important to say that from a practical point of view, the decoder of a spherical code is much more complex than the MAP decoder of an orthogonal modulation. Moreover, we will see in the next sections that, unlike the joint source-channel coding schemes presented in this paragraph, the separate-based one can be easily generalised to other variants of our model, and upper bounds can be easily derived.

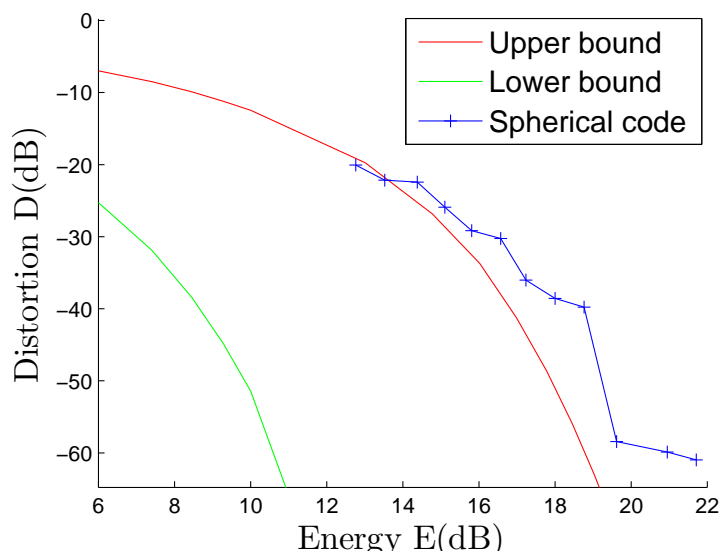


Figure 2.4: Comparison between the spherical code and the upper bound corresponding to our digital code, applied to a source uniformly distributed in an interval of length 0.5.

2.2.7 Extension to Sequence Coding

Due to the slowly time-varying characteristic of the source, we have assumed that just one source component is available to be encoded and then transmitted. We now extend to the case where the sensor can wait until having a sequence of length K of i.i.d. source realisations at the encoder input. Under the mean energy constraint in (2.3), we are interested to see how much the upper bound can be improved by coding a sequence of K source components. Using the same linear uniform quantizer (see Fig. 2.3), each source component is quantized in b representing bits. The quantizer is followed by an orthogonal modulation of size $M_K = 2^{Kb}$ that takes the Kb bits available at the input and maps them onto an Kb -dimensional signal of fixed energy equal to KE . Performing MAP decoding, we have that

$$D_K < D_{QK} + D_{eK}P_{eK} \quad (2.48)$$

where D_{QK} represents the quantization error, D_{eK} the MSE distortion when an error decision has been made and P_{eK} the probability of making an error. Clearly, we have $D_{QK} = D_{Q1} = D_Q$, $D_{eK} \leq D_{e1} = D_e$ and $P_{eK} \leq$

$M_K^\rho e^{\left[-\frac{KE}{2\sigma_z^2}\left(\frac{\rho}{\rho+1}\right)\right]}$. Doing the same optimization procedure as in section 2.2.3, we obtain $D_K < e^{-2b_{Kopt} \log(2)}$ for large amount of energy E with $\rho_{opt} = 1$ and

$$b_{Kopt} = \left\lfloor \frac{KE}{4(K+2)\sigma_z^2 \log(2)} \right\rfloor. \quad (2.49)$$

Letting $K \rightarrow \infty$, the upper bound approaches asymptotically the value $e^{-E/2\sigma_z^2}$ and the gap with the lower bound is reduced to $3dB$.

2.3 System Performance with Noncoherent Reception

Until now, we have assumed that the receiver has full knowledge of the channel. This assumption means that the sensor should allocate a part of his energy to inform the receiver about the channel phase each time it has an information to transmit. Therefore, the energy allocated for the phase knowledge is relatively large compared to the one dedicated for the transmission of information which presents a critical question on how efficiently the limited energy of a sensor battery is used.

In this section, we will study the case where the sensor send no information about the channel phase which will be considered as a random variable denoted by ϕ with uniform distribution. We will adopt the same notations as in previous sections with the difference that the random variables representing the input, output and the noise of the channel are now complex values. The model is depicted in Fig. 2.5. The channel noise \mathbf{Z} is considered to be zero mean circularly symmetric Gaussian noise with complex covariance matrix $2\sigma_Z^2 \mathbf{I}_N$.

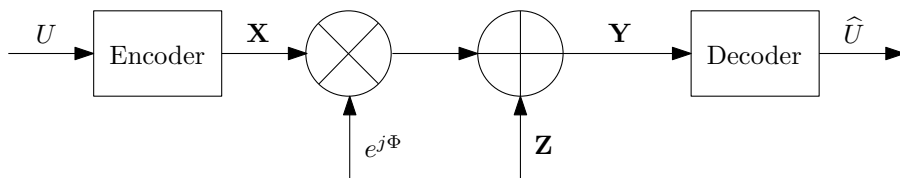


Figure 2.5: System model with phase shift.

2.3.1 Lower Bound

As in section 2.2.1, let us take the more general case where the encoder maps K source components into \mathbf{X} and the decoder maps \mathbf{Y} into $\hat{\mathbf{U}}$. Therefore, we can write

$$I(\mathbf{U}, \hat{\mathbf{U}}) \leq I(\mathbf{X}, \mathbf{Y}) \quad (2.50)$$

$$= h(\mathbf{Y}) - h(\mathbf{Y}|\mathbf{X}) \quad (2.51)$$

$$\leq h(\mathbf{Y}) - h(\mathbf{Y}|\mathbf{X}, e^{j\Phi}) \quad (2.52)$$

$$\leq \sum_{i=1}^N h(Y_i) - h(\mathbf{Z}) \quad (2.53)$$

$$\leq \sum_{i=1}^N \log(\mathbb{E}[|Y_i|^2]) - N \log(2\sigma_z^2) \quad (2.54)$$

$$\leq N \log\left(\frac{\sum_{i=1}^N \mathbb{E}[|Y_i|^2]}{N}\right) - N \log(2\sigma_z^2) \quad (2.55)$$

$$= N \log\left(\frac{KE + 2N\sigma_z^2}{2N\sigma_z^2}\right) \quad (2.56)$$

Making use of the inequality in (2.9), we obtain

$$D_K \geq \frac{1}{\left(1 + \frac{KE}{2N\sigma_z^2}\right)^{2N/K}} \quad (2.57)$$

Letting N goes to infinity gives

$$D_K \geq e^{-E/\sigma_z^2}. \quad (2.58)$$

2.3.2 Upper Bound

Here we consider the same encoding scheme that we have already used in section 2.2.3, which is based on the linear uniform quantizer followed by an orthogonal modulator. As done previously for the coherent reception case, we will compare between two types of decoders: the MAP/ML decoder and the MMSE estimator.

MAP/ML decoder

The MAP decoder is the one which minimizes the probability of error and its corresponding decision rule is given by

$$\hat{m} = \arg \max_{m \in \{1, \dots, M\}} p_m p(\mathbf{y}|\mathbf{s}_m). \quad (2.59)$$

$p(\mathbf{y}|\mathbf{s}_m)$ is obtained by averaging with respect to the phase Φ . We have

$$p(\mathbf{y}|\mathbf{s}_m) = \frac{1}{2\pi} \int_{-\pi}^{\pi} p(\mathbf{y}|\mathbf{s}_m, \phi) d\phi \quad (2.60)$$

$$= \frac{1}{(2\pi\sigma_z^2)^M} e^{-\frac{\|\mathbf{y}\|^2 + \|\mathbf{s}_m\|^2}{2\sigma_z^2}} I_0\left(\frac{|\mathbf{y}^H \mathbf{s}_m|}{\sigma_z^2}\right) \quad (2.61)$$

where we used the integral definition of the modified Bessel function $I_0(z) = \frac{1}{2\pi} \int_{-\pi}^{\pi} e^{z \cos \phi} d\phi$. By considering equal energy signals, the MAP decision rule can be written as

$$\hat{m} = \arg \max_{m \in \{1, \dots, M\}} p_m I_0\left(\frac{|\mathbf{y}^H \mathbf{s}_m|}{\sigma_z^2}\right). \quad (2.62)$$

With the above equation, it is difficult to derive an analytical upper bound on the probability of error and consequently on the distortion. Substituting the MAP by a ML decoder makes the analytical derivations much easier; the resultant decision rule becomes more simple, and is given by

$$\hat{m} = \arg \max_{m \in \{1, \dots, M\}} |\mathbf{y}^H \mathbf{s}_m|^2 \quad (2.63)$$

while in this case, the probability of error can be bounded by (see [53])

$$P_e \leq (M-1)^\rho e^{-\frac{E}{2\sigma_z^2} \left(\frac{\rho}{1+\rho}\right)} \text{ for any } 0 \leq \rho \leq 1. \quad (2.64)$$

Clearly, using the same linear and uniform quantizer as before, the bounds on D_Q and D_e remain unchanged. Therefore, the analytical upper bound on the distortion found in 2.2.3 still holds in the case of noncoherent reception. Moreover, the extension to the case of sequence coding leads to the same upper bounds as in 2.2.7. Note that in the sequel, we will have some numerical results comparing the MAP performance to the analytical upper bound obtained while performing ML decoding.

MMSE Estimator

Now, let us pass to the case where the decoder is an MMSE estimator. The latter is given by

$$\hat{u}(\mathbf{y}) = \frac{\sum_{i=1}^M p_i x_i I_0\left(\frac{\sqrt{E}|y_i|}{\sigma_z^2}\right)}{\sum_{i=1}^M p_i I_0\left(\frac{\sqrt{E}|y_i|}{\sigma_z^2}\right)}. \quad (2.65)$$

Doing similar derivations as for the coherent detection case (section 2.2.5), we obtain

$$D = 1 + \sum_{i=1}^M J_i^2 K_{i,M+1-i} - \sum_{i=1}^M J_i^2 K_{i,i} \quad (2.66)$$

where the integral in the definition of K_{ij} (Eq. (2.36)) is now over \mathbb{C}^M . K_{ij} can be written as a mean with respect to a Gaussian random vector

$$K_{ij} = e^{E/2\sigma_z^2} \mathbb{E}_{\mathbf{Y}} \left[\frac{I_0\left(\frac{\sqrt{E}|y_i|}{\sigma_z}\right) I_0\left(\frac{\sqrt{E}|y_j|}{\sigma_z}\right)}{\sum_{k=1}^M p_k I_0\left(\frac{\sqrt{E}|y_k|}{\sigma_z}\right)} \right] \quad (2.67)$$

where $\mathbf{Y} \sim \mathcal{N}_M^c(0, 2\sigma_z^2 \mathbf{I}_M)$. Thus, the distortion is given by

$$D = 1 - e^{-E/2\sigma_z^2} \sum_{i=1}^M J_i^2 \mathbb{E}_{\mathbf{Y}} \left[\frac{I_0\left(\frac{\sqrt{E}|y_i|}{\sigma_z}\right) (I_0\left(\frac{\sqrt{E}|y_i|}{\sigma_z}\right) - I_0\left(\frac{\sqrt{E}|y_{M+1-i}|}{\sigma_z}\right))}{\sum_{k=1}^M p_k I_0\left(\frac{\sqrt{E}|y_k|}{\sigma_z}\right)} \right]. \quad (2.68)$$

We currently do not have asymptotic expressions of (2.68) as $E \rightarrow \infty$; we will plot in the sequel numerical results representing the system performance using an MMSE estimator, and make performance comparisons between the use of an MMSE estimator and that of a MAP decoder.

2.3.3 Noisy Observations

Until now, we have assumed that the observations collected by the sensor were noiseless. Practically, the sensor has not perfect sensing accuracy and consequently may induce noise to the observations. Therefore, we consider in this section a zero mean Gaussian observation noise of variance σ_w^2 contaminating the source before being observed by the sensor. The corresponding scheme is depicted in Fig. 2.6. The observation noise is denoted by W and the encoder input by $U' = U + W$.

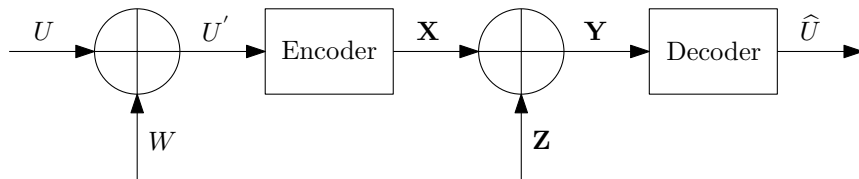


Figure 2.6: The model scheme with noisy observations.

Lower Bound

Let \widehat{U}' denote the MMSE estimator of U given U' , i.e.

$$\widehat{U}' = \mathbb{E}[U|U'] = \frac{1}{1 + \sigma_w^2} U'. \quad (2.69)$$

By introducing \widehat{U}' , the distortion can be written as

$$D = \mathbb{E}[(U - \widehat{U})^2] \quad (2.70)$$

$$= \mathbb{E}[(U - \widehat{U}')^2] + \mathbb{E}[(\widehat{U}' - \widehat{U})^2] + 2\mathbb{E}[(U - \widehat{U}')(\widehat{U}' - \widehat{U})] \quad (2.71)$$

$$= \frac{\sigma_w^2}{1 + \sigma_w^2} + \mathbb{E}[(\widehat{U}' - \widehat{U})^2] \quad (2.72)$$

where we have used the fact that $\mathbb{E}[(U - \widehat{U}')^2] = \frac{\sigma_w^2}{1 + \sigma_w^2}$ and (see the appendix in [54])

$$\mathbb{E}[(U - \widehat{U}')(\widehat{U}' - \widehat{U})] = 0. \quad (2.73)$$

Therefore,

$$\mathbb{E}[(\widehat{U} - \widehat{U}')^2] = D - \frac{\sigma_w^2}{1 + \sigma_w^2}. \quad (2.74)$$

According to the classical information theory, we have

$$I(\mathbf{X}; \mathbf{Y}) \geq I(U'; \widehat{U}) \quad (2.75)$$

$$= I(\widehat{U}'; \widehat{U}) \quad (2.76)$$

$$= h(\widehat{U}') - h(\widehat{U}'|\widehat{U}) \quad (2.77)$$

$$= h(\widehat{U}') - h(\widehat{U}' - \widehat{U}|\widehat{U}) \quad (2.78)$$

$$\geq h(\widehat{U}') - h(\widehat{U}' - \widehat{U}) \quad (2.79)$$

$$\geq \frac{1}{2} \log \frac{1}{(1 + \sigma_w^2)(D - \frac{\sigma_w^2}{1 + \sigma_w^2})}. \quad (2.80)$$

Recalling the inequality in (2.56), we obtain

$$D \geq \frac{e^{-E/\sigma_z^2}}{1 + \sigma_w^2} + \frac{\sigma_w^2}{1 + \sigma_w^2} \quad \text{as } N \longrightarrow \infty. \quad (2.81)$$

Upper Bound

Let us now use the same encoding/decoding schemes that we have been using for the case of noiseless observations. After receiving U' , the sensor encodes the normalized energy random variable $V = \frac{1}{\sqrt{1+\sigma_w^2}}U'$ and sends it over the channel. At the output, we calculate $\hat{U} = \frac{1}{\sqrt{1+\sigma_w^2}}\hat{V}$, where \hat{V} is the estimate of V . The resultant distortion could be written as

$$D = \mathbb{E}[(U - \hat{U}')^2] + \mathbb{E}[(\hat{U}' - \hat{U})^2] \quad (2.82)$$

$$= \frac{\sigma_w^2}{1 + \sigma_w^2} + \frac{1}{1 + \sigma_w^2} \mathbb{E}[(V - \hat{V})^2]. \quad (2.83)$$

As shown in (2.83), any coding scheme that achieves a distortion $D_v \triangleq \mathbb{E}[(V - \hat{V})^2]$ will achieve a distortion $D = \frac{\sigma_w^2}{1 + \sigma_w^2} + \frac{1}{1 + \sigma_w^2} D_v$ with respect to U .

2.3.4 Numerical Results

In all the numerical results, the distortion is plotted versus the energy, and the variance of the channel noise is taken equal to one. Fig. 2.7 shows the inefficiency of the linear encoder compared with the theoretical upper and lower bounds. Note that the curve representing the upper bound is obtained like the following: for each value of E , we find b_{opt} , then we calculate the upper bound over D using the terms in (2.31), (2.32) and (2.105). Also the model presented in Fig. 2.2 is simulated for different number of quantization bits and the simulations are compared to the other curves: it can be seen how the distortion decreases when the energy grows up until arriving to a certain constant or 'residual distortion' that represents the quantization distortion given a fixed number of quantization bits; therefore, beyond a certain amount of energy, the number of quantization bits should be increased in order to decrease the distortion. We can also notice that the linear encoder outperforms the coding scheme presented in Fig. 2.2 in the low energy regime, a fact that reflects the optimality of the uncoded transmission when $E \rightarrow 0$ as shown in section 2.2.2. Fig. 2.8 and Fig. 2.9 show that the different types of encoders and decoders studied in section 2.2.3 and 2.2.5 have comparable performance; therefore, using a MAP decoder instead of an MMSE estimator has practically no effects on the MSE distortion especially when $b > 2$. The analytical upper bound on the distortion D_K (eq.(2.48))

is plotted in Fig. 2.10 for several values of K . This plot shows the improvement that can be made to the upper bound, and consequently to the performance of the system when we code sequences; it shows that even with small length sequences, significant gain can be obtained. Plot 2.11 shows the performance of the MAP-based scheme when noncoherent reception is performed at the receiver. In Fig. 2.12, it is shown that also in the case of noncoherent reception, the MAP decoder and the MMSE receiver have practically the same performance. Fig. 2.13 and 2.14 compare the coherent reception case to the noncoherent one; they show a very small gap in the performance which amounts to say that there is no big loss if we receive noncoherently the transmitted signals.

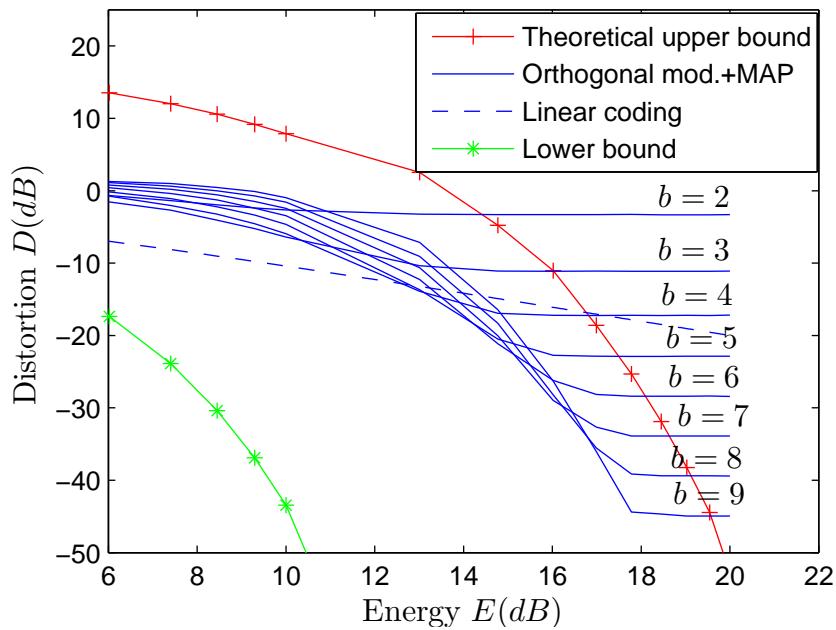


Figure 2.7: Performances of the MAP-based scheme compared to the linear encoder and the theoretical lower bound.

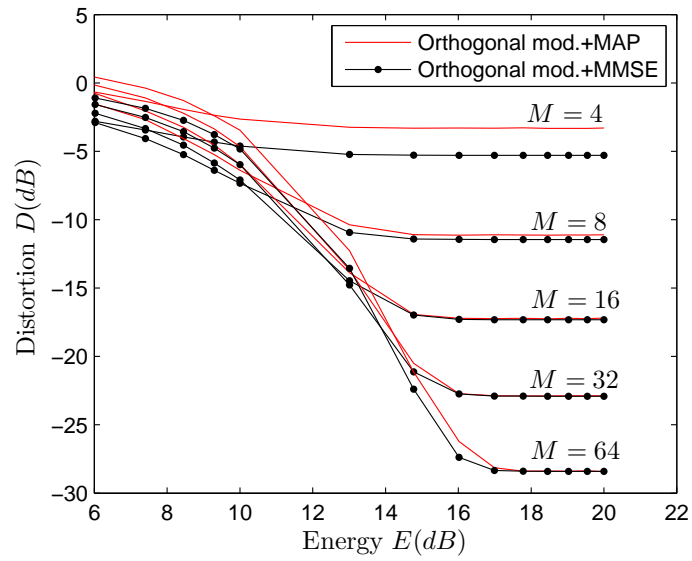


Figure 2.8: Comparison between the MAP and the MMSE based scheme.

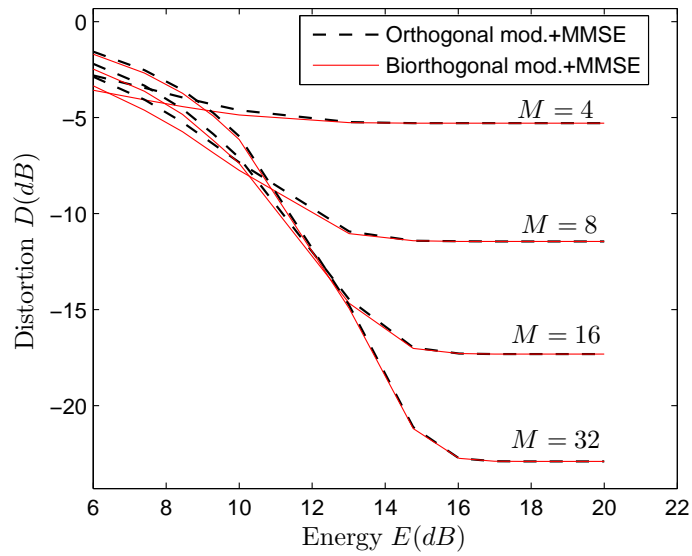


Figure 2.9: Comparison between the orthogonal and the biorthogonal modulation performances combined with the MMSE estimator.

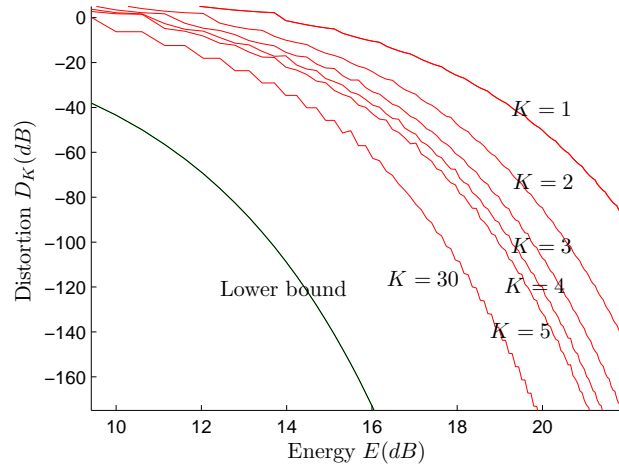


Figure 2.10: The lower bound compared to the upper bound corresponding to sequence coding of length K .

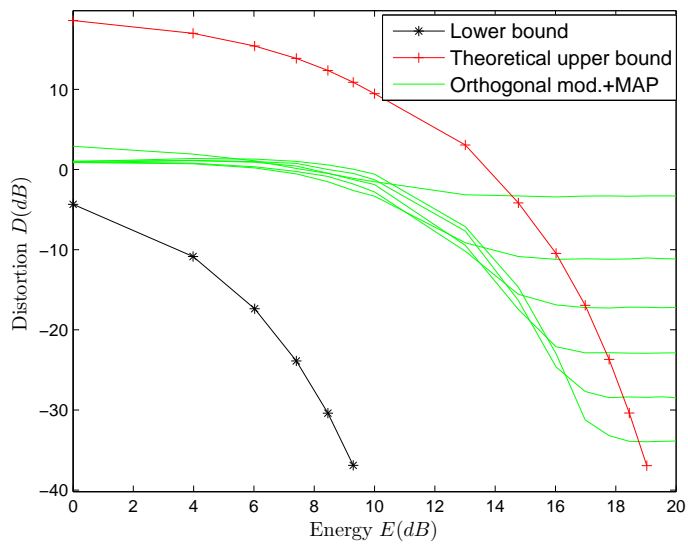


Figure 2.11: Performances of the MAP-based scheme compared to the theoretical lower and upper bound for noncoherent reception.

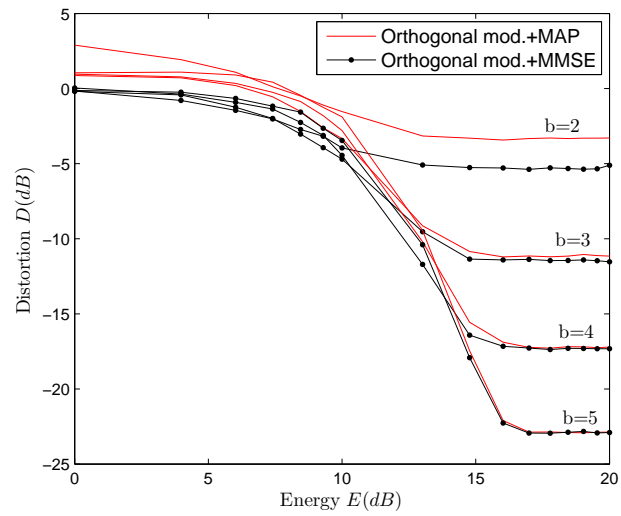


Figure 2.12: Comparison between the MAP and the MMSE-based schemes for the noncoherent reception case.

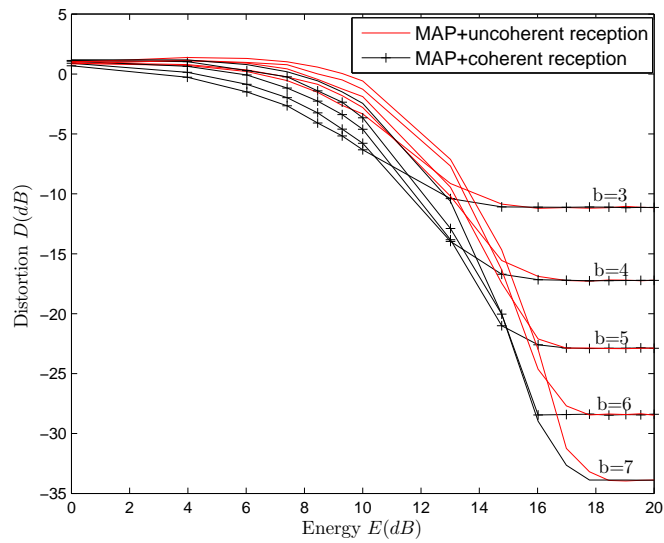


Figure 2.13: Comparison of the performances of the MAP-based scheme in both coherent and noncoherent cases.

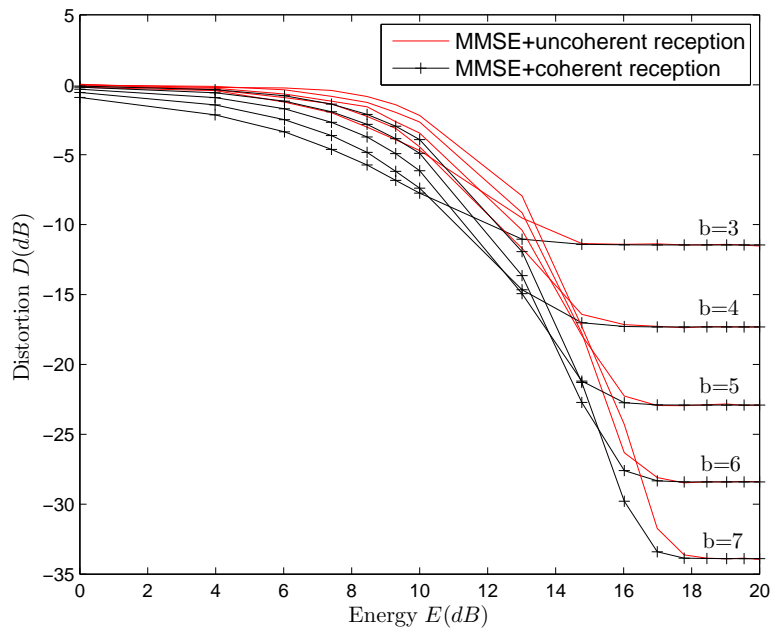


Figure 2.14: Comparison of the performances of the MMSE-based scheme in both coherent and noncoherent cases.

2.4 Multiple sensors

In this section, we consider the case of multiple sensors observing independent sources and sending their observations through a Gaussian multiple access channel to a single receiver. The sources are supposed to be varying very slowly in time and therefore have a low bandwidth. Each sensor m has the possibility of mapping its observation U_m into an infinite dimensional channel. This model can be simply viewed as a generalisation of the one depicted in Fig. 2.1 to the case of multiple sensors. It is presented in Fig. 2.15. The receiver decodes each source U_m into \hat{U}_m . The calculated distortions are defined as

$$D_m = \mathbb{E}[(U_m - \hat{U}_m)^2] \quad \text{for } m = 1, \dots, M \quad (2.84)$$

and the transmitted energy assigned to the sensor m is E_m , $m = 1, \dots, M$.

2.4.1 Lower Bound for the Multiple Sensor Case

As in the previous derivations of the lower bounds, we assume that each sequence $\mathbf{U}_m = (U_{m,1}, \dots, U_{m,K})$ is mapped into a sequence $\mathbf{X}_m = (X_{m,1}, \dots, X_{m,N})$ of length N . The shorthand notation \mathbf{A}_S represents the set of random vectors $\{\mathbf{A}_i, i \in S\}$ where S is a given set. According to the classical information theory, a lower bound on D_m can be found like the following: $\forall S \subseteq \{1, \dots, M\}$, we can write

$$I(\mathbf{U}_S; \hat{\mathbf{U}}_S) = h(\mathbf{U}_S) - h(\mathbf{U}_S | \hat{\mathbf{U}}_S) \quad (2.85)$$

$$\geq h(\mathbf{U}_S) - \sum_{m \in S} h(\mathbf{U}_m | \hat{\mathbf{U}}_m) \quad (2.86)$$

$$\geq h(\mathbf{U}_S) - \sum_{m \in S} h(\mathbf{U}_m - \hat{\mathbf{U}}_m) \quad (2.87)$$

$$\geq h(\mathbf{U}_S) - \sum_{m \in S} \sum_{i=1}^K h(U_{m,i} - \hat{U}_{m,i}) \quad (2.88)$$

$$\begin{aligned} &\geq \frac{|S|K}{2} \log(2\pi e) - \sum_{m \in S} \sum_{i=1}^K \frac{1}{2} \log(2\pi e) \mathbb{E}[(U_{m,i} - \hat{U}_{m,i})^2] \\ &= -\frac{K}{2} \sum_{m \in S} \frac{1}{K} \sum_{i=1}^K \mathbb{E}[(U_{m,i} - \hat{U}_{m,i})^2] \end{aligned} \quad (2.89)$$

$$\geq -\frac{K}{2} \sum_{m \in S} \log D_m = \frac{K}{2} \log \left(\frac{1}{\prod_{m \in S} D_m} \right) \quad (2.90)$$

Due to the data processing inequality, we can also write

$$I(\mathbf{U}_S; \widehat{\mathbf{U}}_S) \leq I(\mathbf{X}_S; \mathbf{Y}) \quad (2.91)$$

$$\stackrel{(a)}{\leq} I(\mathbf{X}_S; \mathbf{Y} | \mathbf{X}_{S^c}) \quad (2.92)$$

$$\leq h(\mathbf{Y} | \mathbf{X}_{S^c}) - h(\mathbf{Z}) \quad (2.93)$$

$$\leq h(\mathbf{Y} - \sum_{m \in S^c} \mathbf{X}_m) - h(\mathbf{Z}) \quad (2.94)$$

$$= h(\sum_{m \in S} \mathbf{X}_m + \mathbf{Z}) - h(\mathbf{Z}) \quad (2.95)$$

$$\leq \sum_{i=1}^N h(\sum_{m \in S} X_{m,i} + Z_i) - h(\mathbf{Z}) \quad (2.96)$$

$$\leq \sum_{i=1}^N \frac{1}{2} \log 2\pi e \left(\sigma_z^2 + \sum_{m \in S} \mathbb{E}[X_{m,i}^2] \right) - \frac{N}{2} \log(2\pi e \sigma_z^2)$$

$$\leq \frac{N}{2} \log \left(\sigma_z^2 + \sum_{m \in S} \frac{1}{N} \sum_{i=1}^N \mathbb{E}[X_{m,i}^2] \right) - \frac{N}{2} \log(\sigma_z^2) \quad (2.97)$$

$$= \frac{N}{2} \log \left(1 + \sum_{m \in S} \frac{K E_m}{N \sigma_z^2} \right) \quad (2.98)$$

where (a) follows from the fact that \mathbf{X}_S and \mathbf{X}_{S^c} are independent. Combining (2.90) and (2.98), we obtain

$$\prod_{m \in S} D_m \geq \left(1 + \sum_{m \in S} \frac{K E_m}{N \sigma_z^2} \right)^{-N/K} \quad \forall S \subseteq \{1, \dots, M\}. \quad (2.99)$$

When the source-channel rate r goes to zero, the set of inequalities in (2.99) becomes

$$D_m \geq e^{-E_m/\sigma_z^2} \quad m = 1, \dots, M \quad (2.100)$$

which represents a set of lower bounds on D_m .

2.4.2 Upper Bound for the Multiple Sensor Case

The coding scheme that can be used in the case of multiple sensors is the same one described in section 2.2: therefore, in each sensor, the observation will be quantized, modulated and then sent through the multiple access

channel. This latter can be transformed into M non-interfering channels by using a suitable MAC protocol like TDMA or FDMA. Doing so, the model can be viewed as M cascaded point-to-point communication schemes where the receivers can perform MAP decoding or MMSE estimation. Therefore, all results on the upper bound obtained in the previous sections are still valid in the case of multiple sensors. Particularly, the distortions that can be achieved while a MAP decoder is implemented at the receiver can be upper bounded by (for high SNRs)

$$D_m \lesssim e^{-E_m/(6\sigma_z^2)} \quad m = 1, \dots, M. \quad (2.101)$$

Notice that when a TDMA protocol is used to avoid the collisions between the transmitted messages, the synchronization of the sensors might be necessary for some applications and not for others: as an example, if the transmission time is very small compared to the channel bandwidth, each sensor (assuming the number of sensor is not too large) can choose randomly its own transmission starting-time without synchronizing with the others, the probability of collision being too small in this case.

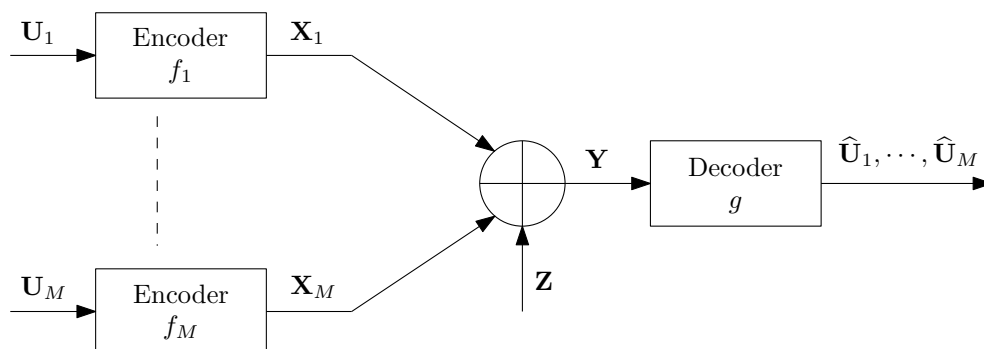


Figure 2.15: The model scheme of multiple sensors observing independent sources.

2.5 Conclusion

As a conclusion, we have derived theoretical lower and upper bounds on the distortion for very-low bandwidth sources. The proposed source-channel coding schemes outperform the linear coding performance and lead to an

exponentially decreasing behaviour of the distortion in E . Also, we have shown that the difference in the performance between a MAP decoder and an MMSE estimator is negligible. We proved that the gap between the lower and the upper bound can be significantly reduced by coding relatively short sequences. We showed that our digital coding scheme based on a linear uniform quantizer followed by an orthogonal modulator and combined with an MMSE or MAP decoder gave practically the same performance with models involving noncoherent detection, noisy observations and multiple sensors.

APPENDIX

2.A Probability of Error

By analogy to what has been done in [55], we obtain for the general case of unequal *a priori* probabilities that

$$P_{e_i} \leq p_i^{-\frac{\rho}{\rho+1}} \int_{\mathbf{Y}} p(\mathbf{y}|x_i)^{\frac{1}{1+\rho}} \left[\sum_{j \neq i} (p_j p(\mathbf{y}|x_j))^{\frac{1}{1+\rho}} \right]^{\rho} d\mathbf{y}, \quad (2.102)$$

ρ being any positive number and P_{e_i} representing the probability of error given that x_i has been sent. Following the same way of derivation as in [53, p. 65], (2.102) becomes

$$P_{e_i} \leq p_i^{-\frac{\rho}{\rho+1}} e^{-\frac{E}{2\sigma_z^2} \left(\frac{\rho}{1+\rho}\right)} \left(\sum_{j \neq i} p_j^{\frac{1}{1+\rho}} \right)^{\rho} \quad (2.103)$$

provided that $0 \leq \rho \leq 1$. Now Let V be a discrete random variable that takes the value $1/p_i$ with probability p_i for $i = 1, \dots, M$. Using Jensen inequality, we have that

$$E[(V)^{\frac{\rho}{\rho+1}}] \leq (E[V])^{\frac{\rho}{\rho+1}} = M^{\frac{\rho}{\rho+1}} \quad (2.104)$$

for any $0 \leq \rho \leq 1$. Thus,

$$P_e \leq e^{-\frac{E}{2\sigma_z^2} \left(\frac{\rho}{1+\rho}\right)} \left(\sum_{i=1}^M p_i^{\frac{1}{1+\rho}} \right)^{\rho+1} \quad (2.105)$$

$$= e^{-\frac{E}{2\sigma_z^2} \left(\frac{\rho}{1+\rho}\right)} \left(\sum_{i=1}^M p_i \left(\frac{1}{p_i} \right)^{\frac{\rho}{1+\rho}} \right)^{\rho+1} \quad (2.106)$$

$$\leq M^{\rho} e^{-\frac{E}{2\sigma_z^2} \left(\frac{\rho}{1+\rho}\right)} \quad (2.107)$$

2.B Lower Bound on D_e

let B denote the event 'An error decision has been made'. Therefore, we can write,

$$\begin{aligned} D_e &= \mathbb{E}[(U - \widehat{X})^2 | B'] \\ &= \mathbb{E}[(U - X)^2] + \mathbb{E}[(X - \widehat{X})^2 | B'] + 2\mathbb{E}[(U - X)(X - \widehat{X}) | B'] \end{aligned} \quad (2.108)$$

$$\stackrel{(a)}{\geq} \mathbb{E}[(U - X)^2] + \mathbb{E}[(X - \widehat{X})^2 | B'] - 2\sqrt{\mathbb{E}[(U - X)^2]\mathbb{E}[(X - \widehat{X})^2 | B']} \quad (2.109)$$

$$= D_Q + (\sqrt{\mathbb{E}[(X - \widehat{X})^2 | B']} - 2\sqrt{D_Q})\sqrt{\mathbb{E}[(X - \widehat{X})^2 | B']} \quad (2.110)$$

Where (a) follows from applying Cauchy-Schwarz inequality for the last term in (2.108). A symmetric quantizer has the following properties (see Eq. (2.26)): for $j = 1, \dots, M/2$

$$x_j = -x_{M+1-j}; \quad (2.111)$$

$$P_{i,j} = P_{i,M+1-j} \quad i = 1, \dots, M \quad \text{and } j \neq \{i, M+1-i\}. \quad (2.112)$$

Therefore, $\mathbb{E}[(X - \widehat{X})^2 | B']$ can be bounded like the following

$$\mathbb{E}[(X - \widehat{X})^2 | B'] = \mathbb{E}[X^2] + \mathbb{E}[\widehat{X}^2 | B'] - 2\mathbb{E}[X\widehat{X} | B'] \quad (2.113)$$

$$= \mathbb{E}[X^2] + \mathbb{E}[\widehat{X}^2 | B'] - 2 \sum_{\substack{i,j=1 \\ j \neq i}}^M p_i P_{ij} x_i x_j \quad (2.114)$$

$$= \mathbb{E}[X^2] + \mathbb{E}[\widehat{X}^2 | B'] + 2 \sum_{i=1}^M p_i P_{i,M+1-i} x_i^2 \quad (2.115)$$

$$> \mathbb{E}[X^2]. \quad (2.116)$$

In order to bound $\mathbb{E}[X^2]$, we can write

$$D_Q = \mathbb{E}[(U - X)^2] = \mathbb{E}[U^2] + \mathbb{E}[X^2] - 2\mathbb{E}[UX] \quad (2.117)$$

$$= \mathbb{E}[U^2] - \mathbb{E}[X^2] - 2\mathbb{E}[X(U - X)]. \quad (2.118)$$

Using Cauchy-Schwarz inequality, (2.118) gives

$$D_Q \geq \mathbb{E}[U^2] - \mathbb{E}[X^2] - 2\sqrt{\mathbb{E}[X^2]\mathbb{E}[(U - X)^2]}. \quad (2.119)$$

Resolving this second order inequality (in $\sqrt{\mathbb{E}[X^2]}$), we obtain

$$\mathbb{E}[X^2] \geq (\sqrt{\mathbb{E}[U^2]} - \sqrt{D_Q})^2 \quad \text{if } \sqrt{\mathbb{E}[U^2]} - \sqrt{D_Q} \geq 0. \quad (2.120)$$

Having a high SNR, implies that $D_Q \ll 1$; combining the inequalities (2.110), (2.116) and (2.120), we conclude that $D_e \gtrsim 1$ and this completes the proof.

2.C Symmetric Encoder Characteristic

Let $I_j =]a_j; b_j[$; due to the symmetry of the encoder, we have that $I_{M+1-j} =]-b_j; -a_j[$. Therefore, for $j = 1, \dots, M/2$ we can write

$$J_j = \int_{a_j}^{b_j} up(u) du = -\frac{1}{\sqrt{2\pi}} \exp\left(-\frac{u^2}{2}\right) \Big|_{a_j}^{b_j} \quad (2.121)$$

$$= -\frac{1}{\sqrt{2\pi}} \left[\exp\left(-\frac{b_j^2}{2}\right) - \exp\left(-\frac{a_j^2}{2}\right) \right] \quad (2.122)$$

and

$$J_{M+1-j} = \int_{-b_j}^{-a_j} up(u) du = -\frac{1}{\sqrt{2\pi}} \exp\left(-\frac{u^2}{2}\right) \Big|_{-b_j}^{-a_j} \quad (2.123)$$

$$= -\frac{1}{\sqrt{2\pi}} \left[\exp\left(-\frac{a_j^2}{2}\right) - \exp\left(-\frac{b_j^2}{2}\right) \right] = -J_j. \quad (2.124)$$

Now, in order to see the equality between K_{ij} and $K_{i,M+1-j}$, we develop $K_{i,M+1-j}$ like the following

$$K_{i,M+1-j} = \int_{-\infty}^{\infty} \frac{p(\mathbf{y}|\mathbf{s}_i)p(\mathbf{y}|\mathbf{s}_{M+1-j})}{\sum_{k=1}^M p_k p(\mathbf{y}|\mathbf{s}_k)} d\mathbf{y} \quad (2.125)$$

$$\stackrel{(a)}{=} \int_{-\infty}^{\infty} \frac{\frac{1}{(2\pi\sigma_z^2)^{M/4}} \exp\left(\frac{-1}{2\sigma_z^2} \|\mathbf{y} - \mathbf{s}_i\|^2\right) \exp\left(\frac{-1}{2\sigma_z^2} \|\mathbf{y} + \mathbf{s}_j\|^2\right)}{\sum_{k=1}^{M/2} p_k \left[\exp\left(\frac{-1}{2\sigma_z^2} \|\mathbf{y} - \mathbf{s}_k\|^2\right) + \exp\left(\frac{-1}{2\sigma_z^2} \|\mathbf{y} + \mathbf{s}_k\|^2\right) \right]} d\mathbf{y} \quad (2.126)$$

$$= \int_{-\infty}^{\infty} \frac{\frac{1}{(2\pi\sigma_z^2)^{M/4}} \exp\left(\frac{-1}{2\sigma_z^2} \|\mathbf{y} - \mathbf{s}_i\|^2\right) \exp\left(\frac{-\sqrt{E}}{\sigma_z^2} y_j\right)}{\sum_{k=1}^{M/2} p_k \left[\exp\left(\frac{\sqrt{E}}{\sigma_z^2} y_k\right) + \exp\left(\frac{-\sqrt{E}}{\sigma_z^2} y_k\right) \right]} d\mathbf{y} \quad (2.127)$$

$$\stackrel{(b)}{=} \int_{-\infty}^{\infty} \frac{\frac{1}{(2\pi\sigma_z^2)^{M/4}} \exp\left(\frac{-1}{2\sigma_z^2} \|\mathbf{y} - \mathbf{s}_i\|^2\right) \exp\left(\frac{\sqrt{E}}{\sigma_z^2} y_j\right)}{\sum_{k=1}^{M/2} p_k \left[\exp\left(\frac{\sqrt{E}}{\sigma_z^2} y_k\right) + \exp\left(\frac{-\sqrt{E}}{\sigma_z^2} y_k\right) \right]} d\mathbf{y} \quad (2.128)$$

$$= K_{i,j}. \quad (2.129)$$

where (a) follows from the fact that $\mathbf{s}_{M+1-j} = -\mathbf{s}_j$ for $j = 1, \dots, M/2$ and (b) from the change of variable $y_j \rightarrow -y_j$.

Chapter 3

Correlated Discrete Sources Over GMACs with Phase Shifts

In this chapter, we address the problem of separate encoding of correlated discrete sources observed by sensor nodes that send their encoded information through a Gaussian multiple access channel (GMAC) with phase shifts. We suppose that the phases are perfectly known at the receiver and unknown to the transmitters. For discrete sources with finite-cardinality alphabets, we prove that the separation theorem holds for both random ergodic and arbitrary non-random models for the phase shifts, and consequently, the strategy of combining Slepian-Wolf coding to capacity achieving channel encoders is optimal for both.

3.1 Introduction

In many sensor network applications, the observations collected by the sensor nodes are spatially correlated, for instance in scenarios where distributed sensing of a random field is performed (e.g. geological exploration, environmental sensing, electromagnetic sensing, etc.). With low-cost radio-equipped sensors, the observations are further encoded and sent through a noisy channel to a collector node where the information is extracted and processed. The main question that arises is how to efficiently encode the data at each node and how to benefit from the correlation between the observed sources. Shannon proved in [33] that, in a point-to-point communication scenario, an optimal way to send a random source through a noisy channel is to compress the source at a rate slightly greater than its entropy, in bits per source letter, and then to encode it at a rate slightly less than the capacity of the channel, in bits per channel use, prior to sending it across the channel. This coding strategy, known as the source-channel coding theorem or the separation theorem, is very useful because it permits one to split the encoder into two separate entities, the first being the source coding block and the second the channel encoder. Unfortunately, this strategy does not lead to optimal system performances in general network scenarios. An example of the latter is considered in [32], where the authors provide bounds on the capacity region for the MAC with arbitrarily correlated sources; they provide sufficient conditions for the correlated sources to be sent over the channel with an arbitrarily small probability of error. Although the resultant rate region contains the one achieved by separation between the source and the channel encoders, it is shown in [56] that it is not the capacity region for reliable transmission. All these results with others in [46] show the sub-optimality of the separation-based coding strategy and open the door toward cooperative coding strategies that try to map the correlation between the sources into correlation between the transmitted signals. One recent example of this is the scheme described in [57].

The coding problem that we consider here is a variation on the same theme. We consider M sensor nodes deployed in a certain area where each of them senses a single spatial dimension of the source and sends a representation of its measurement through a GMAC corrupted by phase shifts. In contrast to the work of El Gamal[58], we assume that no node has side information with respect to its own channel phase shift, and as a result cannot align its phase at the receiver in order to benefit from some generalized form of coherent combining which exploits the source correlation structure. As a side note, any wireless sensor network problem using a real-

valued GMAC implicitly assumes this form of synchronization. In removing the assumption on phase synchronization we focus on the most pertinent channel model in a pragmatic sense. This is especially true in wireless sensor network applications where we often deal with low-cost components, at least when it comes to the links between the sensors and the collector node. Even in relatively high-cost cellular base stations, feedback-based combining schemes are very difficult (and costly) to achieve even for a centralized antenna array, let alone for distributed spatial processing across several base stations. Furthermore, it is conceivable for future low-end sensor networks that the sensors may not even be equipped with radio receivers in order to limit power consumption which is often dominated by the receiver electronics. This, of course, would rule out the possibility of any form of closed-loop synchronisation and necessarily result in phase differences at the receiver. In our problem formulation, we assume that the source is discrete and of finite cardinality per dimension and the goal is to reconstruct the vector source as reliably as possible at the collector node. What remains is to define a set of necessary and sufficient conditions under which the source can be sent and reconstructed with an arbitrarily small probability of decoding error. We consider two cases for phases variation: ergodic random phase sequences and deterministic but arbitrarily-varying phase sequences. By deriving a converse in both cases, we prove that the separation theorem holds for any number M of sensor nodes. Hence, the set of the achievable rates is the intersection of two rate-regions, the first being the Slepian-Wolf rate region [59] and the second, being the capacity region of the GMAC [60]. We discuss several important points concerning the coding theorems stated in this chapter and prove moreover that the separation still holds even when inter-sensor communications are considered under a sum-energy constraint. The latter idea amounts to saying that under a sum-energy constraint, any kind of information exchange between the sensors is useless. Another closely related work is that of Barros and Servetto [61, 31]; in their model the up-link channel is a set parallel non-interfering channels instead of a MAC. They proved that the separation is also optimal in that case and conclude that in the absence of interference, there is nothing to lose by compressing the source dimensions to their most efficient representation (Slepian-Wolf coding) and separately adding capacity-attaining channel codes.

3.2 Model

The system model is depicted in Fig. 3.1. We consider M discrete correlated sources U_1, \dots, U_M of respectively finite alphabets $\mathcal{U}_1, \dots, \mathcal{U}_M$ following the joint probability distribution $p(u_1, \dots, u_M)$. Source vectors $\mathbf{U}_1, \dots, \mathbf{U}_M$ of dimension K are generated by collecting K i.i.d samples of the spatially correlated sources U_1, \dots, U_M respectively. Before being transmitted, these source vectors are encoded separately by M encoders f_1, \dots, f_M . The encoder f_m is a function that maps \mathbf{U}_m onto a sequence of N channel symbols $\mathbf{X}_m \triangleq \{X_{m,n}; n = 1, \dots, N\}$, each of which taken from a finite alphabet \mathcal{X}_m . Thus

$$\begin{aligned} f_m : \mathcal{U}_m^K &\longrightarrow \mathcal{X}_m^N \\ \mathbf{u}_m \in \mathcal{U}_m^K &\longrightarrow \mathbf{x}_m = f_m(\mathbf{u}_m) \in \mathcal{X}_m^N \end{aligned}$$

Let $\mathbf{Z} = \{Z_i; i = 1, \dots, N\}$ denote an i.i.d. sequence drawn according to a Gaussian distribution representing the channel noise where $Z_i \sim \mathcal{N}_C(0, N_0)$, and $\Phi_m = \{\Phi_{m,i}; i = 1, \dots, N\}$ denote the set of random phases induced by the channel and associated to the encoder f_m . Let $\Phi \triangleq \{\Phi_m; m = 1, \dots, M\}$ be perfectly known to the decoder. The received signal is $\mathbf{Y} \triangleq \{Y_i; i = 1, \dots, N\}$ which belongs to the infinite alphabet \mathcal{Y}^N , and Y_i can be written as

$$Y_i = \sum_{m=1}^M X_{m,i} e^{j\Phi_{m,i}} + Z_i. \quad (3.1)$$

We consider the following power constraint

$$\frac{1}{N} \sum_{i=1}^N \mathbb{E} [|X_{m,i}|^2] \leq E_m \quad (3.2)$$

for $m = 1, \dots, M$, where E_m represents the mean energy allowed per transmission for sensor m . For the channel phase sequences Φ_m , we shall consider the following different cases:

1. Φ_m are random, perfectly known to the receiver and unknown to the transmitters, extracted from a jointly stationary and ergodic process $\{\Phi_{1,i}, \dots, \Phi_{M,i}\}$. Furthermore, we assume that $\Phi_{m,i}$ (the i -th marginals of the process) are individually uniformly distributed over $[-\pi, \pi]$ and that the i -th marginal distribution of the phase difference $\Delta\Phi_{m,m',i} \triangleq \Phi_{m,i} - \Phi_{m',i}$ is also uniformly distributed over $[-\pi, \pi]$.

2. Φ_m are *arbitrary* sequences, denoted by ϕ_m since they are non-random. The transmitters have no knowledge of the phase sequences.
3. Φ_m are *arbitrary and constant* sequences, that is, $\Phi_{m,i} = \phi_m$ for all $i = 1, \dots, N$, where ϕ_m is an arbitrary value in $[-\pi, \pi]$. In this case, the phases are constant for the whole duration of transmission but the transmitters have no knowledge about their values.

In section 3.3, one coding theorem will be dedicated to the first phase sequences case, and another one for the last two cases, their corresponding proof being quite similar. After receiving \mathbf{Y} , the decoder generates an estimate $\hat{\mathbf{U}}_m$ on each source \mathbf{U}_m given the full knowledge on Φ . Thus, we have

$$g : \mathcal{Y}^N \times [-\pi; \pi]^{NM} \longrightarrow \mathcal{U}_1^K \times \dots \times \mathcal{U}_M^K \quad (3.3)$$

$$(\mathbf{y}, \phi) \longrightarrow g(\mathbf{y}, \phi) = (\hat{\mathbf{U}}_1, \dots, \hat{\mathbf{U}}_M). \quad (3.4)$$

Given a code, i.e., a mapping $f_m : \mathbf{U}_m \mapsto \mathbf{X}_m$ ($m = 1, \dots, M$), and $g : (\mathbf{Y}, \Phi) \mapsto (\hat{\mathbf{U}}_1, \dots, \hat{\mathbf{U}}_M)$, we define the error probability as

$$P^K(e) = \Pr \left((\mathbf{U}_1, \dots, \mathbf{U}_M) \neq (\hat{\mathbf{U}}_1, \dots, \hat{\mathbf{U}}_M) \right).$$

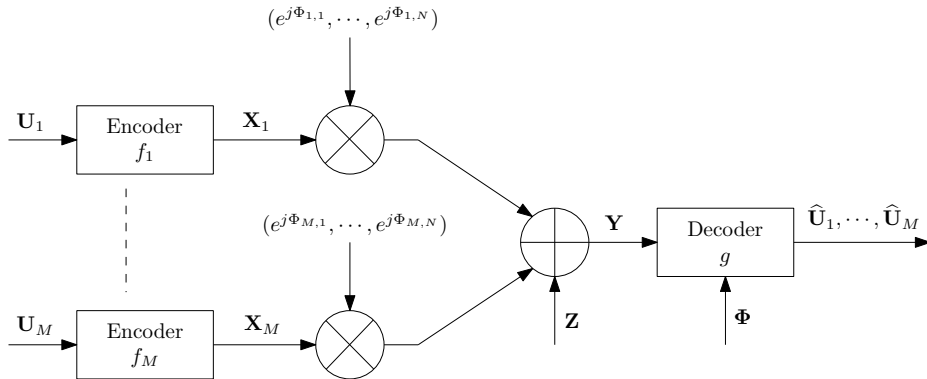


Figure 3.1: Correlated sources over GMAC with phase shifts perfectly known at the receiver

3.3 Coding Theorems for Correlated Sources Over GMAC with Phase Shifts

3.3.1 Ergodic Phase Sequences

For the ergodic phase sequences, we have the following coding theorem:

Theorem 1. *M discrete correlated sources U_1, \dots, U_M of finite alphabets drawn according to $p(u_1, \dots, u_M)$ can be transmitted with an arbitrarily small probability of error over a GMAC with ergodic phases perfectly known at the receiver and with source-channel rate $r \triangleq K/N$, if and only if*

$$H(U_S|U_{S^c}) \leq \frac{N}{K} \log \left(1 + \sum_{m \in S} \frac{E_m}{N_0} \right), \forall S \subseteq \{1, 2, \dots, M\}, \quad (3.5)$$

where the shorthand notation A_S represents the set of random variables $\{A_i, i \in S\}$.

Proof. The proof of this theorem can be divided in two parts: the direct part and the converse.

For the direct part, we have to prove that if the conditions in (3.5) are satisfied, the sources can be transmitted with an arbitrarily small probability of error. In fact, it is clear that, when the bounds on the joint entropy of the sources are satisfied, a simple separated approach that makes use of Slepian-Wolf coding and standard Gaussian superposition coding allows the transmission and the reconstruction of the sources at the receiver with a vanishing probability of error.

The converse part of the proof can be found in Appendix 3.A. It is shown that if the sources are transmitted with an arbitrarily small probability of error, then they must verify the joint entropy conditions in (3.5). This theorem shows that in the case of ergodic phases, a separation-based scheme is optimal. In other words, compressing the sources to their most efficient representations by performing Slepian-Wolf coding, and separately adding capacity-achieving channel encoders is an optimal coding scheme. Moreover, it shows that coding cooperation between the transmitters does not buy anything. \square

3.3.2 Arbitrary Phase Sequences

Assuming that the phase sequences are not random, unknown at the transmitters, but perfectly known at the receiver, we have the following theorem:

Theorem 2. *For the arbitrary phase sequences (or arbitrary and constant phases), M discrete correlated sources U_1, \dots, U_M of finite alphabets can be transmitted reliably over a GMAC with a given source-channel rate r if, and only if their joint entropies satisfy the inequalities in Eq. (3.5).*

Proof for arbitrary phase sequences. The direct part of the proof is the same as for Theorem 1. The converse part can be found in Appendix 3.B.

Proof for arbitrary and constant phase sequences. It is important to point out that this case cannot be considered as a special case of the arbitrary phase sequences. Although the necessary and sufficient transmissibility conditions for the case of arbitrary phase sequences are also necessary and sufficient for the case of arbitrary constant phases, this fact is not immediately evident. Notice also that constant phases reduce the possibility with respect to the arbitrary sequences, therefore, the capacity region may be larger (certainly, not smaller). Hence, we only need to show the converse. In fact, by repeating the derivations in Appendix 3.B while taking into account that the phase sequences are arbitrary and constant, we obtain the following necessary conditions: $\forall S \subseteq \{1, \dots, M\}$,

$$H(U_S|U_{S^c}) \leq \frac{N}{K} \log \left(1 + \sum_{m \in S} \frac{E_m}{N_0} + \frac{1}{NN_0} \inf_{\phi_1, \dots, \phi_M} \left\{ \sum_{i=1}^N T_i \right\} \right) \quad (3.6)$$

where

$$\begin{aligned} \sum_{i=1}^N T_i &= \sum_{\substack{m, m' \in S \\ m' > m}} \sum_{i=1}^N |\rho_{m, m', i}| \cos(\Delta\phi_{m, m'} + \theta_{m, m', i}) \\ &= \sum_{\substack{m, m' \in S \\ m' > m}} \operatorname{Re} \left[\sum_{i=1}^N |\rho_{m, m', i}| e^{j(\Delta\phi_{m, m'} + \theta_{m, m', i})} \right]. \end{aligned} \quad (3.7)$$

By defining the complex number $\rho_{m,m'}$ as

$$\rho_{m,m'} \triangleq \sum_{i=1}^N |\rho_{m,m',i}| e^{j\theta_{m,m',i}}, \quad (3.8)$$

Eq. (3.7) becomes

$$\sum_{i=1}^N T_i = \sum_{\substack{m,m' \in S \\ m' > m}} \operatorname{Re} \left[|\rho_{m,m'}| e^{j(\Delta\phi_{m,m'} + \theta_{m,m'})} \right]. \quad (3.9)$$

Using Eq. (3.9), it can be shown, as in Appendix 3.B, that

$$\inf_{\phi_1, \dots, \phi_M} \sum_{i=1}^N T_i \leq 0. \quad (3.10)$$

Therefore, we deduce that the following conditions must be verified for reliable transmission of the sources

$$H(U_S|U_{S^c}) \leq \frac{N}{K} \log \left(1 + \sum_{m \in S} \frac{E_m}{N_0} \right) \quad \forall S \subseteq \{1, \dots, M\}. \quad (3.11)$$

□

3.4 Discussion

In this section, we discuss several important points that concern the two theorems stated above. For the converse of Theorem 2, we mention here two notes: first, other than providing necessary conditions for reliable communication, this converse gives in addition some constraints or some properties about the family of codes that achieves optimality. In fact, for the case of arbitrary phase sequences, channel symbols at time i corresponding to an optimal code must be uncorrelated, otherwise the code is suboptimal. To see it more clearly, let's take two blocks of channel symbols of length N corresponding to sensors m and m' . Without loss of generality, we will assume $m = 1$ and $m' = 2$. From (3.29) and (3.38), we conclude that any code allowing the reconstruction of the sources with vanishing probability of error must satisfy

$$H(U_1, U_2|U_{S^c}) \leq \frac{N}{K} \log \left(1 + \frac{E_1 + E_2}{N_0} - \frac{2}{NN_0} \sum_{i=1}^N |\rho_{1,2,i}| \right) \quad (3.12)$$

Knowing that the inequality

$$H(U_1, U_2|U_{S_c}) \leq \frac{N}{K} \log \left(1 + \frac{E_1 + E_2}{N_0} \right) \quad (3.13)$$

can be achieved by a separation-based coding scheme, we deduce that if $\rho_{1,2,i} \neq 0$ for at least one i , the optimal system performance cannot be reached. Therefore, any optimal code, including the one based on the source-channel separation, must verify $\rho_{m,m',i} = 0 \quad \forall m, m' \in \{1, \dots, M\}, m \neq m', i = 1, \dots, N$. Similarly, for the case of arbitrary and constant phases, it can be shown that optimal codes should satisfy $\rho_{m,m'} = 0 \quad \forall m, m' \in \{1, \dots, M\}, m \neq m'$.

The second point on this converse is the one related to the interval of values the phase shifts can take. Until now, we have considered that phase shifts can take values in $[-\pi; \pi]$. In fact, Theorem 2 can be extended to the case where the phase shifts belong to the interval $[-\pi/2; \pi/2]$. Therefore, restraining the interval of phase values does not break imperatively the separation optimality. To prove this, it suffices to show that the following inequality

$$\inf_{\underline{\phi}_{M_S}} Q_{M_S}(\underline{\phi}_{M_S}) \leq 0 \quad (3.14)$$

still holds. To this end, by choosing

$$\Delta\phi_{1,2,i} = \begin{cases} \pi/2 - \theta_{1,2,i} & \text{if } \theta_{1,2,i} \in [0; \pi] \\ -\pi/2 - \theta_{1,2,i} & \text{if } \theta_{1,2,i} \in [-\pi; 0[\end{cases} \quad (3.15)$$

it becomes obvious that the infimum over the phase sequences in (3.38) is less or equal to zero. Then, by making similar modifications to the phases in (3.40), it can be easily shown that (3.14) still holds. Notice that, although the separation remains optimal when the phases belong to $[-\pi/2; \pi/2]$, there exist other possibilities of phase intervals for which this optimality still holds (as an example, when the phases take just two different values α and $\alpha + \pi$).

Another important point concerns the fact that in many wireless sensor networks, the sensors may not be at the same distance from the collector node. In that case, we should consider an attenuation factor $\sqrt{\alpha_m}$ associated to each encoder that reflects the quality of the channel between each sender and the receiver. If we assume that these attenuation factors are known at the receiver point, Theorems 1 and 2 can be easily generalised to include this type of model.

The last point we would like to discuss is the utility of information exchange between the sensor nodes under a sum-energy constraint. The question here is to see if we can gain something if the sensors have the possibility

of communicating with each others. The sum-energy constraint is described by the following inequality

$$\frac{1}{N} \sum_{i=1}^N \sum_{m=1}^M \mathbb{E}[|X_{m,i}|^2] \leq \sum_{m=1}^M E_m \quad (3.16)$$

In fact, under (3.16), any kind of communication or information exchange between the sensors is useless and a separation-based coding scheme is optimal. To see it more clearly, assume that the sensors can communicate in a free manner with each others; therefore, each sensor knows perfectly the realisations of all the sources. The converse for this resultant model contains obviously all the achievable performances resulting from any kind of collaboration between the nodes. In that case, one can simply verify that the necessary condition

$$H(U_1, \dots, U_M) \leq \frac{N}{K} \log \left(1 + \sum_{m=1}^M \frac{E_m}{N_0} \right) \quad (3.17)$$

must hold, and this for any kind of phase sequences considered in this chapter. Knowing that the above inequality can be achieved by a separation-based coding scheme without involving any type of collaboration between the sensor nodes, shows that there is no gain in exchanging information using inter-sensor connections.

3.5 Conclusion

In this chapter, we extended the separation theorem to the case of separately encoded correlated discrete sources sent over a GMAC with phase shifts perfectly known at the receiver and unknown to the transmitters. Hence, for different assumptions on the phase shifts, we proved that a set of two-stage encoders performing distributed source coding in the Slepian-Wolf sense and capacity-achieving channel coding leads to optimal system performance. The presented model constitutes one of the rare scenarios in network information theory where the separation theorem holds. While previous works in the literature concerned in sending correlated sources over MAC channels were more focused on cooperative coding strategies and on trying unsuccessfully to find necessary and sufficient conditions for optimality, we showed, by introducing a small and practical variation to the model (which is that of phase shifts unknown at the transmitters and Gaussian channel noise), that the optimal performance can be simply reached with a

separate source-channel coding scheme. In the next chapter, we will try to extend the separation optimality to continuous information sources where the goal will be to reconstruct them at the receiver within a certain allowable distortions.

APPENDIX

3.A Proof of the Converse of Theorem 1

Given a code with a fixed source-channel rate r , Fano's inequality yields

$$\frac{1}{K}H(\mathbf{U}_1, \dots, \mathbf{U}_M | \mathbf{Y}, \Phi) \leq \lambda_K, \quad (3.18)$$

where, for a family of codes of increasing block length and achieving vanishing error probability, we have $\lambda_K \rightarrow 0$ as $K \rightarrow \infty$. Now, we can write $\forall S \subseteq \{1, 2, \dots, M\}$,

$$\begin{aligned} H(U_S | U_{S^c}) &= \frac{1}{K}H(\mathbf{U}_S | \mathbf{U}_{S^c}) \\ &= \frac{1}{K}H(\mathbf{U}_S | \mathbf{U}_{S^c}, \Phi) \\ &= \frac{1}{K}H(\mathbf{U}_S | \mathbf{U}_{S^c}, \mathbf{X}_{S^c}, \Phi) \\ &= \frac{1}{K}I(\mathbf{U}_S; \mathbf{Y} | \mathbf{U}_{S^c}, \mathbf{X}_{S^c}, \Phi) + \frac{1}{K}H(\mathbf{U}_S | \mathbf{U}_{S^c}, \mathbf{X}_{S^c}, \mathbf{Y}, \Phi) \\ &\stackrel{(a)}{\leq} \frac{1}{K}I(\mathbf{U}_S; \mathbf{Y} | \mathbf{U}_{S^c}, \mathbf{X}_{S^c}, \Phi) + \lambda_K \\ &\leq \frac{1}{K} \sum_{i=1}^N H(Y_i | \mathbf{U}_{S^c}, \mathbf{X}_{S^c}, \Phi) - \frac{1}{K}H(\mathbf{Y} | \mathbf{U}_S, \mathbf{U}_{S^c}, \mathbf{X}_{S^c}, \Phi) + \lambda_K \\ &= \frac{1}{K} \sum_{i=1}^N H(Y_i - \sum_{m \in S^c} e^{j\Phi_{m,i}} X_{m,i} | \mathbf{U}_{S^c}, \mathbf{X}_{S^c}, \Phi) - \frac{1}{K}H(\mathbf{Z}) + \lambda_K \\ &\stackrel{(b)}{\leq} \frac{1}{K} \sum_{i=1}^N \mathbb{E}[\log \text{Var}(A_i(\Phi_{1,i}, \dots, \Phi_{M,i}))] - \frac{N}{K} \log N_0 + \lambda_K \end{aligned} \quad (3.19)$$

where (a) follows from

$$\begin{aligned} H(\mathbf{U}_S | \mathbf{U}_{S^c}, \mathbf{X}_{S^c}, \mathbf{Y}, \Phi) &\leq H(\mathbf{U}_S, \mathbf{U}_{S^c} | \mathbf{X}_{S^c}, \mathbf{Y}, \Phi) \\ &\leq H(\mathbf{U}_S, \mathbf{U}_{S^c} | \mathbf{Y}, \Phi) \\ &\leq \lambda_K, \end{aligned} \quad (3.20)$$

$A_i(\phi_{1,i}, \dots, \phi_{M,i}) \triangleq (Y_i - \sum_{m \in S^c} e^{j\Phi_{m,i}} X_{m,i} | \phi_{1,i}, \dots, \phi_{M,i})$, and the expectation in (b) is with respect to $p(\phi_{1,i}, \dots, \phi_{M,i})$. Without loss of generality, we can restrict the code to have mean zero on all components. Therefore,

$$\begin{aligned}
\text{Var}(A_i(\phi_{1,i}, \dots, \phi_{M,i})) &= \text{Var}\left(\sum_{m \in S} e^{j\phi_{m,i}} X_{m,i} + Z_i\right) \\
&= N_0 + \mathbb{E}\left[\sum_{m \in S} \sum_{m' \in S} X_{m,i} X_{m',i}^* e^{j(\phi_{m,i} - \phi_{m',i})}\right] \\
&= N_0 + \mathbb{E}\left[\sum_{m \in S} X_{m,i} X_{m,i}^*\right] + \\
&\quad 2 \sum_{\substack{m, m' \in S \\ m' > m}} \text{Re}\left\{\mathbb{E}\left[X_{m,i} X_{m',i}^* e^{j\Delta\phi_{m,m',i}}\right]\right\} \quad (3.21)
\end{aligned}$$

$\mathbb{E}\left[X_{m,i} X_{m',i}^*\right]$ is a complex number depending on m, m' and i ; we shall call this number $\rho_{m,m',i} = |\rho_{m,m',i}| e^{j\theta_{m,m',i}}$. Letting the average energy of the i -th symbol be denoted by $E_{m,i}$, we can rewrite (3.21) as

$$\text{Var}(A_i(\phi_{1,i}, \dots, \phi_{M,i})) = N_0 + \sum_{m \in S} E_{m,i} + T_i \quad (3.22)$$

where

$$T_i = 2 \sum_{\substack{m, m' \in S \\ m' > m}} |\rho_{m,m',i}| \cos(\Delta\phi_{m,m',i} + \theta_{m,m',i}) \quad (3.23)$$

Using Jensen's inequality, we can write

$$\begin{aligned}
\mathbb{E}[\log \text{Var}(A_i(\Phi_{1,i}, \dots, \Phi_{M,i}))] &\leq \log\left(N_0 + \sum_{m \in S} E_{m,i} + \mathbb{E}[T_i]\right) \\
&= \log\left(N_0 + \sum_{m \in S} E_{m,i}\right) \quad (3.24)
\end{aligned}$$

where the last step follows from the fact that $\Delta\Phi_{m,m',i}$ is uniformly distributed on $[-\pi; \pi]$. Using again Jensen's inequality, we can proceed with (3.19) and write

$$\begin{aligned}
H(U_S | U_{S^c}) &\leq \frac{1}{K} \sum_{i=1}^N \log\left(N_0 + \sum_{m \in S} E_{m,i}\right) - \frac{N}{K} \log N_0 + \lambda_K \\
&\leq \frac{N}{K} \log\left(N_0 + \sum_{m \in S} E_m\right) - \frac{N}{K} \log N_0 + \lambda_K \quad (3.25)
\end{aligned}$$

Letting $K \rightarrow \infty$, we find the necessary conditions

$$H(U_S|U_{S^c}) \leq \frac{N}{K} \log \left(1 + \sum_{m \in S} \frac{E_m}{N_0} \right), \forall S \subseteq \{1, 2, \dots, M\}. \quad (3.26)$$

3.B Proof of the Converse of Theorem 2

Given a code with a fixed source-channel rate r and a fixed ϕ , Fano's inequality yields

$$\frac{1}{K} H_\phi(\mathbf{U}_1, \dots, \mathbf{U}_M | \mathbf{Y}) \leq \lambda_K(\phi) \quad (3.27)$$

where $\lambda_K(\phi)$ is a function depending on K and ϕ . We require that a family of codes of increasing block length achieves vanishing error probability for all possible ϕ since they are unknown at the transmitters, i.e., that $\lambda_K(\phi) \rightarrow 0$ as $K \rightarrow \infty$. Now, we can write,

$$\begin{aligned} H(U_S|U_{S^c}) &= \frac{1}{K} H(\mathbf{U}_S | \mathbf{U}_{S^c}) = \frac{1}{K} H(\mathbf{U}_S | \mathbf{U}_{S^c}, \mathbf{X}_{S^c}) \\ &= \frac{1}{K} \left(I_\phi(\mathbf{U}_S; \mathbf{Y} | \mathbf{U}_{S^c}, \mathbf{X}_{S^c}) + \frac{1}{K} H_\phi(\mathbf{U}_S | \mathbf{U}_{S^c}, \mathbf{X}_{S^c}, \mathbf{Y}) \right) \\ &\leq \frac{1}{K} I_\phi(\mathbf{U}_S; \mathbf{Y} | \mathbf{U}_{S^c}, \mathbf{X}_{S^c}) + \lambda_K(\phi) \\ &\leq \frac{1}{K} \left(\sum_{i=1}^N H_\phi(Y_i | \mathbf{U}_{S^c}, \mathbf{X}_{S^c}) - H_\phi(\mathbf{Y} | \mathbf{X}_1, \dots, \mathbf{X}_M) \right) + \lambda_K(\phi) \\ &\leq \frac{1}{K} \sum_{i=1}^N \log \text{Var}(A_i(\phi_{1,i}, \dots, \phi_{M,i})) - \frac{N}{K} \log N_0 + \lambda_K(\phi) \end{aligned} \quad (3.28)$$

Since these inequalities must hold for every ϕ , we obtain the tightest conditions by taking the infimum of the RSH term in (3.28) with respect to ϕ . Therefore, letting K goes to ∞ , we can write

$$\begin{aligned}
H(U_S|U_{S^c}) &\leq \inf_{\phi} \left\{ \frac{1}{K} \sum_{i=1}^N \log \left(1 + \sum_{m \in S} \frac{E_{m,i}}{N_0} + \frac{T_i}{N_0} \right) \right\} \\
&\leq \frac{N}{K} \inf_{\phi} \left\{ \log \left(1 + \sum_{m \in S} \frac{E_m}{N_0} + \frac{1}{NN_0} \sum_{i=1}^N T_i \right) \right\} \\
&= \frac{N}{K} \log \left(1 + \sum_{m \in S} \frac{E_m}{N_0} + \frac{1}{NN_0} \inf_{\phi} \left\{ \sum_{i=1}^N T_i \right\} \right) \quad (3.29)
\end{aligned}$$

where we have used again Jensen's inequality and the monotonicity of the logarithm in order to take the infimum inside the log. Now, we will prove that the infimum term in (3.29) cannot be positive, i.e.,

$$\inf_{\phi} \left\{ \sum_{i=1}^N T_i \right\} \leq 0. \quad (3.30)$$

Notice that if the chosen code satisfies $\rho_{m,m',i} = 0 \forall m, m', i$, then the equality is achieved in (3.30) for all phase sequences; this point will be discussed in more details in section 3.4. Returning back to the proof of (3.30), let's take $S = \{1, \dots, l\}$ with $2 \leq l \leq M$; note that specifying the subset S is just to simplify notations and the following proof holds $\forall S \subseteq \{1, \dots, M\}$. Define the matrix

$$\underline{\phi}_l \triangleq [\phi_{m,i}] \quad m = 1, \dots, l \quad i = 1, \dots, N \quad (3.31)$$

and

$$Q_l(\underline{\phi}_l) \triangleq \sum_{i=1}^N T_i \quad (3.32)$$

$$= \sum_{i=1}^N \sum_{m=1}^{l-1} \sum_{m'>m}^l \operatorname{Re} \left[|\rho_{m,m',i}| e^{j(\Delta\phi_{m,m',i} + \theta_{m,m',i})} \right]. \quad (3.33)$$

Consequently, proving (3.30) reduces to prove that $\inf_{\underline{\phi}_l} Q_l(\underline{\phi}_l) \leq 0$. To this end, we can first derive a relation between $Q_{l-1}(\underline{\phi}_{l-1})$ and $Q_l(\underline{\phi}_l)$ like the

following

$$\begin{aligned}
Q_l(\underline{\phi}_l) - Q_{l-1}(\underline{\phi}_{l-1}) & \quad (3.34) \\
&= \sum_{i=1}^N \sum_{m=1}^{l-1} \operatorname{Re} \left[|\rho_{m,l,i}| e^{j(\phi_{m,i} - \phi_{l,i} + \theta_{m,l,i})} \right] \\
&= \sum_{i=1}^N \operatorname{Re} \left[e^{-j\phi_{l,i}} \sum_{m=1}^{l-1} |\rho_{m,l,i}| e^{j(\phi_{m,i} + \theta_{m,l,i})} \right] \\
&= \sum_{i=1}^N \operatorname{Re} \left[e^{-j\phi_{l,i}} |\rho_{l,i}| e^{j\theta_{l,i}} \right] \quad (3.35)
\end{aligned}$$

where

$$\rho_{l,i} = |\rho_{l,i}| e^{j\theta_{l,i}} \triangleq \sum_{m=1}^{l-1} |\rho_{m,l,i}| e^{j(\phi_{m,i} + \theta_{m,l,i})}. \quad (3.36)$$

Note that for a given code and a fixed $\underline{\phi}_{l-1}$, the complex number $\rho_{l,i}$ is fixed and is independent from ϕ_l . Now, it becomes easy to prove that $\inf_{\underline{\phi}_l} Q_l(\underline{\phi}_l) \leq 0$. In fact, for $l = 2$ we have

$$Q_2(\phi_1, \phi_2) = \sum_{i=1}^N \operatorname{Re} \left[|\rho_{1,2,i}| e^{j(\Delta\phi_{1,2,i} + \theta_{1,2,i})} \right]. \quad (3.37)$$

By taking $\Delta\phi_{1,2,i} = \pi - \theta_{1,2,i}$, we obtain that

$$\inf_{\phi_2} Q_2(\phi_1, \phi_2) = - \sum_{i=1}^N |\rho_{1,2,i}| \leq 0. \quad (3.38)$$

Suppose now that

$$\inf_{\underline{\phi}_{l-1}} Q_{l-1}(\underline{\phi}_{l-1}) \leq 0$$

and that this infimum is attained for a certain value $\underline{\phi}_{l-1} = \underline{\phi}_{l-1}^*$; using the recurrence relation in (3.35), we can write

$$\begin{aligned}
\inf_{\underline{\phi}_l} Q_l(\underline{\phi}_l) & \leq Q_l(\underline{\phi}_{l-1}^*, \phi_l^*) \\
&= Q_{l-1}(\underline{\phi}_{l-1}^*) - \sum_{i=1}^N |\rho_{l,i}| \\
&\leq 0. \quad (3.39)
\end{aligned}$$

where the entries of $\boldsymbol{\phi}_l^* = (\phi_{l,1}^*, \dots, \phi_{l,N}^*)$ are chosen like the following

$$\phi_{l,i}^* = \theta_{l,i} - \pi \quad \text{for } i = 1, \dots, N. \quad (3.40)$$

Using this result in (3.29) completes the proof of Theorem 2 for arbitrary phase sequences.

Chapter 4

Correlated Continuous Sources Over GMACs with Phase Shifts

In this chapter, we address the problem of separate encoding of correlated continuous sources observed by sensor nodes that send their encoded information through a Gaussian multiple access channel (GMAC) with phase shifts. Actually, this chapter is an extension of the previous one in the sense that it extends the results of separation optimality to continuous sources. In fact, we prove that a coding scheme based on the source-channel separation is practically optimal in the high fidelity regime where small distortions at the receiver are required; this separation quasi-optimality holds for random ergodic and arbitrary non-random models of the phase shifts.

4.1 Introduction

In the previous chapter, we have been dealing with discrete sources where the goal was to reconstruct them at the receiver with an arbitrarily small probability of error. This means that no data loss was allowed in order to recover the information of all the sources at the receiver. In that case, we have proved that the separation theorem holds and consequently, performing separate source-channel coding leads to optimal system performance. In this chapter, we are trying to generalise the separation concept when dealing with continuous sources. Here, we wish to reconstruct the sources at the receiver in order to achieve certain fidelity levels. The encoders being subject to transmission cost constraints, the coding problem is to determine all fidelity levels that could be attained under any coding strategy despite its complexity or incurred delay. Proving the separation for this coding problem needs at least a characterization of the rate-distortion region known also under the multiterminal source coding problem. This latter is one of the most long-standing open problem in information theory. Its resultant rate-distortion region can be viewed as an extension of the Slepian-Wolf region for lossy coding case. Despite the fact that this problem has been subject to extensive work in the literature [62], [63], [64], [65], [66] and [67], no general solution in terms of single letter information quantities is known until now.

Recently, a multi-letter characterization of the rate-distortion region has been found in [68]; the authors proved that the Berger-Tung's inner region [63, 65] extended to multiple-letter representation is exactly the rate-distortion region. Despite the fact that this multi-letter description of the rate-distortion region was crucial to extend the separation result obtained in [61, 31] to the lossy coding case, it is no more helpful, or at least not trivial to use it on our model. For the case of two correlated Gaussian sources, the rate-distortion region has been partially found in [64] and then fully characterized in [69] where the authors proved that the Berger-Tung's inner region is exactly the rate-distortion region. In the high resolution regime, the rate-distortion region has been asymptotically found in [34] for any number of encoders and arbitrarily correlated continuous source distributions, while considering MSE distortion measures at the receiver.

In this chapter, we first study the case of two correlated Gaussian sources separately encoded and sent over a GMAC with phase shifts. While using an MSE distortion measure, we derive an outer region on the set of all achievable distortion pairs (D_1, D_2) given fixed power constraints at the encoders. This region can be also viewed as an outer region on the power constraints (E_1, E_2) that should be taken in order to achieve a fixed distortion pairs

(D_1, D_2) . We prove that in the high fidelity regime, the outer region on the cost constraints achievable set matches asymptotically ($D_1 \rightarrow 0, D_2 \rightarrow 0$) with the inner region obtained by a separation-based coding scheme; hence, in applications where small distortions are needed, the strategy of source-channel separation is practically optimal. Finally, we prove that for low distortions, the separation asymptotically holds for an arbitrary number of encoders and any kind of continuous source distributions while performing MSE distortion measures at the receiver. Note that throughout the chapter, the results hold for both random ergodic and arbitrary non-random phase shifts.

4.2 Model

We consider the same model as the one in chapter 3 (see Fig. 4.3), with the main differences summarized as follows :

- The sources U_1, \dots, U_M are continuous random variables and arbitrarily correlated .
- The goal is no more to decode the sources with an arbitrarily small probability of error, but to reconstruct them in order to achieve some fidelity levels. The fidelity criterion considered here is the squared-error distortion measure defined like the following

$$d(u_i, \hat{u}_i) = (u_i - \hat{u}_i)^2 \quad i = 1, \dots, M. \quad (4.1)$$

For sequence distortions, we will use the following notational convention

$$d(\mathbf{u}_i, \hat{\mathbf{u}}_i) \triangleq \frac{1}{K} \sum_{j=1}^K d(u_{i,j}, \hat{u}_{i,j}) \quad i = 1, \dots, M. \quad (4.2)$$

Using a given code, we can easily determine the average incurred distortions

$$\Delta_i \triangleq \mathbb{E}[d(\mathbf{u}_i, \hat{\mathbf{u}}_i)] \quad i = 1, \dots, M. \quad (4.3)$$

Note that, as in the previous chapter, we consider the following power constraint

$$\frac{1}{N} \sum_{i=1}^N \mathbb{E}[|X_{m,i}|^2] \leq E_m \quad \text{for } m = 1, \dots, M \quad (4.4)$$

where E_m represents the mean energy allowed per transmission for sensor m . The coding problem is addressed like the following: given an an

energy vector (E_1, \dots, E_M) , what are the distortion vectors (D_1, \dots, D_M) that can be attained. Or, fixing a distortion vector (D_1, \dots, D_M) , i.e. $\Delta_1 \leq D_1, \dots, \Delta_M \leq D_M$, what are the achievable energy vectors (E_1, \dots, E_M) . In another words, we are searching for the set of energy vectors (E_1, \dots, E_M) such that there exist a code that permits the reconstruction of the sources at the receiver with average incurred distortions $\Delta_1 \leq D_1, \dots, \Delta_M \leq D_M$. Throughout this chapter, we will use the following notation: $\mathbf{X}_i e^{j\Phi_i} \triangleq (X_{i,1} e^{j\Phi_{i,1}}, \dots, X_{i,N} e^{j\Phi_{i,N}})$. We will consider that the phases are random ergodic, but all results can be trivially generalised to the case of arbitrary non-random phases.

4.3 Two Correlated Gaussian Sources

In this section, the number of encoders M is limited to 2, and the sources U_1 and U_2 are correlated Gaussian random variables with mean zero and covariance matrix

$$\underline{\mathbf{K}} = \begin{bmatrix} 1 & \rho \\ \rho & 1 \end{bmatrix}. \quad (4.5)$$

The model scheme is depicted in Fig. 4.1. In what follows, we will derive an inner and outer region on the achievable distortion couple (D_1, D_2) and prove that for small distortions, a separation-based coding scheme is asymptotically optimal.

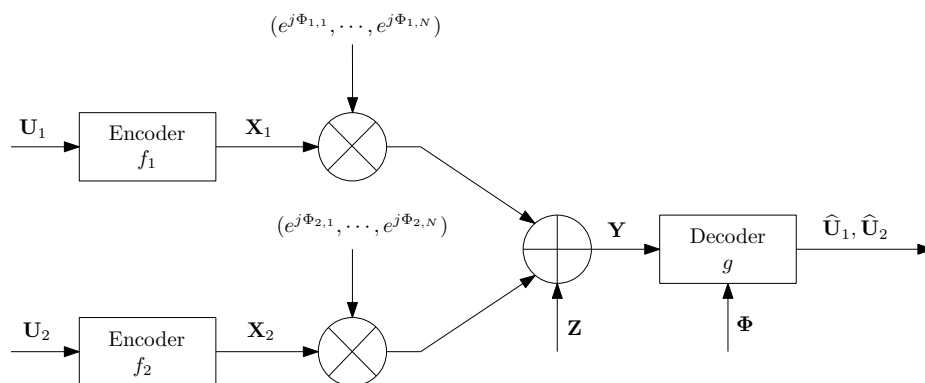


Figure 4.1: Bivariate Gaussian sources over GMAC with phase shifts perfectly known at the receiver

4.3.1 Inner Region

An inner region to all the achievable distortion pairs (D_1, D_2) can be obtained by simply looking to the distortion couples that can be reached by a separate source-channel coding scheme. In fact, the rate-distortion region $\mathcal{R}(D_1, D_2)$ of the quadratic Gaussian two-encoder source coding problem depicted in Fig. 4.2 is given by [64, 69]:

$$\mathcal{R}(D_1, D_2) = \mathcal{R}(D_1) \cap \mathcal{R}(D_2) \cap \mathcal{R}_{sum}(D_1, D_2) \quad (4.6)$$

where the rate regions $\mathcal{R}(D_1), \mathcal{R}(D_2)$ and $\mathcal{R}_{sum}(D_1, D_2)$ are given like the following

$$\mathcal{R}(D_1) = \left\{ (R_1, R_2) : R_1 \geq \frac{1}{2} \log^+ \left[\frac{1}{D_1} (1 - \rho^2 + \rho^2 2^{-2R_2}) \right] \right\}, \quad (4.7)$$

$$\mathcal{R}(D_2) = \left\{ (R_1, R_2) : R_2 \geq \frac{1}{2} \log^+ \left[\frac{1}{D_2} (1 - \rho^2 + \rho^2 2^{-2R_1}) \right] \right\}, \quad (4.8)$$

and

$$\mathcal{R}_{sum}(D_1, D_2) = \left\{ (R_1, R_2) : R_1 + R_2 \geq \frac{1}{2} \log^+ \left[\frac{(1 - \rho^2)\beta(D_1, D_2)}{2D_1D_2} \right] \right\}, \quad (4.9)$$

with

$$\beta(D_1, D_2) = 1 + \sqrt{1 + \frac{4\rho^2 D_1 D_2}{(1 - \rho^2)^2}}. \quad (4.10)$$

The capacity region $C(E_1, E_2)$ of the considered GMAC channel is given by:

$$C(E_1, E_2) = \left\{ (R_1, R_2); R_1 \leq \log \left(1 + \frac{E_1}{N_0} \right), \quad (4.11) \right.$$

$$R_2 \leq \log \left(1 + \frac{E_2}{N_0} \right), \quad (4.12)$$

$$\left. R_1 + R_2 \leq \log \left(1 + \frac{E_1 + E_2}{N_0} \right) \right\}. \quad (4.13)$$

For any set \mathcal{S} and scalar c , we define the multiplication $c\mathcal{S} \triangleq \{cS; S \in \mathcal{S}\}$. Therefore, as a direct result of the separation theorem, the set of pairs (D_1, D_2) such that $r\mathcal{R}(D_1, D_2) \cap C(E_1, E_2) \neq \emptyset$ constitutes an inner bound on the achievable distortion region.

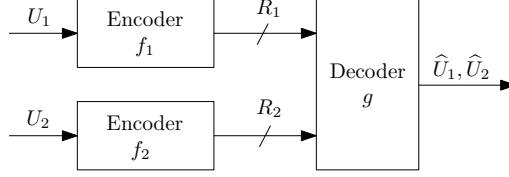


Figure 4.2: Two correlated Gaussian sources separately encoded at rates R_1 and R_2 .

4.3.2 Lower Bounds on the Distortion

In this section, we will derive lower bounds on D_1 and D_2 that will serve as an outer region on the set of all achievable distortion pairs.

Bound on D_1 and D_2

Provided that the considered sources U_1 and U_2 are correlated and Gaussian, they can be related to each other by the following equality

$$U_1 = \rho U_2 + V, \tag{4.14}$$

where V is a Gaussian random variable independent from U_2 , of zero mean and variance $1 - \rho^2$. Now let us split the Gaussian channel noise \mathbf{Z} into two independent Gaussian random vectors \mathbf{Z}_1 and \mathbf{Z}_2 of zero means and covariance matrices $\alpha^2 N_0 \mathbf{I}_N$ and $(1 - \alpha^2) N_0 \mathbf{I}_N$ respectively, α being any real number belonging to $]0; 1[$. For simplicity, let $\mathbf{V}_2 \triangleq (\mathbf{X}_2 e^{j\Phi_2} + \mathbf{Z}_2, \Phi)$. Therefore, we can write

$$I(\mathbf{U}_1; \mathbf{Y} | \mathbf{V}_2) = h(\mathbf{U}_1 | \mathbf{V}_2) - h(\mathbf{U}_1 | \mathbf{Y}, \mathbf{V}_2) \tag{4.15}$$

$$= h(\mathbf{V} + \rho \mathbf{U}_2 | \mathbf{V}_2) - h(\mathbf{U}_1 - \hat{\mathbf{U}}_1 | \mathbf{Y}, \mathbf{V}_2) \tag{4.16}$$

$$\stackrel{(a)}{\geq} \frac{K}{2} \log \left(2^{\frac{2}{K} h(\mathbf{V})} + 2^{\frac{2}{K} h(\rho \mathbf{U}_2 | \mathbf{V}_2)} \right) - h(\mathbf{U}_1 - \hat{\mathbf{U}}_1). \tag{4.17}$$

where $\mathbf{V} = (V_1, \dots, V_K)$ and (a) follows from the entropy power inequality which can be used due to the fact that \mathbf{V} is independent from \mathbf{U}_2 and \mathbf{V}_2 . Besides, we have that

$$h(\mathbf{V}) = \frac{K}{2} \log 2\pi e(1 - \rho^2), \tag{4.18}$$

$$h(\rho\mathbf{U}_2|\mathbf{V}_2) = K \log |\rho| + h(\mathbf{U}_2|\mathbf{V}_2) \quad (4.19)$$

$$= K \log |\rho| + h(\mathbf{U}_2) - I(\mathbf{U}_2; \mathbf{X}_2 e^{j\Phi_2} + \mathbf{Z}_2|\Phi) \quad (4.20)$$

$$\geq K \log |\rho| + \frac{K}{2} \log 2\pi e - N \log \left[1 + \frac{E_2}{(1-\alpha^2)N_0} \right], \quad (4.21)$$

and

$$h(\mathbf{U}_1 - \hat{\mathbf{U}}_1) \leq \sum_{i=1}^K h(U_{1,i} - \hat{U}_{1,i}) \quad (4.22)$$

$$\leq \sum_{i=1}^K \frac{1}{2} \log \left(2\pi e \mathbb{E}[(U_{1,i} - \hat{U}_{1,i})^2] \right) \quad (4.23)$$

$$\leq \frac{K}{2} \log \left(2\pi e \frac{1}{K} \sum_{i=1}^K \mathbb{E}[(U_{1,i} - \hat{U}_{1,i})^2] \right) \quad (4.24)$$

$$\leq \frac{K}{2} \log (2\pi e D_1). \quad (4.25)$$

Combining Eqs. (4.17), (4.18), (4.21) and (4.25), we obtain

$$I(\mathbf{U}_1; \mathbf{Y}|\mathbf{V}_2) \geq \frac{K}{2} \log \left[2\pi e(1-\rho^2) + 2\pi e\rho^2 \left[1 + \frac{E_2}{(1-\alpha^2)N_0} \right]^{\frac{-2N}{K}} \right] - \frac{K}{2} \log (2\pi e D_1) \quad (4.26)$$

$$\geq \frac{K}{2} \log \left(\frac{(1-\rho^2) + \rho^2 \left(1 + \frac{E_2}{(1-\alpha^2)N_0} \right)^{\frac{-2N}{K}}}{D_1} \right). \quad (4.27)$$

An upper bound on $I(\mathbf{U}_1; \mathbf{Y}|\mathbf{V}_2)$ can be found like the following

$$I(\mathbf{U}_1; \mathbf{Y}|\mathbf{V}_2) = h(\mathbf{Y}|\mathbf{V}_2) - h(\mathbf{Y}|\mathbf{U}_1, \mathbf{V}_2) \quad (4.28)$$

$$= h(\mathbf{X}_1 e^{j\Phi_1} + \mathbf{Z}_1|\mathbf{V}_2) - h(\mathbf{Z}_1) \quad (4.29)$$

$$\leq h(\mathbf{X}_1 e^{j\Phi_1} + \mathbf{Z}_1|\Phi) - h(\mathbf{Z}_1) \quad (4.30)$$

$$\leq N \log \left(1 + \frac{E_1}{\alpha^2 N_0} \right). \quad (4.31)$$

From Eqs. (4.27) and (4.31) we get

$$D_1 \geq \frac{(1-\rho^2) + \rho^2 \left(1 + \frac{E_2}{(1-\alpha^2)N_0} \right)^{\frac{-2N}{K}}}{\left(1 + \frac{E_1}{\alpha^2 N_0} \right)^{\frac{2N}{K}}}. \quad (4.32)$$

This inequality holds for all $0 < \alpha < 1$, therefore

$$D_1 \geq \max_{0 < \alpha < 1} \frac{(1 - \rho^2) + \rho^2 \left(1 + \frac{E_2}{(1 - \alpha^2)N_0}\right)^{-\frac{2N}{K}}}{\left(1 + \frac{E_1}{\alpha^2 N_0}\right)^{2N/K}}. \quad (4.33)$$

By analogy, we obtain

$$D_2 \geq \max_{0 < \alpha < 1} \frac{(1 - \rho^2) + \rho^2 \left(1 + \frac{E_1}{(1 - \alpha^2)N_0}\right)^{-\frac{2N}{K}}}{\left(1 + \frac{E_2}{\alpha^2 N_0}\right)^{2N/K}}. \quad (4.34)$$

Bound on the Product $D_1 D_2$

Let us find now a new bound on the product of D_1 and D_2 . On one hand, we have

$$I(\mathbf{X}_1, \mathbf{X}_2; \mathbf{Y} | \Phi) = h(\mathbf{Y} | \Phi) - h(\mathbf{Y} | \mathbf{X}_1, \mathbf{X}_2, \Phi) \quad (4.35)$$

$$= h(\mathbf{Y} | \Phi) - h(\mathbf{Z}) \quad (4.36)$$

$$\leq N \log \left(1 + \frac{E_1 + E_2}{N_0}\right) \quad (4.37)$$

On the other hand, we have

$$I(\mathbf{X}_1, \mathbf{X}_2; \mathbf{Y} | \Phi) = I(\mathbf{X}_1, \mathbf{X}_2; \mathbf{Y}, \Phi) \quad (4.38)$$

$$\geq I(\mathbf{U}_1, \mathbf{U}_2; \hat{\mathbf{U}}_1, \hat{\mathbf{U}}_2) \quad (4.39)$$

$$= h(\mathbf{U}_1, \mathbf{U}_2) - h(\mathbf{U}_1, \mathbf{U}_2 | \hat{\mathbf{U}}_1, \hat{\mathbf{U}}_2) \quad (4.40)$$

$$= h(\mathbf{U}_1, \mathbf{U}_2) - h(\mathbf{U}_1 - \hat{\mathbf{U}}_1, \mathbf{U}_2 - \hat{\mathbf{U}}_2 | \hat{\mathbf{U}}_1, \hat{\mathbf{U}}_2) \quad (4.41)$$

$$\geq h(\mathbf{U}_1, \mathbf{U}_2) - h(\mathbf{U}_1 - \hat{\mathbf{U}}_1, \mathbf{U}_2 - \hat{\mathbf{U}}_2) \quad (4.42)$$

$$\geq h(\mathbf{U}_1, \mathbf{U}_2) - h(\mathbf{U}_1 - \hat{\mathbf{U}}_1) - h(\mathbf{U}_2 - \hat{\mathbf{U}}_2) \quad (4.43)$$

$$\geq \frac{K}{2} \log(2\pi e)^2 (1 - \rho^2) - \frac{K}{2} \log(2\pi e)^2 D_1 D_2 \quad (4.44)$$

$$= \frac{K}{2} \log \left(\frac{1 - \rho^2}{D_1 D_2} \right) \quad (4.45)$$

Combining Eqs. (4.37) and (4.45), we obtain

$$D_1 D_2 \geq \frac{1 - \rho^2}{\left(1 + \frac{E_1 + E_2}{N_0}\right)^{2N/K}} \quad (4.46)$$

4.4 Outer Region and High Fidelity Regime

Let us define three regions of distortion couples like the following: \mathcal{R}_1 the region such that Eqs.(4.33) and (4.34) are satisfied, and \mathcal{R}_2 defined by Eq. (4.46). Therefore, the intersection between these two regions constitutes an outer region on the achievable distortions. Throughout this section, we will consider ourselves working in a high fidelity regime where our interest is to achieve small distortions D_1 and D_2 . This regime is interesting from practical point of view where in most applications we seek to reconstruct all the sources with high fidelity. We will prove that in this regime, the separation theorem asymptotically holds. First, let us define a loose but simple outer region like the following: let $\alpha \rightarrow 1$ in Eq. (4.32); this gives

$$D_1 \geq \frac{(1 - \rho^2)}{\left(1 + \frac{E_1}{N_0}\right)^{2N/K}}. \quad (4.47)$$

By analogy, we obtain

$$D_2 \geq \frac{(1 - \rho^2)}{\left(1 + \frac{E_2}{N_0}\right)^{2N/K}}. \quad (4.48)$$

For fixed (E_1, E_2) , Eqs. (4.47),(4.48) and (4.46) define an outer region on the achievable distortion couple (D_1, D_2) . Equivalently, for fixed (D_1, D_2) , the same inequalities define an outer region on the achievable energy couple (E_1, E_2) that will be denoted by \mathcal{R}_{out} . For small distortion couples and hence high rates, the rate region of the sources can be approximated by

$$\mathcal{R}(D_1, D_2) \simeq \left\{ (R_1, R_2) : \begin{aligned} R_1 &\geq \frac{1}{2} \log^+ \left[\frac{1 - \rho^2}{D_1} \right], \\ R_2 &\geq \frac{1}{2} \log^+ \left[\frac{1 - \rho^2}{D_2} \right], \\ R_1 + R_2 &\geq \frac{1}{2} \log^+ \left[\frac{(1 - \rho^2)}{D_1 D_2} \right] \end{aligned} \right\} \quad (4.49)$$

It is straightforward to see that by combining the inequalities in (4.49) with those of the GMAC capacity region while taking into account the source-channel rate gives the same distortion-cost inequalities that define the outer region \mathcal{R}_{out} . This implies that for small distortion couples, the set of achievable energy couples (E_1, E_2) can be asymptotically reached by using a separation-based coding scheme.

4.5 Generalisation

Let us now generalise the concept of separation optimality for any number of encoders and any kind of continuous source distributions. The model scheme is depicted in Fig. 4.3. For the converse, we can write $\forall S \subseteq \{1, \dots, M\}$,

$$I(\mathbf{Y}; \mathbf{U}_S | \mathbf{U}_{S^c}, \Phi) = h(\mathbf{U}_S | \mathbf{U}_{S^c}, \Phi) - h(\mathbf{U}_S | \mathbf{U}_{S^c}, \mathbf{Y}, \Phi) \quad (4.50)$$

$$\geq \sum_{j=1}^K h(U_{S,j} | U_{S^c,j}) - \sum_{i \in S} h(\mathbf{U}_i | \mathbf{U}_{S^c}, \mathbf{Y}, \Phi) \quad (4.51)$$

$$\geq Kh(U_S | U_{S^c}) - \sum_{i \in S} h(\mathbf{U}_i | \mathbf{Y}, \Phi) \quad (4.52)$$

$$= Kh(U_S | U_{S^c}) - \sum_{i \in S} \sum_{j=1}^K h(\mathbf{U}_i - \hat{\mathbf{U}}_i | \mathbf{Y}, \Phi) \quad (4.53)$$

$$\geq Kh(U_S | U_{S^c}) - \sum_{i \in S} h(\mathbf{U}_i - \hat{\mathbf{U}}_i) \quad (4.54)$$

$$\geq Kh(U_S | U_{S^c}) - \sum_{i \in S} \sum_{j=1}^K h(U_{i,j} - \hat{U}_{i,j}) \quad (4.55)$$

$$\geq Kh(U_S | U_{S^c}) - \frac{1}{2} \sum_{i \in S} \sum_{j=1}^K \log 2\pi e \mathbb{E}[(U_{i,j} - \hat{U}_{i,j})^2]$$

$$\geq Kh(U_S | U_{S^c}) - \frac{K}{2} \sum_{i \in S} \log 2\pi e D_i \quad (4.56)$$

$$\geq Kh(U_S | U_{S^c}) - \frac{K}{2} \log(2\pi e)^{|S|} \prod_{i \in S} D_i. \quad (4.57)$$

Besides, we have

$$I(\mathbf{Y}; \mathbf{U}_S | \mathbf{U}_{S^c}, \Phi) = h(\mathbf{Y} | \mathbf{U}_{S^c}, \Phi) - h(\mathbf{Y} | \mathbf{U}_S, \mathbf{U}_{S^c}, \Phi) \quad (4.58)$$

$$= h(\mathbf{Y} | \mathbf{U}_{S^c}, \mathbf{X}_{S^c}, \Phi) - h(\mathbf{Z}) \quad (4.59)$$

$$\leq h(\mathbf{Y} | \mathbf{X}_{S^c}, \Phi) - h(\mathbf{Z}) \quad (4.60)$$

$$\leq h\left(\sum_{i \in S} \mathbf{X}_i e^{j\Phi_i} + \mathbf{Z} | \Phi\right) - h(\mathbf{Z}) \quad (4.61)$$

$$\leq N \log\left(1 + \frac{\sum_{i \in S} E_i}{N_0}\right) \quad (4.62)$$

Combining Eqs. (4.57) and (4.62) gives us the following necessary conditions: $\forall S \subseteq \{1, \dots, M\}$

$$Kh(U_S|U_{S^c}) - \frac{K}{2} \log(2\pi e)^{|S|} \prod_{i \in S} D_i \leq N \log \left(1 + \frac{\sum_{i \in S} E_i}{N_0} \right). \quad (4.63)$$

Note that in the high fidelity regime, the rate-distortion region of the sources $\mathcal{R}(D_1, \dots, D_M)$ can be approximated by (see [34]):

$$\mathcal{R}(D_1, \dots, D_M) \simeq \left\{ (R_1, \dots, R_M); \sum_{i \in S} R_i \geq h(U_S|U_{S^c}) - \frac{1}{2} \log(2\pi e)^{|S|} \prod_{i \in S} D_i \right. \\ \left. \forall S \subseteq \{1, \dots, M\} \right\} \quad (4.64)$$

The capacity region $C(E_1, \dots, E_M)$ of a GMAC is defined like the following

$$C(E_1, \dots, E_M) = \left\{ (R_1, \dots, R_M); \sum_{i \in S} R_i \leq \log \left(1 + \frac{\sum_{i \in S} E_i}{N_0} \right) \right. \\ \left. \forall S \subseteq \{1, \dots, M\} \right\} \quad (4.65)$$

Combining the inequalities defining the rate-distortion region with that of the capacity region while taking into account the source-channel rate K/N , leads to the conclusion of the quasi-optimality of the separation in the high fidelity regime.

4.6 Conclusion

In this chapter, we derived an outer region on the achievable distortions for two correlated Gaussian sources sent through a GMAC channel with phase shifts. In that case, we showed that the source-channel separation is quasi-optimal in the high fidelity regime; hence, for practical applications where the goal is to achieve small distortions, a separation-based coding is asymptotically optimal. At the end, we generalise the asymptotic optimality of the separation for any number of encoders and any continuous source distributions.

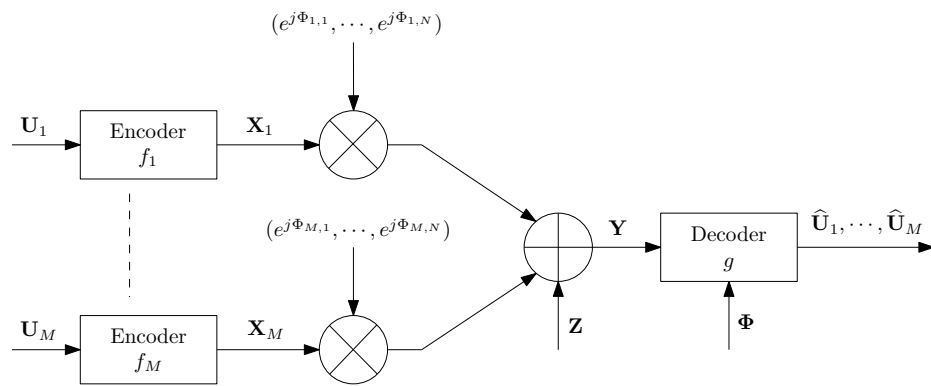


Figure 4.3: Model scheme of M arbitrarily correlated sources sent through a GMAC with phase shifts perfectly known at the receiver

Chapter 5

Distributed Sensing of Random Fields

We consider a wireless sensor network deployed in an area to measure the realization of a finite multi-dimensional, time-varying physical random field. Each sensor observes one noisy realization of the field, maps it linearly into a signal with a signature and sends it across a white Gaussian multiple access channel, under a constraint on the total energy given to all the sensors per field realization. The receiver or the 'collector node' receives all the signals and tries to construct an estimate of the field within a certain mean distortion based on the MSE fidelity criterion. We derive, under the total energy constraint, a lower-bound on the distortion, an achievable one, and another lower-bound under a TDMA transmission scheme. In the case of the non-existence of the observation noise, we find the asymptotic decreasing behavior of the achievable distortion as a function of the number of sensors. Moreover, we derive a lower-bound on the distortion over all possible encoding techniques, assuming a free collaboration and information exchange between the sensors. We compare these bounds for a particular example with another bound on the achievable distortion [70].

5.1 Introduction

Wireless sensor networks are typically used to monitor some spatial characteristics of a field in the area over which the network is deployed. Examples of fields include temperature, electromagnetic radiation, natural or induced vibration, or auditory levels. In such networks, sensors make measurements of the field, process them locally, potentially with the help of neighboring nodes, and then collectively transmit the measurements over a wireless channel to one or more collector nodes. The collector nodes process the received data in order to extract and analyze the spatial characteristics of the field.

While a sensor network is application-dependent, we restrict our work to an application where the sensors have to track a time-varying random field and send back their measurements to one collector node through a white Gaussian multiple-access channel. As in the previous chapters, we address the problem of coding the sensed information at each sensor node before transmitting it through the channel. However, in this application, we consider a random field that has relatively fast variations in time, therefore the coding strategy adopted in chapter 2 for slowly time-varying sources does not apply anymore. Furthermore, the goal now is to reconstruct an estimate of the random field at the receiver instead of reconstructing the sensor measurements as it has been always done in the previous chapters. Notice also that phase shifts are not considered in the channel model, therefore the results obtained in chapter 3 and 4 do not hold anymore and optimal coding strategies are not known yet.

For achievable schemes, we assume a linear encoder in each sensor that maps the sensed value into the amplitude of a *signature* waveform which is transmitted across the channel. As is common in the literature, we consider that the sensing process is imperfect, so that the sensed values are subject to additive Gaussian observation noise. The choice of linear encoder is motivated firstly by its simplicity, and secondly by its optimality in the point-to-point communication model where a Gaussian source is sent over an AWGN channel [38], [35]. The latter is true only in the case where the number of channel uses per source symbol is one. Moreover, recent results in [36] show the optimality of linear encoders for a simple sensor network model where a single Gaussian source is observed by multiple noisy Gaussian sensors, and these observations have to be transmitted via the standard Gaussian multiple-access channel. This is again for the case where a single source letter is available per channel use.

In this chapter, we consider sensor networks with a constraint on the total radiated signal energy and we seek to minimize the distortion between

the random field and its reconstructed estimate at the collector node. A similar model has been studied by Gastpar and Vetterli in [70],[71], [72], and, under certain field configurations, the achievable distortion we find here can be compared to the scheme in [70] and clearly outperforms it. Other than demonstrating an achievable scheme, we derive a lower-bound on the distortion over all possible total energy distributions and all signatures, and another more general lower-bound which is not limited to linear encoders. This latter bound assumes that the sensors can communicate with each other freely in order to exchange information. Under a TDMA transmission scheme, a lower-bound on the distortion is derived, which we find to be independent of the number of sensors. This result shows the sub-optimality of TDMA in the ideal case where the sensor observations are not corrupted by noise, since the other schemes exhibit decreasing distortion with the number of sensors.

Concerning the notations used in this chapter, a bold letter (eg: \mathbf{a}) denotes a vector, while bold and underlined letter (eg: $\underline{\mathbf{a}}$) denotes a matrix. The i^{th} singular value and the i^{th} eigenvalue of a matrix $\underline{\mathbf{a}}$ are denoted respectively by $\sigma_i(\underline{\mathbf{a}})$ and $\mu_i(\underline{\mathbf{a}})$. $E[\cdot]$ denotes the mean value over all random variables inside the brackets.

5.2 Model

The sensor network model is depicted in Fig.5.1. We consider a field $F(\mathbf{x})$ occupying a certain area \mathcal{A} and depending on the spatial-coordinate vector \mathbf{x} . We assume that the field $F(\mathbf{x})$ can be represented in a finite-dimensional orthonormal basis of space functions $\phi_i(\mathbf{x})$ for $i = 1, \dots, N'$, by considering that the energy of the field lying outside the basis is too small and could be neglected. Then

$$F(\mathbf{x}) = \sum_{i=1}^{N'} \sqrt{\lambda_i} U_i \phi_i(\mathbf{x}) \quad (5.1)$$

where each λ_i is a constant representing the energy of the field in the i^{th} dimension and $\mathbf{U} = (U_1, \dots, U_{N'})^t$ is a Gaussian random vector with mean zero and identity covariance matrix.

In the area \mathcal{A} , M sensors are randomly deployed, having $\mathbf{x}_1, \dots, \mathbf{x}_M$ as space coordinates. The sensor k senses the value $R(\mathbf{x}_k)$, a noisy version of the field at position \mathbf{x}_k :

$$R(\mathbf{x}_k) = F(\mathbf{x}_k) + W_k \quad (5.2)$$

where W_k for $k = 1, \dots, M$ are i.i.d Gaussian observation noise with zero-mean and variance σ_W^2 ; this value is mapped onto the signal

$$S_k(R(\mathbf{x}_k), t) = \sum_{i=1}^N S_{ki} \gamma_i(t) \quad \text{for } t \in [0, T]$$

where the set $\{\gamma_1(t), \gamma_2(t), \dots, \gamma_N(t)\}$ forms an orthonormal basis for the signal space and S_{ki} is the projection of the signal on $\gamma_i(t)$. The vector \mathbf{S}_k representing the signal components is taken equal to

$$\mathbf{S}_k = \begin{pmatrix} S_{k1} \\ S_{k2} \\ \vdots \\ S_{kN} \end{pmatrix} = \sqrt{\frac{E_k}{E[R^2(\mathbf{x}_k)]}} R(\mathbf{x}_k) \boldsymbol{\psi}_k \quad (5.3)$$

where E_k is the mean energy attributed to the sensor k and $\boldsymbol{\psi}_k$ a normalized vector representing a signature. A mean total energy E_T being dedicated to all the sensors in order that each one transmit one signal, the energy constraint could be written as

$$\sum_{k=1}^M E_k \leq E_T. \quad (5.4)$$

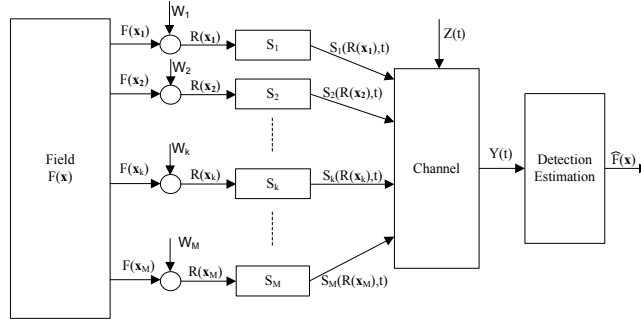


Figure 5.1: The scheme of the considered wireless sensor network model

After the processing stage, the sensors send simultaneously their signals to the collector node through a Gaussian multiple access channel. The output $Y(t)$ of the channel can be written like

$$Y(t) = \sum_{k=1}^M \sqrt{\alpha_k} S_k(R(\mathbf{x}_k), t) + Z(t)$$

with α_k representing an attenuation factor proportional to the distance between the sensor k and the collector node, and $Z(t)$ the white Gaussian noise with zero mean and σ_Z^2 as power spectral density. The baseband expression of $Y(t)$ implies an adjustment at the sensor transmitters of the phases induced by the channel.

At the detection, we calculate $\widehat{F}(\mathbf{x})$, the estimate of $F(\mathbf{x})$ for all $\mathbf{x} \in \mathcal{A}$. Here, we assume that $\alpha_1, \dots, \alpha_M$ and $\mathbf{x}_1, \dots, \mathbf{x}_M$ are perfectly known to the collector node. The distortion measure is the mean squared error, and the total mean distortion that we want to minimize is equal to

$$D = \int_{\mathbf{x} \in \mathcal{A}} E \left[(F(\mathbf{x}) - \widehat{F}(\mathbf{x}))^2 \right] d\mathbf{x} \quad (5.5)$$

5.3 Performance Limits Of Linear Coding

In this section, we'll focus on the linear mapping scheme that we have presented in our model, in order to test its performance in terms of minimal achievable distortion. In other words, with a such linear coding done by the sensors in the processing stage and under the sum-energy constraint, we aim to find the total energy distribution E_1, \dots, E_M over the sensors and the appropriate choice of the signatures $\boldsymbol{\psi}_1, \dots, \boldsymbol{\psi}_M$ that will minimize the total mean distortion. We put all these variables in a matrix $\underline{\mathbf{A}} \triangleq (\sqrt{E_1}\boldsymbol{\psi}_1, \dots, \sqrt{E_M}\boldsymbol{\psi}_M)$ and let $\underline{\mathbf{A}} = \underline{\mathbf{U}}_A \underline{\boldsymbol{\Sigma}}_A \underline{\mathbf{V}}_A^t$ be the singular value decomposition of $\underline{\mathbf{A}}$. Then, the total energy constraint could be written as

$$\sum_{i=1}^p \sigma_i^2(\underline{\mathbf{A}}) \leq E_T \quad (5.6)$$

where $p = \min(M, N)$. Consequently, our goal will be to find the minimal achievable distortion corresponding to a certain matrix $\underline{\mathbf{A}}$ satisfying (5.6). Unfortunately, this problem is quite hard to resolve, therefore, we limit ourselves to a lower-bound and the resulting distortion of a particular encoding scheme which yields an upper-bound on any optimal scheme.

5.3.1 Achievable Distortion

Developing (5.5), the distortion could be written as

$$D = \sum_{i=1}^{N'} \lambda_i E \left[(U_i - \widehat{U}_i)^2 \right] \quad (5.7)$$

where $\hat{\mathbf{U}}$ is the estimate of \mathbf{U} . In order to minimize the distortion, the best estimator to be chosen is the minimum mean squared error (MMSE) estimator. This latter is equal to

$$\hat{\mathbf{U}} = E[\mathbf{U}\mathbf{Y}^t] (E[\mathbf{Y}\mathbf{Y}^t])^{-1} \mathbf{Y}, \quad (5.8)$$

\mathbf{Y} being the projection of $Y(t)$ on the signal space basis. let

$$\underline{\boldsymbol{\gamma}} = \begin{pmatrix} \frac{\alpha_1}{E[R^2(\mathbf{x}_1)]} & 0 & 0 \\ 0 & \ddots & 0 \\ 0 & 0 & \frac{\alpha_M}{E[R^2(\mathbf{x}_M)]} \end{pmatrix}, \quad (5.9)$$

$$\underline{\mathbf{B}} = \begin{pmatrix} \sqrt{\frac{\lambda_1 \alpha_1}{E[R^2(\mathbf{x}_1)]}} \phi_1(\mathbf{x}_1) & \dots & \sqrt{\frac{\lambda_{N'} \alpha_1}{E[R^2(\mathbf{x}_1)]}} \phi_{N'}(\mathbf{x}_1) \\ \vdots & & \vdots \\ \sqrt{\frac{\lambda_1 \alpha_M}{E[R^2(\mathbf{x}_M)]}} \phi_1(\mathbf{x}_M) & \dots & \sqrt{\frac{\lambda_{N'} \alpha_M}{E[R^2(\mathbf{x}_M)]}} \phi_{N'}(\mathbf{x}_M) \end{pmatrix};$$

therefore, (5.7) gives us

$$D = \sum_{i=1}^{N'} \lambda_i \left[1 - \boldsymbol{\Gamma}_i^t \underline{\mathbf{h}}^t (\sigma_Z^2 \mathbf{I}_N + \underline{\mathbf{A}} \underline{\mathbf{C}} \underline{\mathbf{A}}^t)^{-1} \underline{\mathbf{h}} \boldsymbol{\Gamma}_i \right], \quad (5.10)$$

where $\boldsymbol{\Gamma}_i = (0, \dots, 0, 1, 0, \dots, 0)^t$ is the vector that has the i^{th} component equal to 1 and all other components equal to zero, $\underline{\mathbf{h}} = \underline{\mathbf{A}} \underline{\mathbf{B}}$ and $\underline{\mathbf{C}} = \sigma_W^2 \underline{\boldsymbol{\gamma}} + \underline{\mathbf{B}} \underline{\mathbf{B}}^t$. Being symmetric, the eigenvalue decomposition of the matrix $\underline{\mathbf{C}}$ could be written as $\underline{\mathbf{C}} = \underline{\mathbf{U}}_C \underline{\boldsymbol{\mu}}_C \underline{\mathbf{U}}_C^t$ where

$$\underline{\boldsymbol{\mu}}_C = \mathbf{diag}(\mu_1(\underline{\mathbf{C}}), \dots, \mu_M(\underline{\mathbf{C}})) \quad (5.11)$$

with $\mu_1(\underline{\mathbf{C}}) \geq \dots \geq \mu_M(\underline{\mathbf{C}})$, and $\underline{\mathbf{U}}_C$ the matrix of the corresponding eigenvectors.

Hence, by choosing $\underline{\mathbf{V}}_A = \underline{\mathbf{U}}_C$, and then, using Lagrange multipliers [73] in order to optimize the resultant distortion with respect to the singular values of $\underline{\mathbf{A}}$ subject to (5.6), we obtain

$$D_{ach} = \sum_{i=1}^{N'} \lambda_i - \sum_{i=1}^{N'} \sum_{j=1}^p \frac{\lambda_i l_{ij}^2 \gamma_j^+}{\mu_j(\underline{\mathbf{C}}) [\sigma_Z^2 + \gamma_j^+]} \quad (5.12)$$

where $\mathbf{l}_i = (l_{i,1}, \dots, l_{i,M}) = \boldsymbol{\Gamma}_i^t \underline{\mathbf{B}}^t \underline{\mathbf{U}}_C$,

$$\gamma_j^+ = \max \left\{ 0, \sqrt{\frac{\sigma_Z^2 \sum_{k=1}^{N'} \lambda_k l_{kj}^2}{\delta}} - \sigma_Z \right\} \quad (5.13)$$

and δ is such that

$$\sum_{j=1}^p \frac{\gamma_j^+}{\mu_j(\mathbf{C})} = E_T \quad (5.14)$$

5.3.2 Lower-Bound

We will derive here a lower-bound over all achievable distortions while the sensors are performing the linear mapping described in the previous section. Let q be the rank of \mathbf{B} , $\mathbf{U}_B \mathbf{\Sigma}_B \mathbf{V}_B^t$ its ordered ($\sigma_1(\mathbf{B}) \geq \dots \geq \sigma_q(\mathbf{B})$) singular value decomposition and $r = \min(p, q)$. Let also $\underline{\mathbf{h}}^t \underline{\mathbf{h}} = \mathbf{V} \underline{\boldsymbol{\mu}} \mathbf{V}^t$ be the ordered eigenvalue decomposition ($\mu_1(\underline{\mathbf{h}}^t \underline{\mathbf{h}}) \geq \dots \geq \mu_{N'}(\underline{\mathbf{h}}^t \underline{\mathbf{h}})$) of $\underline{\mathbf{h}}^t \underline{\mathbf{h}}$, v_{ij} the entries of \mathbf{V} and λ_{\min} the minimum of $\{\lambda_1, \dots, \lambda_{N'}\}$. Any achievable distortion will be lowered by canceling the effect of the observation noise or equivalently by taking $\sigma_W = 0$. Therefore, we have the following inequalities

$$D \geq \sum_{i=1}^{N'} \sum_{j=1}^{N'} \lambda_i \frac{\sigma_Z^2 v_{ij}^2}{\sigma_Z^2 + \mu_j(\underline{\mathbf{h}}^t \underline{\mathbf{h}})} \quad (5.15)$$

$$\geq \lambda_{\min} \sum_{j=1}^{N'} \frac{\sigma_Z^2}{\sigma_Z^2 + \mu_j(\underline{\mathbf{h}}^t \underline{\mathbf{h}})} \quad (5.16)$$

$$= \lambda_{\min} \sum_{j=1}^r \frac{\sigma_Z^2}{\sigma_Z^2 + \mu_j(\underline{\mathbf{h}}^t \underline{\mathbf{h}})} + \lambda_{\min}(N' - r) \quad (5.17)$$

The eigenvalues of $\underline{\mathbf{h}}^t \underline{\mathbf{h}}$ are constrained by (see [74] p.171)

$$\prod_{i=1}^r \mu_i(\underline{\mathbf{h}}^t \underline{\mathbf{h}}) \leq \left(\prod_{i=1}^r \sigma_i^2(\mathbf{A}) \right) \left(\prod_{i=1}^r \sigma_i^2(\mathbf{B}) \right) \quad (5.18)$$

Maximizing the right hand side of (5.18) subject to the sum energy constraint, gives that for every matrix \mathbf{A} satisfying (5.6),

$$\prod_{i=1}^r \mu_i(\underline{\mathbf{h}}^t \underline{\mathbf{h}}) \leq \left(\frac{E_T}{r} \right)^r \left(\prod_{i=1}^r \sigma_i^2(\mathbf{B}) \right) \quad (5.19)$$

Then, minimizing (5.17) over (5.19) gives the following result (the proof is put in Appendix 5.A)

$$D_{lower} = \lambda_{\min} \frac{r^2 \sigma_Z^2}{r \sigma_Z^2 + E_T \sqrt[r]{\prod_{i=1}^r \sigma_i^2(\mathbf{B})}} + \lambda_{\min}(N' - r) \quad (5.20)$$

$$\text{for } \frac{E_T}{r} \sqrt[r]{\prod_{i=1}^r \sigma_i^2(\mathbf{B})} \geq (2r - 1) \sigma_Z^2. \quad (5.21)$$

5.4 General Lower-Bound

Until now, we have dealt with linear encoders that just forward their observed values across the channel. Such encoders are known to have some advantages in terms of low complexity and delay. It is natural to consider the distortion achievable with more general encoders. In this section, we derive a more general lower-bound on the distortion over all possible encoders, all total energy distributions and all signatures; note that, as said previously, the separation theorem does not hold because of having to code correlated observations over a multiple access channel. Thus, doing multi-terminal source coding, then, using capacity-achieving channel encoders does not lead to an optimal distortion and consequently to a lower-bound. Therefore, we will assume that the sensors can communicate freely with each other, an assumption that will render our model equivalent to a point-to-point communication model on which the separation theorem holds and an achievable lower-bound is well-known. A similar lower-bound has been found in [70] (see also [75], [54]) and can be applied for the special case of our random field where $\lambda_1 = \dots = \lambda_{N'}$; we generalise this result for general $\lambda_1, \dots, \lambda_{N'}$ in order to obtain the lower-bound that we seek. Since the observations are noisy versions of the field, the lower-bound is equal to $D_{remote}(C)$, where

$$D_{remote}(R) = \min_{p(\hat{\mathbf{u}}/\mathbf{r}): I(\hat{\mathbf{U}};\mathbf{R}) \leq R} \sum_{i=1}^{N'} \lambda_i E[(U_i - \hat{U}_i)^2] \quad (5.22)$$

is the remote distortion rate function of the source vector \mathbf{U} , $\mathbf{R} = (R(\mathbf{x}_1), \dots, R(\mathbf{x}_M))$ and C is the capacity of the N uses of the multiple input one output channel. Let

$$\underline{\Phi} = \begin{pmatrix} \sqrt{\lambda_1} \phi_1(\mathbf{x}_1) & \dots & \sqrt{\lambda_{N'}} \phi_{N'}(\mathbf{x}_1) \\ \vdots & & \vdots \\ \sqrt{\lambda_1} \phi_1(\mathbf{x}_M) & \dots & \sqrt{\lambda_{N'}} \phi_{N'}(\mathbf{x}_M) \end{pmatrix} \quad (5.23)$$

and

$$\underline{\Phi}' = \underline{\Phi} \text{diag}(\sqrt{\lambda_1}, \dots, \sqrt{\lambda_{N'}}). \quad (5.24)$$

We find that

$$D_{\text{remote}}(C) = \sum_{i=1}^{N'} [\lambda_i - \sigma_i^2 + \min\{\sigma_i^2, \delta\}] \quad (5.25)$$

with

$$\frac{1}{2} \sum_{i=1}^{N'} \left(\log \frac{\sigma_i^2}{\delta} \right)^+ = C \quad (5.26)$$

where $\sigma_1^2, \dots, \sigma_{N'}^2$ are the eigenvalues of the matrix $\underline{\Phi}'^t (\underline{\Phi}' \underline{\Phi}'^t + \sigma_W^2 \mathbf{I}_M)^{-1} \underline{\Phi}'$ and

$$C = \frac{N}{2} \log \left(1 + \frac{E_T \sum_{i=1}^M \alpha_i}{N \sigma_Z^2} \right) \quad (5.27)$$

5.5 Ideal Model

Consider an ideal sensor network model in which the node's sensing ability is perfect, in the sense that the observations collected by the sensors are no longer corrupted by observation noise. Assume that the signal space dimension is larger or equal to the field dimension and that $\alpha_i < \infty$ for $i = 1, \dots, M$. In that case, by choosing $\underline{\mathbf{V}}_A = \underline{\mathbf{U}}_B$ and $\sigma_1(\underline{\mathbf{A}}) = \dots = \sigma_{N'}(\underline{\mathbf{A}}) = \sqrt{\frac{E_T}{N'}}$,

$$D = \sum_{i=1}^{N'} \sum_{j=1}^{N'} \lambda_i \frac{\sigma_Z^2 v_{B_{ij}}^2}{\sigma_Z^2 + \frac{E_T}{N'} \sigma_j^2(\underline{\mathbf{B}})} \quad (5.28)$$

is achievable where $v_{B_{ij}}$ are the entries of $\underline{\mathbf{V}}_B$.

5.5.1 Scaling Law

Let $\mathbf{b}(\mathbf{x}_i)$ be the i^{th} line vector in $\underline{\mathbf{B}}$ corresponding to a sensor at position \mathbf{x}_i . Here, we assume that $\phi_i(\mathbf{x}_j) < \infty$ for $i = 1, \dots, N'$ and $j = 1, \dots, M$. Suppose that there exists N' areas $\mathcal{A}_1, \dots, \mathcal{A}_{N'} \subset \mathcal{A}$ such that $\forall \mathbf{x}_1 \in \mathcal{A}_1, \dots, \forall \mathbf{x}_{N'} \in \mathcal{A}_{N'}$, the vectors $\mathbf{b}(\mathbf{x}_1), \dots, \mathbf{b}(\mathbf{x}_{N'})$ are linearly independent. Suppose also, that the position of every sensor, which is random, follows a certain probability density function $p(\mathbf{x})$ defined on \mathcal{A} and is independent from the positions of the other sensors. Thus, the probability that

a sensor belongs to an area \mathcal{A}_i is

$$c_i \triangleq \int_{\mathcal{A}_i} p(\mathbf{x}) d\mathbf{x} \quad (5.29)$$

Denote by n_i the number of sensors in \mathcal{A}_i after throwing M sensors and let $n = \min\{n_1, \dots, n_{N'}\}$. Therefore, with the line vectors of \mathbf{B} , it can be at least constructed n full ranked N' -dimensional square matrices denoted by $\mathbf{B}_1, \dots, \mathbf{B}_n$. Then, for $i = 1, \dots, N'$, we have the following result (see [76] p.176)

$$\frac{n}{M} d_{\min} \leq \frac{\sigma_i^2(\mathbf{B})}{M} \leq d_{\max} \quad (5.30)$$

where

$$d_{\min} = \min_{i=1, \dots, n} \left[\min_{\mathbf{s}^t \mathbf{s} = 1} \|\mathbf{B}_i \mathbf{s}\|^2 \right] \quad (5.31)$$

and

$$d_{\max} = \max_{i=1, \dots, M} \left[\max_{\mathbf{s}^t \mathbf{s} = 1} (\mathbf{b}(\mathbf{x}_i) \mathbf{s})^2 \right] \quad (5.32)$$

Due to the field and channel assumptions, d_{\min} and d_{\max} are strictly positive and bounded constants. Note that $\lim_{M \rightarrow \infty} \frac{n}{M} = c$ where $c = \min\{c_1, \dots, c_{N'}\}$. Hence, the achievable distortion in (5.28) scales asymptotically as $\frac{1}{M}$. This scaling behavior is under investigation in the case where the sensors have no information about the channel.

5.5.2 Comparison With a TDMA Scheme

In a TDMA transmission scheme, the number of sensors is equal to the signal space dimension and the matrix $\underline{\psi} \triangleq (\psi_1, \dots, \psi_M)$ is unitary. Therefore,

$$\sum_{i=1}^r \sigma_i^2(\underline{\mathbf{h}}) = \sum_{i=1}^M \alpha_i E_i \leq E_T \alpha_{\max} \quad (5.33)$$

with $\alpha_{\max} = \max_{i=1, \dots, M} \alpha_i$. Then, an easily lower-bound on the achievable distortion could be found. In fact, minimizing (5.17) under (5.33) leads to

$$D_{TDMA} \geq \frac{\lambda_{\min} \sigma_Z^2 r^2}{\sigma_Z^2 r + \alpha_{\max} E_T} + \lambda_{\min}(N' - r). \quad (5.34)$$

Compared to the achievable distortion in (5.28) which scales asymptotically like $1/M$, the left-hand side term in (5.34) does not depend on the number

of sensors. This leads to the conclusion of the sub-optimality of such a transmission scheme especially when the number of sensors becomes large. Note that this lower-bound is also true when observation noise exists.

5.6 Numerical Results

A simple sensor network model is considered to illustrate and compare some of the bounds derived in the above sections; The area \mathcal{A} is partitioned in ten smaller areas $\mathcal{A}_1, \dots, \mathcal{A}_{10}$. These are put in a vector $\mathcal{A} \triangleq (\mathcal{A}_1, \dots, \mathcal{A}_{10})$. The space functions are taken equal to

$$\phi_i(\mathbf{x}) = \begin{cases} \frac{1}{\sqrt{\mathcal{A}_i}} & \text{if } \mathbf{x} \in \mathcal{A}_i \\ 0 & \text{if } \mathbf{x} \notin \mathcal{A}_i \end{cases}$$

for $i = 1, \dots, 10$.

In the figures 5.2(a) and 5.2(b), our achievable distortion outperforms the Gastpar-Vetterli result especially for relatively small total energy. The distortion is due to the channel noise and to the observation noise, thus when the total energy increases, the influence of the channel noise on the distortion decreases. Therefore, it will be essentially caused by the observation noise, the influence of which being independent from the total energy. That's the reason why, the slope of the curves in 5.2(a) and 5.2(b) (except D_{lower} because it only depends on the channel noise) tends to zero when the total energy becomes relatively large. Comparing the curves corresponding to D_{ach} and D_{lower} , we see that the gap between them starts very small and then becomes larger which is due, as mentioned above, to the fact that the lower-bound does not take into account the observation noise. Note that the large difference between the two lower-bound curves for relatively small total energy reveals nothing on the efficiency of linear encoders, because of the free information exchange assumption taken in the calculation of the general lower bound ($D_{remote}(C)$) that render it non-achievable in general. In any case, $D_{remote}(C)$ still have the utility of giving us a lower-bound on the distortion over all possible encoders even if it is not achievable. At the end, comparing 5.2(a) to 5.2(b) reveals the decreasing behavior for all the distortion curves when the number of sensors increases.

5.7 Conclusion

In this chapter, we investigated the coding problem of a wireless sensor network tracking a random time-varying random field. Particularly, We anal-

ysed the performance of a linear coding scheme performed at each sensor node and derived upper and lower bounds on the optimal achievable performance. Under a sum energy constraint, we found the asymptotic decreasing behavior of the distortion as a function of the number of sensors.

APPENDIX

5.A Proof of D_{lower}

In fact, the minimization problem that we have is equivalent to minimize a function f of a vector

$$f(\mathbf{y}) = \sum_{i=1}^r \frac{a^2}{a^2 + y_i} \quad (5.35)$$

over

$$\Omega \triangleq \{\mathbf{y} \in \mathbb{R}^r : y_1 \geq 0, \dots, y_r \geq 0, \prod_{i=1}^r y_i \leq b\} \quad (5.36)$$

where a and b are constants. For convexity considerations, it is assumed that $b \geq [(2r-1)a^2]^r$. In that case, denoting by y^* the vector that minimizes $f(\mathbf{y})$ over Ω , and taking $\mathbf{y}_1 \triangleq ((2r-1)a^2, \dots, (2r-1)a^2) \in \Omega$, we obtain $f(\mathbf{y}^*) \leq f(\mathbf{y}_1) = \frac{1}{2}$. Thus y^* should belong to Ω' where

$$\Omega' \triangleq \{\mathbf{y} \in \mathbb{R}^r : y_1 \geq a^2, \dots, y_r \geq a^2, \prod_{i=1}^r y_i = b\}. \quad (5.37)$$

Letting $\mathbf{y} = (e^{t_1}, \dots, e^{t_r})$ where $\mathbf{t} \triangleq (t_1, \dots, t_r) \in \mathbb{R}^r$, leads to the equivalence between the minimization of $f(\mathbf{y})$ over Ω (or over Ω') and that of another function g defined as

$$g(\mathbf{t}) = \sum_{i=1}^r \frac{a^2}{a^2 + e^{t_i}} \quad (5.38)$$

over

$$\Omega_t \triangleq \{\mathbf{t} \in \mathbb{R}^r : t_1 \geq \ln(a^2), \dots, t_r \geq \ln(a^2), \sum_{i=1}^r t_i = \ln(b)\}$$

which is a convex optimization problem. Thus, using Lagrange multipliers, we obtain

$$g(\mathbf{t}^*) = \frac{ra^2}{a^2 + \sqrt[r]{b}} \quad (5.39)$$

where \mathbf{t}^* is the vector in Ω_t that minimizes $g(\mathbf{t})$.

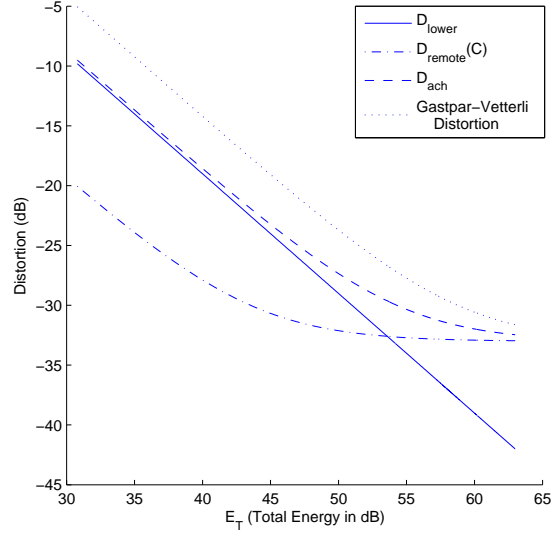
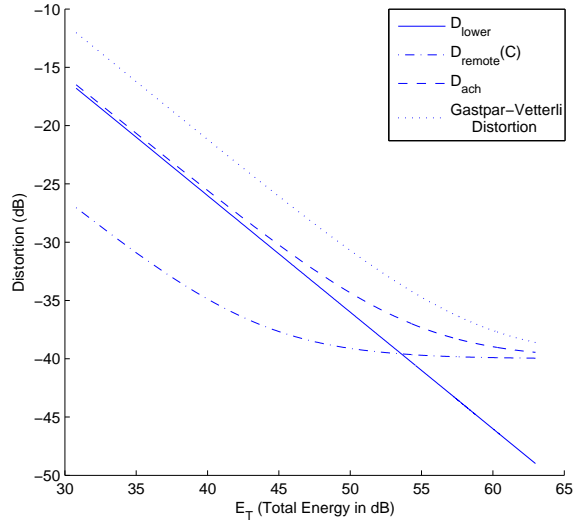
(a) Number of sensors $M=200$ (b) Number of sensors $M=1000$

Figure 5.2: Comparison between D_{lower} , D_{ach} , $D_{remote}(C)$ and Gastpar-Vetterli distortion: $\mathcal{A} = [9, 15, 18, 12, 6, 7, 3, 13, 7, 10]$, $N = N' = 10$, $\lambda_1 = \dots = \lambda_{10} = 10$, $\alpha_i = 1$ for $i = 1, \dots, M$, $\sigma_Z = 1.5$, $\sigma_W = 0.01$

Chapter 6

Conclusions and Future Work Directions

In this thesis, we addressed the coding problem in wireless sensor network models where sensor nodes send simultaneously their observed data through a noisy MAC to a certain receiver. As coding strategies in WSNs are application-dependent, we limited our study to three types of applications for which we proposed different encoding techniques adapted with the characteristics of each one and derived bounds on the optimal performance that could be achieved.

In the first application, we considered independent sources, varying very slowly in time and observed by a network of spatially separated sensor nodes; we assumed there that sensor nodes are obliged to encode one source sample and send it directly through the channel since encoding an i.i.d. sequence of source samples will induce an undesirable delay in reconstructing the source estimates at the receiver. Due to the slowly time-varying characteristics of the sources and hence to the long interval of time existing between two i.i.d source samples, it is assumed that each sensor node can map its observed source sample into an infinite-dimensional channel with fixed energy constraint. We derived upper and lower bounds on the optimal achievable performance using standard inequalities in information theory and proposed a simple digital code that exhibits an exponential decreasing behavior with the fixed quantity of energy dedicated to each source sample. In addition, we

worked on different model variants, such as the one involving noisy observations at the sensor nodes or assuming noncoherent detection at the decoder. For all these variants, we obtained theoretical bounds on the performance and showed through simulations the efficiency of our proposed code.

In the second application, we supposed that the sources observed by the sensor nodes are correlated. We assumed here a Gaussian multiple access channel with phase shifts unknown at the transmitters but perfectly known at the receiver. Unlike the first application, sensor nodes had the possibility of encoding very long blocks regardless of the delay that might be induced in reproducing them at the receiver. We proved that the separation theorem holds for lossless transmission of arbitrarily correlated discrete sources of finite alphabets; in other words, the coding strategy based on separating the source coding from the channel coding is optimal. This separation holds for ergodic random and arbitrary non-random phase shifts. Hence, unlike the case where the phases are known at the transmitters, the separation performance is optimal even if the transmitted sources are correlated. For lossy coding of arbitrarily correlated continuous sources, the separation result obtained for the discrete source case is extended by proving its asymptotic optimality in the high fidelity regime; this optimality holds when the fidelity criterion is the MSE distortion.

In the last application, we considered a physical random field generated by a fixed number of Gaussian random variables and monitored by a wireless sensor network deployed over an area. We assumed here a real Gaussian multiple access channel with no phase shifts. We investigated the performance of linear coding performed at each sensor node while an MMSE estimator is used at the decoder to reconstruct an estimate of this field. We derived bounds on the performance and found the asymptotic decreasing behavior of the distortion with the number of sensor nodes.

Future Work Directions

Although we have derived coding schemes and coding strategies for wireless sensor network applications, the results obtained can still be improved and generalized:

In the first part of the thesis, the lower bound on the distortion was derived using Shannon mutual information. This lower bound is known to be achieved when encoding sequences of infinite blocklength which is not the case when dealing with low bandwidth sources. New results obtained in [77], show that the lower bound can be improved by using Rényi information measure. Even if this improvement can just be exploited numerically,

it would be very interesting to see how much we can approach the derived upper bound that decays like $e^{-E/6}$.

In the second part of the thesis, a number of issues remain to be investigated; it is interesting to treat the case of very low bandwidth correlated sources and to propose a practical coding scheme adapted with these kind of sources. More deep work have to be done to see whether or not the exact separation optimality in the continuous source case can be obtained instead of the asymptotic optimality already derived. Another important issue is to see if the separation optimality can be extended to other kind of communication scenarios including those where the information is relayed through multiple sensors to the receiver.

Bibliography

- [1] J.M. Kahn, R.H. Katz, and K.S.J. Pister, “Next century challenges: mobile networking for smart dust,” in *Proceedings of the Fifth Annual International Conference on Mobile Computing and Networks (MobiCOM '99)*, Washington, USA, 1999, pp. 271–278.
- [2] D. Culler, D. Estrin, and M. Srivastava, “Overview of sensor networks,” *IEEE Computer Magazine*, vol. 37, Aug. 2004.
- [3] C. Chong and S.P. Kumar, “Sensor networks: evolution, opportunities and challenges,” *IEEE Proceedings*, vol. 91, pp. 1247–1256, Aug. 2003.
- [4] I.F. Akyildiz, Y. Sankarasubramaniam, and E. Cayirci, “A survey on sensor networks,” *IEEE Communications Magazine*, vol. 40, pp. 102–114, Aug. 2002.
- [5] A. Bharathidasan and V. Ponduru, “Sensor networks: an overview,” in *Technical report, Dept. of Computer Science, University of California, Davis, CA*, 2002.
- [6] A.A. Ahmed, H. Shi, and Y. Shang, “A survey on network protocols for wireless sensor networks,” in *International Conference on Information Technology: Research and Education ITRE'03*, Aug. 2003.
- [7] R. Szewczyk, A. Mainwaring, J. Polastre, J. Anderson, and D. Culler, “An analysis of a large scale habitat monitoring application,” in *The Second ACM Conference on Embedded Networked Sensor Systems*, Nov. 2004.
- [8] K. Martinez, P. Padhy, A. Riddoch, H.L.R. Ong, and J.K. Hart, “Glacial environment monitoring using sensor networks,” in *REAL-WSN'05*, Sweden, Nov. 2005.

-
- [9] D. Estrin, R. Govindan, J. Heidemann, and S. Kumar, “Next century challenges: Scalable coordination in sensor networks,” in *Proceedings of the Fifth Annual International Conference on Mobile Computing and Networks (MobiCOM '99)*, Washington, USA, 1999, pp. 263–270.
- [10] Ivan Stojmenović, *Handbook of sensor networks: algorithms and architectures*, John Wiley & Sons, 2005.
- [11] M. Ilyas and I. mahgoub, *Handbook of sensor networks: compact wireless and wired sensing systems*, CRC Press LLC, 2005.
- [12] R.B. Alley, “Continuity comes first: recent progress in understanding subglacial deformation,” in *Geological Society Special Publication*, 2000, vol. 176, pp. 171–180.
- [13] J.K. Hart and J. Rose, “Approaches to the study of glacier bed deformation,” in *Quaternary International*, 2001, vol. 86, pp. 45–58.
- [14] R. Szewczyk et al., “Lessons from a sensor network expedition,” in *1st European Workshop on Wireless Sensor Networks (EWSN '04)*, Berlin, Jan. 2004, pp. 307–322.
- [15] “<http://envisense.org/floodnet.htm>,” .
- [16] “<http://envisense.org/secoas.htm>,” .
- [17] C.R. Baker et al., “Wireless sensor networks for home health care,” in *21st International Conference on Advanced Information Networking and Applications Workshops (AINAW'07)*, May 2007.
- [18] C. Intanagonwiwat, R. Govindan, D. Estrin, J. Heidemann, and F. Silva, “Directed diffusion for wireless sensor networking,” *IEEE/ACM Transactions on Networking*, vol. 11, pp. 2–16, Feb. 2003.
- [19] W. Heinzelman, A. Chandrakasan, and H. Balakrishnan, “Energy-efficient communication protocol for wireless microsensor networks,” in *Proceedings of the 33rd Annual Hawaii International Conference on System Sciences (HICSS'00)*, Jan. 2000.
- [20] S. Lindsey and C. Raghavendra, “Pegasis: power-efficient gathering in sensor information systems,” in *International Conference on Communication Protocols*, 2001, pp. 149–155.

-
- [21] A. Manjeshwar and D.P. Agarwal, "Teen: a routing protocol for enhanced efficiency in wireless sensor networks," in *1st International Workshop on Parallel and Distributed Computing Issues in Wireless Networks and Mobile Computing*, Apr. 2001.
- [22] A. Manjeshwar and D.P. Agarwal, "Apteen: a hybrid protocol for efficient routing and comprehensive information retrieval in wireless sensor networks," in *Proceedings of the 16th International Parallel and Distributed Processing Symposium (IPDPS'02)*, 2002, pp. 195–202.
- [23] F. Ye, A. Chen, S. Liu, and L. Zhang, "A scalable solution to minimum cost forwarding in large sensor networks," in *Proceedings the IEEE International Conference on Computer Communications and Networks (ICCCN)*, 2001, pp. 304–309.
- [24] V. Rodoplu and T.H. Meng, "Minimum energy mobile wireless networks," *IEEE Journal on Selected Areas in Communications*, vol. 17, pp. 1333–1344, Aug. 1999.
- [25] J. Al-Karaki and A. Kamal, "On the optimal data aggregation and in-network processing based routing in wireless sensor networks," *Technical Report, Iowa State University*, 2003.
- [26] Q. Li, J. Aslam, and D. Rus, "Hierarchical power-aware routing in sensor networks," in *In Proceedings of the DIMACS Workshop on Pervasive Networking*, May 2001.
- [27] S.J. Baek, G. Veciana, and X. Su, "Minimizing energy consumption in large-scale sensor networks through distributed data compression and hierarchical aggregation," *IEEE Journal on Selected Areas in Communications*, vol. 22, pp. 1130–1140, Aug. 2004.
- [28] X. Li, H. Kang, and H-H. Chen, "Sensing workload scheduling in hierarchical sensor networks for data fusion applications," in *Proceedings of the 2007 international conference on Wireless communications and mobile computing*, 2007, pp. 214–219.
- [29] D. Marco and D.L. Neuhoff, "Reliability vs. efficiency in distributed source coding for field-gathering sensor networks," in *Third International Symposium on Information Processing in Sensor Networks IPSN'04*, 2004, pp. 161–168.

-
- [30] L. Sankaranarayanan, G. Kramer, and N.B. Mandayam, “Hierarchical sensor networks: capacity bounds and cooperative strategies using the multiple-access relay channel model,” in *First Annual IEEE Communications Society Conference on Sensor and Ad Hoc Communications and Networks (SECON 2004)*, Oct. 2004, pp. 191–199.
- [31] J. Barros and S.D. Servetto, “Network information flow with correlated sources,” *IEEE Transactions on Information Theory*, vol. 52, pp. 155–170, Jan. 2006.
- [32] T.M. Cover, A. El Gamal, and M. Salehi, “Multiple access channels with arbitrarily correlated sources,” *IEEE Transactions on Information Theory*, vol. 26, pp. 648–657, Nov. 1980.
- [33] C.E. Shannon, “A mathematical theory of communication,” *Bell System Technical Journal*, vol. 27, pp. 379–423, 623–656, Nov. 1948.
- [34] R. Zamir and T. Berger, “Multiterminal source coding with high resolution,” *IEEE Transactions on Information Theory*, vol. 45, pp. 106–117, Jan. 1999.
- [35] T.J. Goblick, “Theoretical limitations on the transmission of data from analog sources,” *IEEE Transactions on Information Theory*, vol. 11, pp. 558–567, Oct. 1965.
- [36] M. Gastpar, “Uncoded transmission is exactly optimal for a simple gaussian sensor network,” in *Proc. 2007 Information Theory and Applications Workshop*, San Diego, CA, USA, Jan. 29 - Feb. 2 2007.
- [37] P. Elias, “Networks of gaussian channels with applications to feedback systems,” *IEEE Transactions on Information Theory*, vol. 13, pp. 493–501, July 1967.
- [38] M. Gastpar, *To code or not to code*, Ph.D. thesis, EPFL, Dec. 2002.
- [39] B. Hochwald and K. Zeger, “Tradeoff between source and channel coding,” *IEEE Transactions on Information Theory*, vol. 43, pp. 1412–1424, Sept. 1997.
- [40] B. Hochwald and K. Zeger, “Tradeoff between source and channel coding on a gaussian channel,” *IEEE Transactions on Information Theory*, vol. 44, pp. 3044–3055, Nov. 1998.

-
- [41] J.M. Wozencraft and I.M. Jacobs, *Principles of Communication Engineering*, John Wiley & Sons, Inc, 1965.
- [42] V.A. Vaishampayan and I.R. Costa, “Curves on a sphere, shift-map dynamics, and error control for continuous alphabet sources,” *IEEE Transactions on Information Theory*, vol. 49, pp. 1658–1672, July 2003.
- [43] B. Chen and G.W. Wornell, “Analog error-correcting codes based on chaotic dynamical systems,” *IEEE Transactions on Communications*, vol. 46, pp. 881–890, July 1998.
- [44] P.A. Floor and T.A. Ramstad, “Noise analysis for dimension expanding mappings in source-channel coding,” in *IEEE 7th Workshop on Signal Processing Advances in Wireless Communications*, July 2006.
- [45] P.A. Floor, T.A. Ramstad, and N. Wernersson, “Power constrained channel optimized vector quantizers used for bandwidth expansion,” in *4th International Symposium Workshop on Wireless Communication Systems*, Oct. 2007, pp. 667–671.
- [46] T.M. Cover and J.A. Thomas, *Elements of Information Theory*, New York: John Wiley & Sons, 1991.
- [47] H.L. Van Trees, *Detection, Estimation and Modulation Theory*, John Wiley and Sons, 2001.
- [48] A.V. Balakrishnan, “A contribution to the sphere-packing problem of communication theory,” *Journal of Mathematical Analysis and Applications*, vol. 3, pp. 485–506, Dec. 1961.
- [49] B. Dunbridge, “Asymmetric signal design for the coherent gaussian channel,” *IEEE Transactions on Information Theory*, vol. 13, pp. 422–431, July 1967.
- [50] M. Steiner, “The strong simplex conjecture is false,” *IEEE Transactions on Information Theory*, vol. 40, pp. 721–731, May 1994.
- [51] A.J. Kurtenbach and P.A Wintz, “Quantizing for noisy channels,” *IEEE Transactions on Communication Technology*, vol. 17, pp. 291–302, Apr. 1969.
- [52] P.A Wintz and A.J. Kurtenbach, “Analysis and minimization of message error in pcm telemetry,” Tech. Rep. TR-EE67-19, Purdue University, Lafayette, Ind, December 1967.

-
- [53] A.J. Viterbi and J.K. Omura, *Principles of Digital Communication and Coding*, McGraw-Hill Publishing Company, 1979.
- [54] J.K. Wolf and J. Ziv, "Transmission of noisy information to a noisy receiver with minimum distortion," *IEEE Transactions on Information Theory*, vol. 16, pp. 406–411, July 1970.
- [55] R.G. Gallager, "A simple derivation of the coding theorem and some applications," *IEEE Transactions on Information Theory*, vol. 11, pp. 3–18, Jan. 1965.
- [56] G. Dueck, "A note on the multiple access channel with correlated sources," *IEEE Transactions on Information Theory*, vol. 27, pp. 232–235, Mar. 1981.
- [57] A.D. Murugan, P.K. Gopala, and H. El Gamal, "Correlated sources over wireless channels: cooperative source-channel coding," *IEEE Journal on Selected Areas in Communications*, vol. 22, pp. 988–998, Aug. 2004.
- [58] H. El Gamal, "On the scaling laws of dense wireless sensor networks: the data gathering channel," *IEEE Transactions on Information Theory*, vol. 51, pp. 1229–1234, Mar. 2005.
- [59] D. Slepian and J.K. Wolf, "Noiseless coding of correlated information sources," *IEEE Transactions on Information Theory*, vol. 19, pp. 471–480, July 1973.
- [60] R. Ahlswede, "Multi-way communication channels," in *Proc. 2nd Int. Symp. on Information Theory*, Tsahkadsor, Armenian S.S.R., Hungarian Acad. Sc., pp. 23-52, 1973.
- [61] J. Barros and S.D. Servetto, "Reachback capacity with non-interfering nodes," in *IEEE Symposium on Information Theory (ISIT)*, Yokohama, Japan, 2003.
- [62] A. D. Wyner and J. Ziv, "The rate-distortion function for source coding with side information at the decoder," *IEEE Transactions on Information Theory*, vol. 22, pp. 1–10, Jan. 1976.
- [63] T. Berger, *The Information Theory Approach to Communications*, vol. 229 of *CISM Courses and Lectures*, chapter Multiterminal source coding, pp. 171–231, Springer-Verlag, New York, 1978.

- [64] Y. Oohama, “Gaussian multiterminal source coding,” *IEEE Transactions on Information Theory*, vol. 43, pp. 1912–1923, Nov. 1997.
- [65] S.Y. Tung, *Multiterminal source coding*, Ph.D. thesis, School of Elect. Eng., Cornell Univ., Ithaca, NY, May 1978.
- [66] P. Viswanath, *Advances in Network Information Theory*, chapter Sum rate of multiterminal Gaussian source coding, pp. 43–60, DIMACS Series in Discrete Mathematics and Theoretical Computer Science. American Mathematical Society, Providence, RI, 2004.
- [67] A.D. Wyner, “The rate-distortion function for source coding with side information at the decoder-ii: General sources,” *Inf. Contr.*, vol. 38, pp. 60–80, July 1978.
- [68] J. Xiao and Z. Luo, “Multiterminal sourcechannel communication over an orthogonal multiple-access channel,” *IEEE Transactions on Information Theory*, vol. 53, pp. 3255–3264, Sept. 2007.
- [69] A.B. Wagner, S. Tavildar, and P. Viswanath, “Rate region of the quadratic gaussian two-encoder source-coding problem,” *IEEE Transactions on Information Theory*, vol. 54, pp. 1938–1961, May 2008.
- [70] M. Gastpar and M. Vetterli, “Power-bandwidth-distortion scaling laws for sensor networks,” in *3rd international symposium on information processing in sensor networks (IPSN’04)*, Berkeley, CA, Apr. 2004.
- [71] M. Gastpar and M. Vetterli, “Scaling laws for homogeneous sensor networks,” in *Allerton Conference*, Monticello, Illinois, Oct. 2003.
- [72] JM. Gastpar and M. Vetterli, “Power, spatio-temporal bandwidth, and distortion in large sensor networks,” *IEEE Journal on Selected Areas in Communications*, vol. 23, pp. 745–754, Apr. 2005.
- [73] S. Boyd and L. Vandenberghe, *Convex Optimization*, Cambridge University Press, 2004.
- [74] R.A. Horn and C.R. Johnson, *Topics in Matrix Analysis*, Cambridge University Press, 1991.
- [75] T. Berger, *Rate Distortion Theory: A Mathematical Basis for Data Compression*, Prentice-Hall, Englewood Cliffs, NJ, 1971.
- [76] R.A. Horn and C.R. Johnson, *Matrix Analysis*, Cambridge University Press, 1985.

- [77] A. Ingber, I. Leibowitz, R. Zamir, and M. Feder, “Distortion lower bounds for finite dimensional joint source-channel coding,” in *IEEE Symposium on Information Theory (ISIT)*, 2008, pp. 1183–1187.